The Dissertation Committee for Diana Kathryn Snelling Certifies that this is the approved version of the following dissertation:

BIODEGRADABLE MICRODEVICES FOR BIOLOGICAL DETECTION AND SMART THERAPY

Committee:

Nicholas A. Peppas, Supervisor

Jennifer Maynard

Donald R. Paul

Isaac C. Sanchez

Muhammad Zaman

BIODEGRADABLE MICRODEVICES FOR BIOLOGICAL DETECTION AND SMART THERAPY

by

Diana Kathryn Snelling, B.S.

Dissertation

Presented to the Faculty of the Graduate School of

The University of Texas at Austin

in Partial Fulfillment

of the Requirements

for the Degree of

Doctor of Philosophy

The University of Texas at Austin

May 2010

Acknowledgements

I would first like to acknowledge the steadfast support I have received from my family. I want to thank my parents, Larry and Kathy Snelling, for their love and unwavering confidence in my abilities. I count myself very fortunate to have such wonderful parents. I would also like to thank my husband, Tom Van Blarcom, for his loving encouragement of this work. He inspires me daily to be the best scientist that I can be.

I would like to thank my advisor, Professor Nicholas Peppas, for his guidance and providing an exceptionally rich graduate experience. I thank him for making me a more worldly scientist by enabling research-related travel on four continents over the past four years. I feel so fortunate to have had a graduate adviser who genuinely cared about all of his students and advised accordingly.

I would like to acknowledge the contributions of my labmates, the Peppamers: Omar, Steve, Daniel, Justin, Adam, Carolyn, Melissa, Maggie, Marty, Brandon, David, and Bill. Their collaborative spirit improved the quality of my research, and their occasional antics made my time in the lab a lot of fun. I would like to thank my undergraduate assistants who have been a privilege with

which to work. Thanks go to Yonic Medina, Sonia Gelani, Barbara Ekerdt, Daniel Ayoub, Lauren Collins, and Sukeert Manral. Their countless hours in the lab and questioning minds greatly improved the quality of this thesis.

I would like to thank Professor Teruo Okano and his students at Tokyo Women's Medical University for sharing their expertise and outstanding research facilities. My unique experiences with novel micropatterning techniques and large animal studies there added breadth to my graduate experience. Thanks to these fantastic hosts for making my time in Japan thoroughly enjoyable. I would also like to thank Professor J. Justin Gooding and Peter Reece at the University of New South Wales who guided and supported the portion of this thesis involving porous silicon rugate filters. They were extraordinarily helpful and committed to making my short time at UNSW highly productive.

I would like to acknowledge the financial support of the National Science Foundation for both a Graduate Research Fellowship and funding through the East Asia and Pacific Summer Internship program. I would also like to thank the University of Texas and the Cockrell School of Engineering for graduate fellowships.

Special thanks go to the ChEetahs who provided an outstanding outlet for any research-related frustration. And finally, I would like to thank my undergraduate research adviser, Professor Jacques Zakin, who started me on this journey.

Biodegradable Microdevices for Biological Detection and Smart Therapy

Publication No._____

Diana Kathryn Snelling, Ph.D.
The University of Texas at Austin, 2010

Supervisor: Nicholas A. Peppas

Biodegradable, pH-responsive hydrogel networks composed of poly(methacrylic acid) crosslinked with varying mol percentages of polycaprolactone diacrylate were synthesized. These materials were characterized using NMR and FTIR. The equilibrium and dynamic swelling properties of these pH-responsive materials were studied. Also, the materials' degradation was characterized using swelling studies and gel permeation chromatography.

Methods were developed to incorporate these novel hydrogels as sensing components in silicon-based microsensors. Extremely thin layers of hydrogels were prepared by photopolymerizion atop silicon microcantilever arrays that served to transduce the pH-responsive volume change of the material into an optical signal. Organosilane chemistry allowed covalent adhesion of the hydrogel to the silicon beam. As the hydrogel swelled, the stress generated at

the surface between the hydrogel and the silicon caused a beam deflection downward. The resulting sensor demonstrated a maximum sensitivity of 1nm/4.5E-5 pH unit. Sensors were tested in protein-rich solutions to mimic biological conditions and found to retain their high sensitivity. The existing theory was evaluated and developed to predict deflection of these composite cantilever beams.

Another type of hydrogel-based microsensor was fabricated utilizing porous silicon rugate filters as transducers. Porous silicon rugate filters are garnering increased attention as components of *in vivo* biosensors due to their ability for remote readout through tissue. Here, the biodegradable, pH-responsive hydrogel was polymerized within the pores of a porous silicon rugate filter to generate a novel, completely degradable sensor. Silicon was electrochemically etched in hydrofluoric acid to generate the porous silicon rugate filter with its reflectance peak in the near infrared region. Poly(methacrylic acid) crosslinked with polycaprolactone diacrylate was polymerized within the pores using UV free radical photopolymerization. The reflectance peak of this sensor varied linearly with pH in the region pH 2.2 to 8.8. This work shows promise towards utilizing porous silicon rugate filters as transducers for environmentally responsive hydrogels for biosensing applications.

Table of Contents

List of Tables

List of Figures

CHAPTER 1: INTRODUCTION

Significant developments in bionanotechnology and advanced biomaterials facilitate the design and production of systems that not only respond to physiological conditions but act in a specific way to provide a therapeutic effect. Intelligent therapeutic delivery systems can respond to pH, temperature, ionic strength or the concentrations of undesirable components in the body. Essentially, these processes involve a mimicking of natural responses in the body to different concentrations of hydrogel ions or target biomolecules. For example, insulin can be released in response to the sensed serum glucose level.

In our laboratory, we have studied a variety of mostly non-biodegradable, biomimetic systems that establish the principles for this work. It is an effort to revolutionize medicine that we tailor therapeutics based on an individual's genetic predisposition towards disease.

Biosensors can provide feedback control by recognizing changes in its surrounding physiological or biological fluid and then taking "action", either in terms of simple movement of a device component or release of one or more drugs. In recent years we have seen an explosion in the field of such novel sensors and microfabricated devices for drug delivery. Such devices provide a platform for well-controlled functions in the micro- or nano-level. They include nanoparticulate systems, recognitive molecular systems, biosensing devices, and microfabricated and microelectronic devices. The synthesis and characterization

of biomimetic gels for drug and protein delivery systems is a significant focus of recent research [1].

There are numerous techniques for microfabrication of patterned polymer surfaces and microchips for medical devices [2]. While silicon has been the choice material for much of the research done with MEMs, the methacrylates and acrylates could provide an inexpensive base for future work. Several applications have already been suggested including patterned surfaces for cell adhesion, biosensors, microfluidic devices, and arrays for chemical screening.

The physicochemical understanding of such hydrogels under the conditions of application is neither simple nor well developed. Considering that all these carriers are ionic hydrogels, and that several ionic and macromolecular components are involved, with associated thermodynamically non-ideal interactions, it is evident that analysis and prediction of their swelling and response behavior is rather complex [3].

Environmentally responsive hydrogels lend themselves naturally to utilization in microfabricated devices. Polymerization of the required monomers and crosslinking agents can be done by free-radical polymerization using UV light, thus enabling photolithographic techniques to be adjusted to pattern these materials on the microscale. When hydrogels are immobilized within microstructures, the ability of the hydrogel to function is improved. There are many advantages of utilizing hydrogels in this way. First, hydrogels can be deposited permanently in specific locations of a substrate where they can exhibit

their unique physiologically-responsive characteristics repeatedly. Second, the hydrogels mechanical failure is less of an issue when the primary action is swelling against a well-defined structure. Finally, the reduced size of these hydrogel microstructures leads to faster mass transfer and chemomechanical response [4].

While biosensors and sensing devices are usually made of non-biodegradable sensing materials and substrates, environmentally sensitive hydrogel networks whose crosslinks are degradable by hydrolysis can have a significant advantage over their nondegradable counterparts. Hydrogels are capable of serving multiple functions within the body and many of these functions are only required temporarily. They are particularly useful in “feedback control devices” where an input leads to an output through a simple or complex function, unique of the polymer used. One example is a biochemical sensor which is dependent on an enzyme.

Our laboratory has investigated the use of glucose oxidase immobilized in a swollen poly(methacrylic acid) network for the purpose of sensing glucose and responding with swelling or deswelling that can provide insulin delivery. Hydrogels can serve a dual role in sensors by first immobilizing the enzyme near the electrode surface and second, allowing the responsiveness of the gel to sense the change [5]. However, since the enzymes become inactive and degrade with time, it is desirable and more practical that the hydrogel network do the same.

Other examples of feedback control devices include responsive hydrogel nanoparticles for targeted drug delivery. Our laboratory has investigated temperature-responsive polymer-gold nanocomposites as intelligent therapeutic systems [6]. Through spatial and temporal controlled drug delivery, injectable nanoparticle carriers have the ability to revolutionize disease treatment [7].

With the advantages of a novel degradable hydrogel network come the additional challenges of understanding the responsive swelling as the crosslinks holding together the network are being cleaved. The microsensors produced for this dissertation employ very slowly degrading hydrogel networks as sensing elements that present a useable lifetime in the device. Previous studies were more concerned with mass or structural integrity losses, as many of this type of materials have been designed for structural applications in the body. A broader understanding of degradation is needed for these materials to be useful in new and more complex application such as biosensing. Structural integrity is much less of an issue in biosensing applications because the network is covalently attached to a rigid scaffold.

The synthesis of responsive hydrogels which provided tunable degradation rates was desired. Put another way, it was preferred to produce hydrogels with different lifetimes as sensing elements. This was dependent among other things on the number and length of the crosslinks. Degradation occurs via a variable number of hydrolytically labile bonds in the material. The

concentration of those bonds is easily changed, and thus the resulting sensing lifetime can be changed [8].

A complete MEMS/BioMEMS sensor usually consists of three elements [9]. First is the sensing element. Here poly(methacrylic acid) networks with hydrolytically degradable crosslinks were used. Poly(methacrylic acid) systems are especially interesting to biological applications because their pKa is so near to biological pH. Second, a transducer is required to convert the sensing element into our third required element, a measurable output. This thesis includes the experimental results of utilizing two different transducers, each of which offers unique advantages. Microcantilevers utilize a unique sensing mechanism since they provide mechanical amplification of a signal due to change in the surface properties [10]. This heightens the sensitivity for which very small volume changes in the hydrogel can be precisely observed.

This thesis focused on using biodegradable, environmentally-responsive hydrogels as sensing components in novel microscale devices. The hydrogels utilized as sensing elements were composed of pH-responsive, poly(methacrylic acid) crosslinked with biodegradable, polycaprolactone diacrylate. Two transducers were employed to create novel microsensors. The first was microcantilever arrays, and the second was porous silicon rugate filters. The microcantilever array transducer offered the advantages of ultrasensitive pH response and the opportunity for diverse sensing utilizing different hydrogels on the various beams. The porous silicon rugate filter transducer offered the

advantages of optical readout through tissue and being hydrolytically degradable, thus creating a completely biodegradable microsensor.

Within this thesis, the dissertation work is divided into many chapters. Chapter 2 offers detailed background on responsive hydrogel materials and their application in microsensors. Chapter 3 describes the overall objectives of this research. The synthesis and characterization of the various hydrogel materials is described in Chapter 4. Important studies involving the swelling and degradation behavior of these responsive hydrogels is included in Chapter 5. In Chapter 6, the fabrication and testing of microsensors which utilize microcantilever transducers along with these hydrogels is described. In this chapter also, the theory to describe composite cantilever deflection is presented and developed. Chapter 7 details the fabrication and testing of porous silicon rugate filter microsensors utilizing the same hydrogels. Finally, the overall conclusions drawn from this work are summarized in Chapter 8.

REFERENCES

1. Bayer, C.L. and N.A. Peppas, *Advances in recognitive, conductive and responsive delivery systems.* J Control Release, 2008.
2. Qin, D., Y.N. Xia, and G.M. Whitesides, *Rapid prototyping of complex structures with feature sizes larger than 20 mu m.* Adv Mater, 1996. **8**(11): p. 917.3.
3. Peppas, N.A., *Kinetics of Smart Hydrogels*, in *Reflexive Polymers and Hydrogels*, N. Yui, R.J. Mrsny, and K. Park, Editors. 2004, CRC Press LLC. p. 99-113.
4. Lei, M., et al., *Integration of hydrogels with hard and soft microstructures.* J Nanosci Nanotechno, 2007. **7**(3): p. 780-789.
5. Calvert, P., *Gel sensors and actuators.* Mrs Bull, 2008. **33**(3): p. 207-212.
6. Owens, D.E., et al., *Temperature-responsive polymer-gold nanocomposites as intelligent therapeutic systems.* J Biomed Mater Res A, 2007. **83A**: p. 692-695.
7. Owens, D.E. and N.A. Peppas, *Opsonization, biodistribution, and pharmacokinetics of polymeric nanoparticles.* Int J Pharm, 2006. **307**(1): p. 93-102.
8. Chao, G.T., et al., *Synthesis, characterization, and hydrolytic degradation behavior of a novel biodegradable pH-sensitive hydrogel based on*

polycaprolactone, methacrylic acid, and poly(ethylene glycol). J Biomed Mater Res A, 2008. **85A**(1): p. 36-46.

9. Buerk, D.G., *Biosensors, Theory and Applications*. 1993, Lancaster, PA: Technomic Publishing Company, Inc.

10. Hilt, J.Z., *Novel micro- and nanoscale diagnostic and therapeutic devices based on intelligent polymer networks*, in *Chemical Engineering*. 2004, The University of Texas: Austin, TX.

CHAPTER 2: BACKGROUND

2.1 Introduction to hydrogel-based biosensing

Several decades of research have contributed to our understanding of stimuli-responsive hydrogels so that they can now be utilized in an abundance of sensing applications. A comprehensive knowledge of their physical and chemical properties exists along with how the materials interact with living systems. Alongside, theory has evolved to explain the unique interaction of these systems with their environment and other external stimuli. Engineers are now poised to develop and utilize novel sensing systems that allow the biological processes of life to be monitored like never before.

Hydrogels are water-swollen hydrophilic crosslinked polymers, that do not dissolve in water or biological fluids because of chemical or physical crosslinks [1]. Certain hydrogels can sense changes in their environment on a molecular level which lead to changes in their swollen volume. These are commonly referred to as environmentally-responsive hydrogels. Large changes in the swelling ratio of these hydrogels can be observed with changes in the pH, temperature, ionic strength, nature of the swelling agent, and electromagnetic radiation [2]. Biomolecules are commonly immobilized within environmentally-responsive hydrogels to yield biosensing materials. The most common of these

is the immobilization of glucose oxidase within pH-responsive hydrogels to make glucose-sensitivie materials.

pH-Responsive hydrogels are anionic, cationic, or amphiphilic. Anionic hydrogels exist in a collapsed state at low pH. When the pH of the external environment is raised above the pK_a of the gel, they begin to swell. This is due to ionization of the side groups and repulsion of the like-charged chains. The charge repulsion is more powerful than other forces such as hydrogen bonding which exist between the chains in the collapsed state. At the molecular level and if the swelling is isotopic, this increase in volume corresponds to an increase in the network mesh size. Cationic hydrogels show the opposite behavior which is swelling at low pH and collapsing at high pH (Figure 2.1).

Environmentally-responsive hydrogels lend themselves naturally to utilization in microfabricated devices. Polymerization of the required monomers and crosslinking agents can be done by free-radical polymerization using UV light, thus enabling photolithographic techniques to be adjusted to pattern these materials on the microscale. When hydrogels are immobilized on top of or within microstructures, the ability of the hydrogel to function is improved.

There are many advantages of utilizing hydrogels in this way. Hydrogels can be deposited permanently in specific locations of a substrate where they can exhibit their unique physiologically-responsive characteristics repeatedly. Their mechanical failure is less of an issue when the primary action is swelling against a well-defined structure. Finally, the reduced size of these hydrogel

microstructures leads to faster mass transfer and chemomechanical response [3].

2.1.1 Kinetics of hydrogel-based sensors

To better understand the kinetic response of hydrogel-based sensors, we must first understand the kinetic response of the hydrogel itself. The swelling and shrinking of hydrogels requires transport of the stimulus into the network followed by water transport into or out of the network [4]. An interesting complexity in this system is that shrinking of the gel can generally occur more rapidly than its swelling. The characteristic response time in a hydrogel sensor is dependent on the square of the distance, so the hydrogel thickness should be as small as possible [5]. This is why microfabrication techniques are actively investigated with hydrogels.

It is interesting to note that the type of transducer can further slow the kinetics of the sensor. If the method of transduction is based on measurement of the changes of the optical transparency or conductivity of the material, then free swelling kinetics can apply. If the volume change of the gel must be transduced mechanically, such as by the use of microcantilevers, then the sensor will be inherently slower. The external force required slows the sensor performance versus our free swelling models [5].

2.2 Traditional application of hydrogels in biosensing

2.2.1 Hydrogel as immobilizing scaffold for biomolecules

The first examples of hydrogels in biosensing employed hydrogels for the immobilization of biomolecules to measure biospecific interactions. In one such example, Fagerstam et al. [6] covalently attached biomolecules to thin hydrogel films atop surface plasmon resonance chips to measure biomolecular interaction kinetics and concentration. Solutions containing biomolecules of interest were flowed over the hydrogel and small mass changes were measured with a sensitivity of 10 pg/mm^2. Some advantages of this early biosensor include that it did not require any biomolecular labeling and the sensor chip could be used repeatedly.

Immobilization of nucleic acids on solid supports has been widely used in the detection of DNA and other biomolecules in sensor technology. Because three dimensional hydrogel matrices offer significant advantages for capturing probes over more conventional two dimensional rigid substrates and the ability to provide a solution-mimicking environment, they are becoming increasingly attractive as desired supports for bio-analysis [7].

The use of hydrogels to immobilize enzymes for improved and sustained activity of biomolecules is not limited to the microscale. While commonly employed in lab-on-a-chip technologies, these materials also perform favorably in large-scale bioreactors as well. Hydrogel microspheres containing immobilized enzymes were used to monitor packed-bed bioreactor by Guiseppi-Elie et al. [8].

Enzyme activity was tested after the materials were stored in buffer at 4°C for one year. The materials retained 80% of their initial activity. This high stability shows promise towards the utilization of hydrogel-based biosensing materials on a variety of scales. Since scale-up is of common concern in the practice of chemical engineering, it is important to note that hydrogel-based biosensing elements have shown desireable performance at a variety of scales.

2.2.2 Hydrogels for improved biocompatibility of sensors

Biofouling is one of the most significant hurdles to the advancement of novel biosensor. The innate biocompatibility and tunable permeability of hydrogels is exploited in many applications for *in vivo* sensing. Baxamusa et al. deposited ultrathin films of poly(hydroxyethyl methacrylate) (PHEMA) by photoinitiated chemical vapor deposition (piCVD) onto bare silicon for biosensor applications [9]. The mesh size was engineered to allow only small molecules to permeate with the exclusion of proteins that would otherwise adhere to the silicon. The coated sensor demonstrated 8-times less adhesion of bovine serum albumin (BSA) than the bare silicon surface. This piCVD method allowed the application of thin hydrogel films over sodium-sensing optodes without degradation of their response time or sensitivity.

2.3 Recent Trends: The State of the Technology

2.3.1 Optical Biosensors

Bowman et al. have used polymerization-based amplification to detect proteins and other biomolecules. Their method involves selective polymer formation only when the biomolecule of interest is present. Recently, they fabricated a novel biosensor to detect avian flu [10]. First, the sensor surface functionalized with antibody was exposed to a solution containing the analyte of interest and an antibody-functionalized photoititiator. This resulted in the photoinitiator being bound to the substrate only when the analyte was present. Next, a monomer solution was introduced, and the sensor was exposed to UV light. Crosslinked hydrogel formed only when flu nucleoproteins were present. The hydrogel was visually apparent, making this simple assay one which requires no additional equipment to interpret the readout.

These sensors are particularly well suited for use in resource poor settings around the world for many reasons. They are inexpensive and robust. The photopolymerization is initiated by UV light that is easily sourced from the sun worldwide. Finally, optical biosensors whose outputs are designed to be readout by the unaided human eye, such as the one described above, is essential in third-world biosensing since additional equipment would not be available. It is important to note that the above-mentioned characteristics that benefit resource poor settings would also be beneficial in many point of care sensing devices.

Many hydrogel-based biosensors rely on a change to the equilibrium swollen volume of the hydrogel to measure chemical or biomolecular changes in the sensing environment. One such example is an optical sensor fabricated by Tierney et al. [11]. Hydrogel was adhered to the end of an optical fiber from which very sensitive swelling changes could be measured. Light was reflected at the fiber/hydrogel and hydrogel/liquid interfaces, and the difference in that length was measured and correlated to hydrogels swelling. Tierney et al. measured an acrylamide-based hydrogel at the end of the fiber with a precision of 2 nm.

The very small hydrogel volumes utilized with this responsive hydrogel and fiber-optic transducer are critical for sensor performance. Sensor response times are limited by diffusion into and out of the hydrogel. With the fiber optical transducer free swelling dynamics can apply and the transducer causes no delay in sensor response. The choice of an optical fiber transducer is beneficial to the sensor's response time.

Biosensing arrays are of particular interest in the field of hydrogel-based biosensor. It is commonly proposed to produce diverse sensing arrays by photopolymerizing many different hydrogels onto the same substrate, such as silicon, forming complex biochips. Covalent adhesion of each hydrogel to a specific location on the substrate makes it possible to track the response of each hydrogel throughout testing. Meiring et al. offered an alternative to this complex method of biochip fabrication [12]. Instead of adhering the hydrogels to a common substrate, Meiring simply fabricated individual hydrogel disks with a

coding system of dots. The identity of each hydrogel disk sensor was determined using pattern-recognition software. A 98% recognition accuracy was demonstrated with nondefective sensors. This new method for generating arrays of hydrogels for biosensing would be beneficial for quick and inexpensive biochemical testing.

There is a trend in hydrogel-based biosensors to enable visual output that can be read with the unaided eye. One type of output that is particularly useful in this manner is a hydrogel that simply changes color. A dye used to optically monitor pH was covalently bound within the hydrogels allowing for significant color changes to be observed [13]. Fluorescent dyes are also commonly immobilized within a hydrogel network. A shift in the wave length of fluorescence and the intensity of fluorescence can result from interactions between biomolecules and fluorescent molecules within the swollen hydrogel [14].

Another method to utilize fluorescence in optical biosensor involves fluorescence quenching. In one technology, uric acid was immobilized in a polyurethane hydrogel next to a metal-organic probe [15]. Fluorescence was quenched by oxygen to enable continuous optical monitoring. The biosensors produced were stable to 1 month with common interferents. These fully reversible optical biosensors demonstrated significant stability for fluorescence-based monitoring.

2.3.2 Photonic Hydrogel Sensors

Silicon-based photonic sensors have shown much promise for *in vivo* biosensing because of their potential for remote readout through several centimeters of tissue. However, the application of photonic sensor technologies *in vivo* has been limited due to the biocompatibility issues of silicon. Recently, photonic hydrogel sensors have been produced by photopolymerizing the hydrogel within the voids of a silicon photonic sensor. Wu et al. [16] fabricated a sensor to detect cholic acid from a molecularly imprinted photonic hydrogel. The MIP was photopolymerized within the voids of a colloidal crystal array. Then the silica was etched away using hydrofluoric acid to leave only photonic hydrogel. Wu observed a concentration dependent absorbance peak shift with cholic acid, which was not observed with molecular analogs dehydrocholic acid or deoxycholic acid. Additionally, the non-imprinted hydrogel showed no significant peak shift with all three molecules.

Similarly, Asher et al. used physically crosslinked poly(vinyl alcohol) (PVA) to make thermoreversible photonic crystals for sensor applications [17]. PVA was chosen for its biocompatibility and ability to generate thicker volumes than other photopolymerized networks. These networks were chemically modified with carboxyl or amine groups and their diffraction monitored at different pH. A pH-responsive hydrogel photonic sensor was demonstrated.

Maurer et al. fabricated a photonic hydrogel sensors for the detection of cholesterol [18]. A polymerized crystalline colloid array composed of

poly(acrylamide-*co*-glycidyl methacrylate) functionalized with cholesterol oxidase was used to detect biologically significant concentrations of cholesterol in solution. A diffraction peak wavelength shift of 63nm was observed, which showed promise towards use as an optical cholesterol sensor. The stability of this enzyme sensor was tested with thermal and pH variation, storage time, and repeated use.

2.3.3 Nanoparticle-composite hydrogels for sensing

Some hydrogel-based biosensors utilize silver or gold nanoparticles to transduce volume changes of the environmentally-responsive hydrogel. As the volume swelling ratio, q, of the hydrogel increases in response to an external stimuli, the interparticle distance of the nanoparticles increases. The interparticle distance of silver or gold nanoparticles determines the absorbance spectrum of the material. Noble metal nanoparticles have unique optical properties which are described by Mie theory.

In this way, Endo et al. fabricated a novel glucose sensor from silver nanoparticles and pH-responsive hydrogel immobilized with glucose oxidase [19]. Upon exposure to glucose solution, the network swelled, producing a localized surface plasmon resonance (LSPR)-based optical biosensor. The resulting sensor showed excellent selectivity for glucose versus mannitol and sucrose.

2.3.4 Gelation as a Sensing Mechanism

Hydrogel gelation can be utilized as a sensing mechanism in certain biosensors. Knerr et al. utilized a mechanism by which hydrogelation of special peptides occurs only in the presence of zinc [20]. They proposed this hydrogel as a sensing element for sensors which detect toxic levels of zinc pollution. The special peptide sequence which was designed for these bionsensors only folds in the presence of zinc. Thus no hydrogel will form, and the protein will not fold, in an environment without zinc. This concept for the development of novel, bio-based sensors can be extended to a variety of environmental conditions. Special peptides can be designed which undergo folding only when triggered by a wide variety of environmental changes, such as temperature, pH, or ionic strength. In this way, hydrogelation based on special peptides can be utilized as a sensing mechanism in a variety of sensors.

2.3.5 Dual Monitoring from Hydrogel Sensing Element

One method for miniaturizing the sensing elements needed to monitor bioprocessing is the creation of a dual-purpose environmentally-sensitive hydrogel. Kocincova et al. synthesized a hydrogel which was responsive to both pH and oxygen concentration by embedding organosilica microparticles and poly(methacrylic acid)-based microbeads into polyurethane hydrogel [21]. In this way, simultaneous dual monitoring was achieved from one hydrogel. The novel dual-responsive hydrogel was used to monitor bacterial growth rates in culture with the optical readout being based on fluorescence.

2.3.6 Electrical Transducers

Recently, conductive polymers have been incorporated with environmentally-responsive hydrogels to form novel biosensors. Conductive polymers possess delocalized charge along the chain backbone. Similar to their use in semiconductor manufacture, dopants are added to improve the conductivity of the polymer. Conductive polymers based on polyaniline and polypyrrole within crosslinked poly(hydroxyl-ethyl methacrylate) (pHEMA) hydrogels were made biospecific and demonstrated as glucose or urea sensors [22]. A simple transducer which can respond to hydrogen peroxide is beneficial coupled with glucose oxidase and other enzymes.

Research with conductive hydrogels for protein sensing has been conducted in our lab. Bayer and Peppas have utilized polyaniline (PANI) doped with a polymer acid for the purpose of transducing recognition events within a molecularly imprinted polymer (MIP). It is theorized that charged amino acids within the recognized protein will compete with the polymer acid and cause changes to the conductivity of the material [23]. This method for generating protein-specific sensing materials is particularly desirable because MIPs are inexpensive to synthesize and highly stable. Additionally, it should be possible to synthesize conductive MIPs responsive to a wide variety of different proteins.

Sheppard et al. microfabricated a conductimetric pH sensor by photopolymerizing pH-responsive hydrogel atop planar interdigitated electrode arrays [24]. Copolymers of pHEMA and N,N-dimethylaminoethylmethacrylate

(DMAEMA) crosslinked with tetraethylene diacrylate were used. It was found that the conductivity of the thin hydrogel film changed as the swollen volume of the hydrogel changed in response to environmental pH. The conductivity varied as a result of changes in the ion mobility within the hydrogel. These sensors were most sensitive around the biological pH, about pH 7.4, and demonstrated a linear response over the range of about pH 7 to 8.

2.3.7 Magnetic Transducers

Magnetoelastic sensors are of interest to biosensing primarily for their small size and remote sensing. The sensor is interrogated by a metallic field pulse, and a resulting resonance frequency is measured. Ruan coated a magnetoelastic sensor with a pH-responsive, poly(acrylic acid-co-isooctyl acrylate) hydrogel to measure small mass changes in the material [25]. A pH resolution of 0.02 pH was achieved over the range of pH 4.4 to 8.5. For sensors with approximately 1.4 μm thickness, a response time of 120 seconds was observed.

Building up this work, Zourob et al. synthesized an organophosphorous pesticide sensing element by immobilizing organophosphorous hydrolase within a pH-responsive hydrogel [26]. A magnetoelastic sensor was utilized as the transducer for this sensor as well. The reaction of certain pesticides with organophosphorous hydrolase caused a drop in pH and a change to the volume and elasticity of the hydrogel. The sensor output was monitored wirelessly via

magnetic field, and the sensor was able to detect pesticides of 10^{-7} molar concentrations.

2.3.8 Responsive hydrogel with pressure sensor chips

Several authors have investigated the use of standard pressure sensing chips with environmentally responsive hydrogels to yield novel microsensors. Sorber et al. utilized pH-responsive poly(acrylic acid) (PAA)-based hydrogel with a piezoresistive pressure sensor chip [27]. The authors wanted to better understand the chemical changes within the hydrogel and not just the volume changes that could be transduced by the pressure chip. They used FT-IR to study chemical changes within the hydrogel and found them to be in excellent agreement with the electrical signal from the chip.

Lei et al. also utilized a pressure sensor for the transduction of pH-responsive hydrogel, but their work was particularly interesting since the resulting sensor was capable of wireless monitoring [28]. As with other pressure-based hydrogel sensors, a stiff, porous membrane on one side of the material was required. A thin glass diaphragm was deflected when the hydrogel swelled causing the capacitor plates to become closer together. This resulted in a resonant frequency change which could be sensed remotely. A sensitivity of 1.16MHz/pH was seen over the range 3.0 - 6.5, and a response time of 45 minutes.

2.3.9 Microcantilever-based Sensors

Silicon-based microcantilever beams have received much attention as transducers in MEMS-based sensors. This attention is primarily due to their extreme sensitivity, very small size, and inexpensive microfabrication by methods established in the semiconductor industry. Microcantilevers can generate an optical output via the deflection of a laser beam such as in Atomic Force Microscopy (AFM) (Figure 2.2) or an electronic output utilizing piezoresistive microcantilevers (Figure 2.3). Hydrogels can be polymerized covalently to silicon microcantilevers using self assembled monolayers (SAMs) with appropriate functionality.

Hilt et al. fabricated an ultrasensitive microsensor by micropatterning pH-responsive poly(methacrylic acid) highly crosslinked with poly(ethylene glycol) onto silicon microcantilevers [29]. A single silicon microcantilever was fabricated atop a microwell by etching (Figure 2.4). The hydrogel was selectively polymerized atop the beam using a photolithography mask, and the hydrogel remained adhered to the silicon surface through swelling and deswelling because an organosilane agent was used. The sensor demonstrated a maximum sensitivity of 1e-5/pH unit. The microcantilever-based sensors produced by Hilt et al. were most sensitive in the region just below the biological pH of 7.4.

Microcantilever-based sensors have also been fabricated by photopolymerizing a pH-responsive hydrogel beneath the microcantilever beam. Microcantilevers of 500 μm were used with a maximum deflection of 42 μm

observed at high pH. Lei et al. generated a pH microsensor with a linear deflection in the range of pH 3 to 6 [30]. This linear behavior was not seen in the free swelling hydrogel over the same pH range. An advantage of micropatterning the hydrogel beneath the beam is that it protects the hydrogel which lacks the mechanical strength of the silicon. A disadvantage, however, is that significantly less hydrogel surface area is exposed and thus a slower sensor response time would be expected due to diffusion limitations.

Since the successful transduction of environmentally-responsive hydrogels by microcantilevers has been demonstrate, it may seem that the next logical step would be to employ nanocantilevers for improved sensitivity. Nanomechanical cantilever active probes have been used for ultrasmall mass detection, on the order of picograms [31]. This has been achieved by measuring a shift in the piezoelectrically driven resonance frequency of the nanocantilever, and not by measuring deflection. However, the deflection of microcantilever beams by hydrogel swelling is generated by a uniform force at the interface between the silicon beam and the covalently adhered hydrogel. And thus, it should not be assumed that composite cantilevers, composed of hydrogel and silicon, would directly mimic the mass-based sensitivities observed by nanocantilevers.

2.3.10 QCM-based Sensors

Quartz crystal microbalance (QCM) have been utilized with stimuli-responsive hydrogels to generate novel microsensors for a variety of

environmental conditions. A pH microsensor based on QCM was investigated by Richter [32]. A uniform film on one side of the resonater was generated by spincoating a pH-sensitive polymer mixture and then thermally initiating crosslinking to form a hydrogel. Real-time monitoring in liquid media was achieved with this microsensor. It was concluded that quartz crystal microbalances make excellent transducers for pH-responsive hydrogels, primarily because they utilize thin hydrogel films which generate the fastest responses.

A particularly interesting hydrogel-based QCM sensor was fabricated for nucleotide sensing by Kanekivo et al. [33]. Nucleotide-responsive hydrogels were utilized with QCM as a sensor for nucleotide detection. These hydrogels bound adenosine monophosphate (AMP) or adenosine triphosphate (ATP) both by boronic acid-*cis*-diol complexation and electrostatic interaction between the cationic unit and the phosphate group. A QCM-based sensor was fabricated from dextran hydrogels crosslinked with peptides for the detection of proteases [34]. Different protease/peptide sequence pairs were tested and the systems were found to be rather specific. Very highly crosslinked films, between 25% and 75%, were used. This QCM-based biosensor was particularly interesting because a degradable hydrogel was utilized.

2.3.11 Hydrogels in Sensing Arrays

Hydrogels are an ideal material for use in the fabrication of diverse sensing arrays. Diverse sensing arrays are sometimes referred to as an “electric

tongue" or an "electric nose", and much research has been conducted towards this end. First, hydrogels are amenable to diverse biosensing arrays since they can be easily micropatterned by photolithography and other microfabrication techniques developed by the semiconductor industry. The performance of thin hydrogel films in sensing is almost always superior to that of thicker films. The ability to use very small volumes of hydrogel is critical to the economics of biosensing array fabrication. While traditional monomers tend to be inexpensive, the biomolecules used in many of the responsive hydrogels presented in this chapter are not. The diversity of responsive hydrogels available for fabrication enables a bright future for hydrogels in biosensing and specifically the formation of diverse biosensing arrays.

2.4 Conclusions and the future for hydrogels in biosensing

It is evident that hydrogels have a bright future in the field of biosensing and specifically for the fabrication of microscale biosensors. Hydrogels have grown beyond their early uses as a scaffold for the immobilization of biomolecules and to discourage protein adhesion and promote biocompatilibity of sensors. Now many stimuli responsive hydrogels have been utilized as a direct means of sensing a variety of environmental conditions. A wide variety of techniques have been demonstrated to transform the volume change experienced by stimuli-repsonsive hydrogels into an easy-to-read signal. With the aid of these transducers, hydrogel-based microsensors can generate outputs such as optical, electronic, and magnetic. The author believes that the most

promising application of hydrogels in biosensing will be their use in diverse sensing arrays.

FIGURES

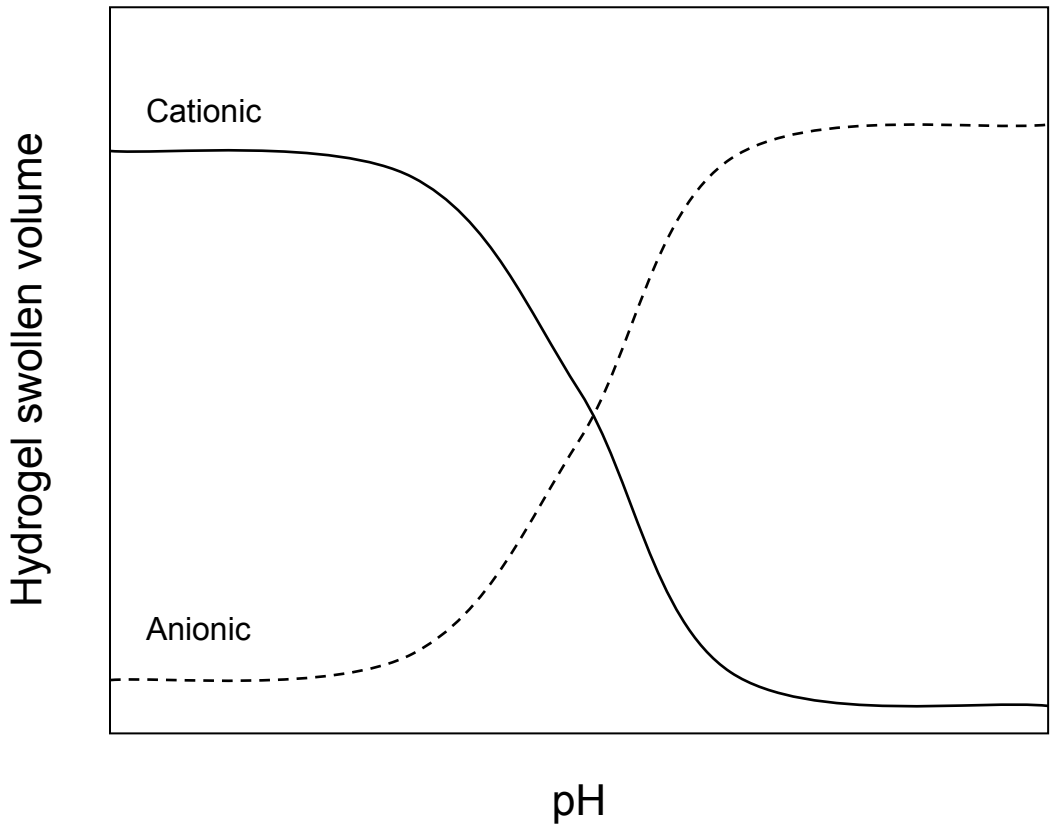

Figure 2.1 Cationic and Anionic pH-responsive hydrogel swelling

Cationic hydrogels are highly swollen at low pH while anionic hydrogels swell greatly at high pH. The pH-responsive swelling in both types is due to repulsion from like-charged polymer chains.

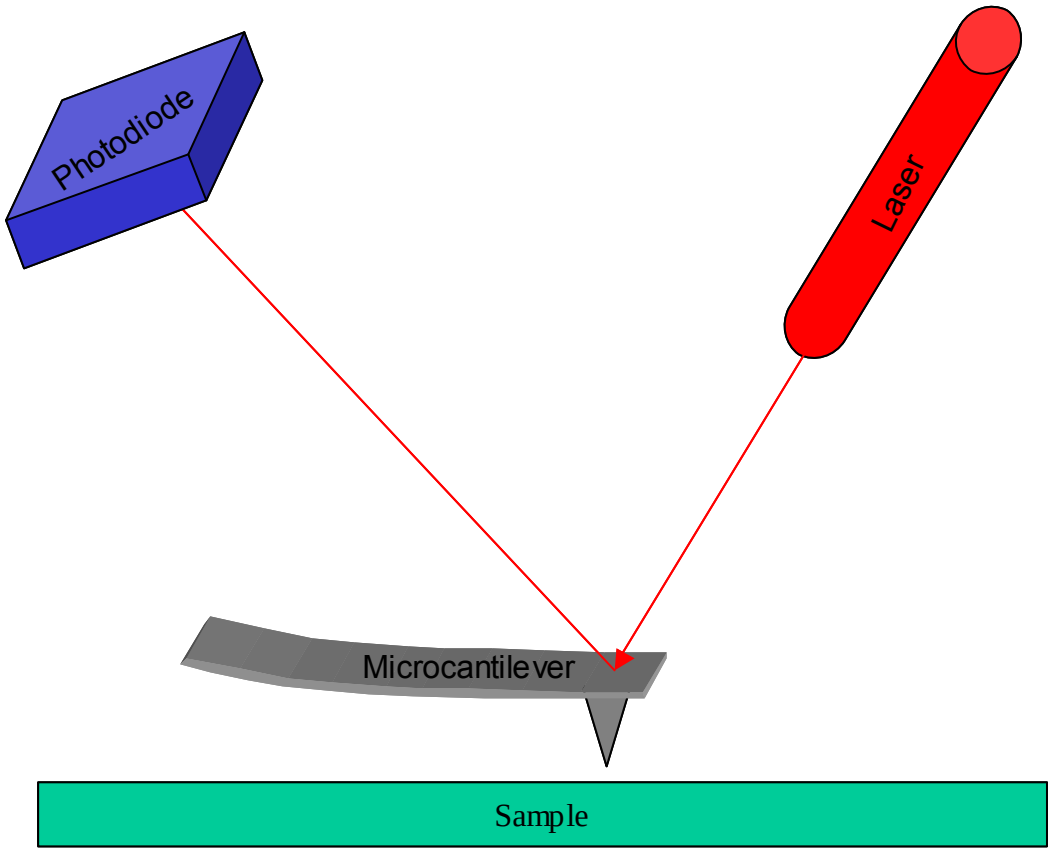

Figure 2.2 Microcantilever's role in Atomic Force Microscopy

In Atomic Force Microscopy, microcantilever beam is deflected as its tip interacts with a sample surface. Microcantilever deflection is measured by a change in the position of a laser beam reflected off the microcantilever onto a photodiode.

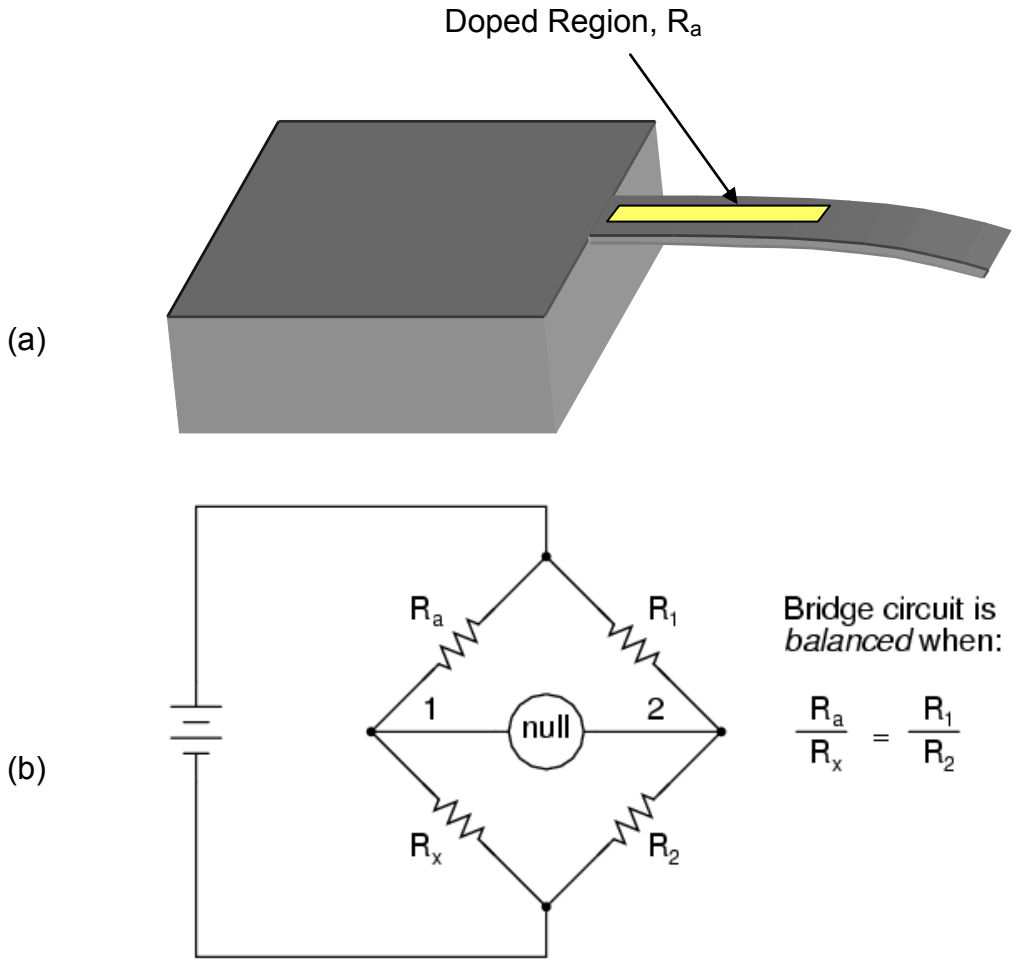

Figure 2.3 Piezoresistive Microcantilevers

Piezoresistive microcantilevers can be used to when an electronic output is desired from microsensors. (a) Piezoresistive microcantilever contains a doped region of resistivity, Ra. (b) A wheatstone bridge is utilized with piezoresistive cantilevers to measure deflection based on changes in resistivity.

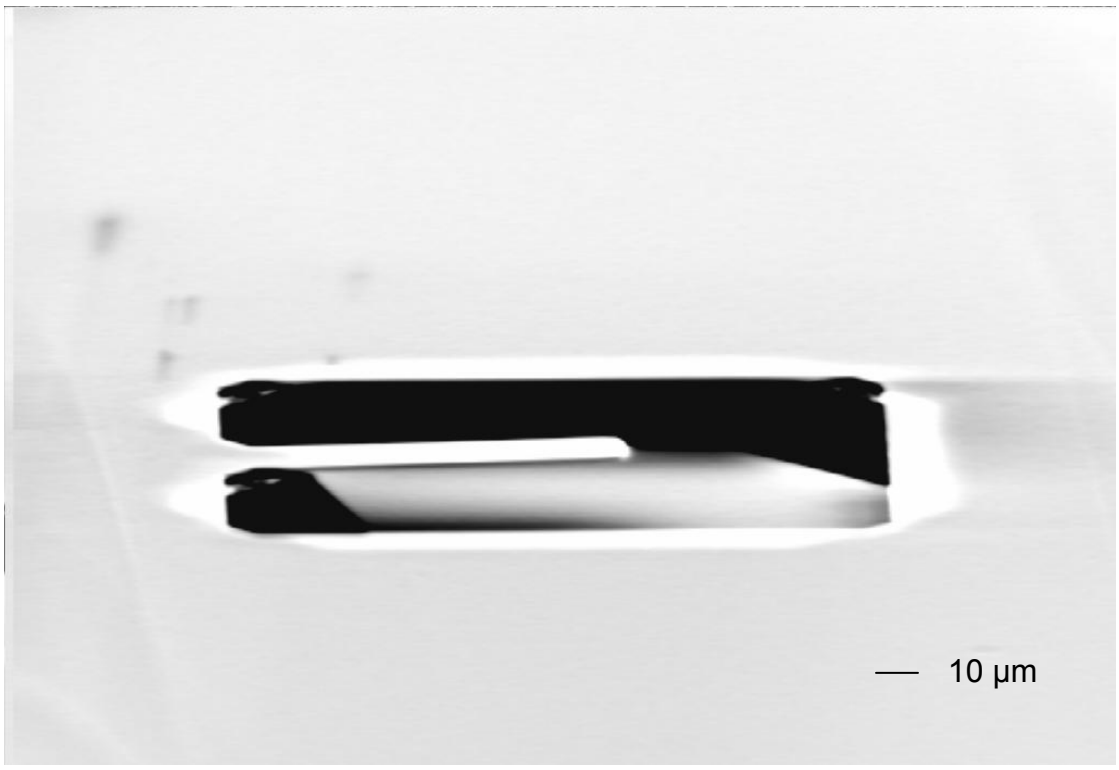

Figure 2.4 Single cantilever with microwell

Silicon was etched to yield a single microcantilever beam of 100 µm length atop a microwell.

REFERENCES

1. Lowman, A.M. and N.A. Peppas, *Solute transport analysis in pH-responsive, complexing hydrogels of poly(methacrylic acid-g-ethylene glycol).* J Biomat Sci-Polym E, 1999. **10**(9): p. 999-1009.
2. Peppas, N.A., et al., *Hydrogels in biology and medicine: From molecular principles to bionanotechnology.* Adv Mater, 2006. **18**(11): p. 1345-1360.
3. Lei, M., et al., *Integration of hydrogels with hard and soft microstructures.* J Nanosci Nanotechno, 2007. **7**(3): p. 780-789.
4. De, S.K., et al., *Equilibrium swelling and kinetics of pH-responsive hydrogels: Models, experiments, and simulations.* J Microelectromech S, 2002. **11**(5): p. 544-555.
5. Richter, A., et al., *Review on hydrogel-based pH sensors and microsensors.* Sensors, 2008. **8**: p. 561-581.
6. Fagerstam, L.G., et al., *Biospecific interaction analysis using surface-plasmon resonance detection applied to kinetic binding-site and concentration analysis.* J Chromatogr, 1992. **597**: p. 397-410.
7. Tang, J., Xiao, P.F., *Polymerizing immobilization of acrylamide-modified nucleic acids and its applications.* Biosens Bioelectron, 2009. **24**(7): p. 1817-1824.

8. Guiseppi-Elie, A., et al., *Enzyme microgels in packed-bed bioreactors with downstream amperometric detection using microfabricated interdigitated microsensor electrode arrays*. Biotechno Bioeng, 2001. **75**(4): p. 475-484.
9. Baxamusa, S.H. et al., *Protection of sensors for biological applications by photoinitiated chemical vapor deposition of hydrogel thin films*. Biomacromolecules, 2008. **9**(10): p. 2857-2862.
10. Sikes, H.D., et al., *Antigen detection using polymerization-based amplification*. Lab Chip, 2009. **9**(5): p. 653-656.
11. Tierney, S., et al., *Determination of swelling of responsive gels with nanometer resolution. Fiber-optic based platform for hydrogels as signal transducers*. Anal Chem, 2008. **80**(13): p. 5086-5093.
12. Meiring, J.E., et al., *Pattern recognition of shape-encoded hydrogel biosensor arrays*. Opt Eng, 2009. **48**(3).
13. Mohr, G.J., et al., *Design of acidochromic dyes for facile preparation of pH sensor layers*. Anal Bioanal Chem, 2008. **392**(7): p. 1411-1418.
14. Thete, A.R. et al., *A hydrogel based fluorescent micro array used for the characterization of liquid analytes*. Anal Chim Acta, 2009. **633**(1): p. 81-89.
15. Schrenkhammer, P., Wolfbeis, O.S., *Fully reversible optical biosensors for uric acid using oxygen transduction*. Biosens Bioelectron, 2008. **24**(4): p. 994-999.
16. Wu, Z., *Direct and label-free detection of cholic acid based on molecularly imprinted photonic hydrogels*, J Mater Chem, 2008. **18**: p. 5452-5458.

17. Asher, S.A., et al., *Enabling thermoreversible physically cross-linked polymerized colloidal array photonic crystals*. Chem Mater, 2008. **20**(24): p. 7501-7509.

18. Maurer, M.K., et al., *Cholesterol oxidase functionalization of a polymerized crystalline colloidal array*. Sensor Actuat B-Chem, 2008. **134**(2): p. 736-742.

19. Endo, T., et al., *Stimuli-responsive hydrogel–silver nanoparticles composite for development of localized surface plasmon resonance-based optical biosensor*. Anal Chim Acta, 2008. **611**(2): p. 205-211.

20. Knerr, P.J., et al., *Zinc-triggered hydrogelation of designed beta-hairpin peptides*. Biopolymers, 2007. **88**(4): p. 639.

21. Kocincova, A.S., et al., *Multiplex bacterial growth monitoring in 24-well microplates using a dual optical sensor for dissolved oxygen and pH*. Biotechnol Bioeng, 2008. **100**(3): p. 430-438.

22. Brahim, S., et al., *Chemical and biological sensors based on electrochemical detection using conducting electroactive polymers*. Microchim Acta, 2003. **143**(2): p. 123-137.

23. Bayer, C.L. and N.A. Peppas, *Advances in recognitive, conductive and responsive delivery systems.* J Control Release, 2008.

24. Sheppard, N.F., et al., *Microfabricated conductimetric pH sensor*. Sensor Actuat B-Chem, 1995. **28**(2): p. 95-102.

25. Ruan, C.M., et al., *A mass-sensitive pH sensor based on a stimuli-responsive polymer*. Anal Chim Acta, 2003. **497**(1): p. 123-131.

26. Zourob, M., et al., *A wireless magnetoelastic biosensor for the direct detection of organophosphorus pesticides*. Analyst, 2007. **132**(4): p. 338-343.

27. Sorber, J., et al., *Hydrogel-based piezoresistive pH sensors: Investigations using FT-IR attenuated total reflection spectroscopic Imaging.* Anal Chem, 2008. **80**(8): p. 2957-2962.

28. Lei, M., et al., *Integration of hydrogels with hard and soft microstructures.* J Nanosci Nanotechno, 2007. **7**(3): p. 780-789.

29. Hilt, J.Z., et al., *Ultrasensitive biomems sensors based on microcantilevers patterned with environmentally responsive hydrogels*. Biomed Microdevices, 2003. **5**(3): p. 177-184.

30. Lei, M., et al., *Integration of hydrogels with hard and soft microstructures.* J Nanosci Nanotechno, 2007. **7**(3): p. 780-789.

31. Salehi-Khojin A., et al., *Nanomechanical cantilever active probes for ultrasmall mass detection*. J Appl Phys, 2009. **105**(1).

32. Richter, A., et al., *Characterization of a microgravimetric sensor based on pH sensitive hydrogels*, Sensor Actuat B-Chem, 2004. **99**(2): p. 579-585.

33. Kanekiyo, Y., et al., *Novel nucleotide-responsive hydrogels designed from copolymers of boronic acid and cationic units and their applications as a*

QCM resonator system to nucleotide sensing. J Polym Sci A1, 2000. **38**(8): p. 1302-1310.

34. Stair, J.L., et al., *Sensor materials for the detection of proteases*. Biosens Bioelectron, 2009. **24**(7): p. 2113-2118.

CHAPTER 3: OBJECTIVES

The advantages of producing environmentally-responsive hydrogel microstructures are well known in the field of stimuli-responsive materials. The most obvious advantage being that the reduced length scales of these materials lead to faster mass transfer and thus chemomechanical response. This faster response is highly desirable in sensing applications. When hydrogel microstructures can be utilized with silicon-based transducers, the fabrication of novel microscale sensors is possible. The mechanical properties of the hydrogel microstructures are improved by their covalent immobilization on silicon substrates.

The overall goal of this research was to fabricate silicon-based microsensors which utilize biodegradable, stimuli-responsive hydrogel networks as the sensing components. This is a step toward the development of *in vivo* biosensors. The specific aims of this research are as follows:

(1) Synthesis and characterization of novel, biodegradable pH-responsive hydrogel networks composed of poly(methacrylic acid) and polycaprolactone.

(2) Investigation of the equilibrium and kinetic pH-responsive swelling and degradation properties of these materials

(3) Fabrication of microcantilever-based sensors which utilize biodegradable, pH-responsive hydrogels and evaluation of their performance as sensors.

(4) Development of theory to allow the prediction of microcantilever-based sensor sensitivity based on bulk hydrogel swelling properties.

(5) Fabrication of biodegradable microsensors composed of pH-responsive hydrogels and porous silicon rugate filters as biodegradable transducers.

Within this body of work, these specific aims have been addressed in multiple chapters. Specific Aim #1 was addressed in Chapter 4. Chapter 5 describes the work completed towards Specific Aims #2. Specific Aims #3 and #4 are both addressed in Chapter 6. Finally, the work to complete Specific Aim #5 was described in Chapter 6. Chapter 7 summarizes general conclusions arrived at through the investigation of all five Specific Aims.

CHAPTER 4: SYNTHESIS AND CHARACTERIZATION OF PH-RESPONSIVE HYDROGELS COMPOSED OF POLY(METHACRYLIC ACID) AND POLYCAPROLACTONE

4.1 Introduction

Hydrogels have special properties that make them ideal materials for applications in the human body. First, the elastic nature of these materials allows them to be implanted *in vivo* with minimal irritation to the surrounding tissues since the implant and the tissue have similar mechanical properties. Second, low interfacial tension between the implanted hydrogel and associated water molecules discourages both cell adhesion and protein absorption to the materials.

Current studies of implantable hydrogels have been directed towards the development of biodegradable systems. A primary advantage of degradable systems is that no secondary surgery would be required to remove the implant [1]. This approach would reduce concerns in third world nations where trained practitioners may implant drug delivery devices during a mass campaign and then leave patients with no properly trained surgeons for follow-up [2].

Hydrogels are water-swollen networks composed of hydrophilic polymers, but prevented from dissolving in water by chemical or physical crosslinks [3]. A common way of producing a biodegradable hydrogel network is by utilizing crosslinks that are biodegradable. Since the crosslinks are the component of the

hydrogel network preventing dissolution of the hydrophilic polymer chains, then as they are cleaved, the network becomes less densely crosslinked with larger mesh sizes until finally full dissolution occurs and no solid phase remains. Biodegradable crosslinks have become popular in the areas of targeted drug delivery and tissue engineering. However, reports on hydrogel systems that are both environmentally responsive and biodegradable are still quite limited [4].

Siepmann and Gopferich [5] give careful consideration to the various terms used to describe biodegradable systems. They draw a distinction between degradation and erosion that will be used in this document. Degradation describes the cleavage of a polymer chain while erosion is material loss from the polymer bulk. Biodegradation and bioerosion are appropriately used to distinguish when a biological system is involved in the processes. Following these definitions, bioerosion can easily be measured gravimetrically while biodegradation can be better shown by demonstrating changes in the molecular weight distribution of polymer chains utilizing gel permeation chromatography (GPC). As crystallinity can greatly influence the degradation and erosion rates of polymeric biomaterials, differential scanning calorimetry (DSC) is another experimental tool of importance in this study.

Certain hydrogels can sense changes in their environment on a molecular level which lead to macroscale changes in the hydrogel's swollen volume. These are commonly referred to as environmentally-responsive hydrogels. Large changes in the swelling ratio of these hydrogels can be observed with changes in

the pH, temperature, ionic strength, nature of the swelling agent, and electromagnetic radiation [6]. Within the category of pH-responsive hydrogels, there are both anionic and cationic.

Anionic hydrogels exist in a collapsed state at low pH and when the pH of the external environment is raised above the pK_a of the gel, they begin to swell. This is due to ionization of the side groups and repulsion of the like-charged chains. The charge repulsion is more powerful than other forces such as hydrogen bonding which exist between the chains in the collapsed state. At the molecular level, this increase in volume corresponds to an increase in the network mesh size (Figure 4.1). Cationic hydrogels show the opposite behavior, which is swelling at low pH and collapsing at high pH.

Our laboratory has extensively studied pH-responsive hydrogels, particularly for applications in intelligent drug delivery. We have applied anionic hydrogels for oral protein delivery. Anionic hydrogels protect the protein from enzymatic degradation and the harsh acidic environment of the stomach and release the protein in the upper small intestines for absorption [7]. Cationic hydrogel nanoparticles have been designed for intracellular delivery. Following endocytosis, the acidic environment of the lysosome causes nanocarriers to swell, disrupting the lysosome, and resulting in release in the cytoplasm [8]. Common ionic polymers employed in this field of study include polyacrylamide, poly(acrylic acid), poly(methacrylic acid), poly(diethyl aminoethyl methacrylate), and poly(dimethyl aminoethyl methacrylate) [9].

Temperature-responsive hydrogels are the most extensively investigated intelligent hydrogels at present, especially in drug delivery systems [10]. Poly(N-isopropyl acrylamide) or PNIPAAm is the most popular temperature-responsive hydrogel for biomedical applications. Perhaps this is because the material's critical point (otherwise known as the upper critical miscibility temperature) is just below the average temperature of the human body, in fact at 32 °C.

It has been suggested that clinical applications of PNIPAAm are limited because this material is not biodegradable. For this reason, Lee and Cheng [10] synthesized PNIPAAm with polycaprolactone crosslinks. These particular crosslinks are advantageous as they are slowly degraded by hydrolysis and catalyzed by enzymes in the body. Also the degradation products are known to be biocompatible. Porous gels were prepared by polymerizing in DMSO below the freezing point. These porous gels showed more rapid degradation when studied *in vitro* in PBS with lipase at 37°C. Lee and Cheng reported 15% degradation, by weight, after 40 days. The swelling and deswelling kinetics were faster with increased porosity as well.

In this chapter, we report on the synthesis and characterization of biodegradable, pH-responsive hydrogels composed of poly(methacrylic acid) and polycaprolactone diacrylate. This particular biodegradable, pH-responsive hydrogel was investigated for several reasons. First, the pK_a of poly(methacrylic acid) is such that small changes just below the biological pH of 7.4 result in a change to the swollen volume of the hydrogel. Since the ultimate application of

these materials is intended for *in vivo* pH sensing, a hydrogel which is pH-responsive over a particular pH range had to be chosen. Second, the choice of polycaprolactone diacrylate as the crosslinker was due to its demonstrated biocompatibility and long degradation time. Finally, the molar feed ratios of poly(methacrylic acid) to polycaprolactone diacrylate were chosen for investigation based on desiring a particular volume swelling ratio for fabricating microcantilever sensors.

The synthesis was done via bulk, UV-photopolymerization to generate thin hydrogel films which were subsequently washed and cut into disks. Hydrogel networks which do not readily undergo hydrolysis were synthesized using poly(ethylene glycol) diacrylate as the crosslinker. These nondegradable materials were studied alongside the degradable ones. Extensive characterization was carried out to better understand the chemical makeup of these hydrogels including FTIR spectroscopy and NMR spectroscopy. Gel permeation chromatography was conducted to enable use of the Flory-Rehner equation and then the network mesh size could be calculated. An Instron was used to analyze the mechanical properties of hydrogels. Such studies were critical for estimating how hydrogels will perform when used as microsensing components in sensors.

4.2 Materials and Methods

4.2.1 Synthesis of Polycaprolactone Diacrylate

Polycaprolactone diacrylate was synthesized for use as a biodegradable crosslinker in these pH-responsive hydrogels [12]. The functional diacrylate ends are necessary so that the polycaprolactone can be UV-photopolymerized into the hydrogel network using a free radical photoinitiator. Polycaprolactone diol (Sigma-Aldrich Inc., St. Louis, MO) was purchased with the following number average molecular weights: 530, 1250, and 2000 Daltons.

In a typical synthesis, 5.0 g polycaprolactone diol with number average molecular weight of 1250 Daltons was added to a 250 mL round bottom flask. The flask was then purged with dry nitrogen to remove water from the system. 40mL of dry benzene (Sigma-Aldrich Inc., St. Louis, MO) was added to the flask via syringe and the mixture was stirred until all polycaprolactone diol was dissolved. 1.22 mL of triethylamine (Sigma-Aldrich Inc, St. Louis, MO) was added. 1 mL of acryloyl chloride (Alfa Aesar, Ward Hill, MA) was added to 5 mL of dry benzene and stirred to form a homogenous mixture. This mixture was added to the reaction flask dropwise over 15 minutes. The reaction flask was placed in a 40ºC oil bath and stirred for 5 hours under nitrogen.

After the reaction was complete, the product was vacuum filtered through P5 filter paper to remove the byproduct precipitate, triethylamine hydrochloride. The polycaprolactone diacrylate product was recovered by adding the filtrate dropwise to excess n-Hexane (Sigma-Aldrich Inc, St. Louis, MO). The precipitate

was recovered and then dried at reduced pressure using a rotary evaporator at 40ºC for at least two hours [10].

4.2.2 Characterization of Polycaprolactone Diacrylate by ^{1}H NMR Spectroscopy

Product purity resulting from the polycaprolactone diacrylate synthesis was analyzed using proton nuclear magnetic resonance spectroscopy. A Varian Mercury 400 was utilized for these studies. Approximately 20 mg of polycaprolactone diacrylate was dissolved in 1 mL of deuterated chloroform ($CDCl_3$) with tetramethylsilane (TMS) for use as an internal reference in the spectra (Cambridge Isotope Laboratories). Polycaprolactone diol was studied in the same solvent for comparison. Spinworks 2.5 software was used to process the data. The appearance of acrylation peaks in the range of 5.8 to 6.5 PPM and integration of these peaks allowed for the calculation of extent of reaction. Consistent purity of polycaprolactone diacrylate was necessary to synthesize consistently crosslinked hydrogel networks.

4.2.3 Preparation of Degradable Hydrogel Films

Thin hydrogel films composed of poly(methacrylic acid) crosslinked with polycaprolactone diacrylate were synthesized according to the following procedure. Polycaprolactone diacrylate and methacrylic acid (Sigma-Aldrich Inc., St. Louis, MO) were added to a small glass vial (Figure 4.2). This vial was placed in a warm water bath to aid in the dissolution of the solid polycaprolactone

diacrylate. The ratio of these two monomers was varied to produce hydrogels with 2.5, 5, 10, and 20% by molar feed ratio of crosslinking. The vial was covered in aluminum foil to prevent light from initiating polymerization.

The UV-free radical initiator, 2,2-dimethoxy-2-phenylacetophenone (DMPA, Sigma-Aldrich Inc., St. Louis, MO), was added to the monomer solution at a ratio of 4 percent of monomer weight. A vortex mixer was used to ensure complete dissolution of the initiator. The monomer solution was pipetted between two glass microscope slides separated by a U-shaped Teflon® spacer. Thickness of the Teflon® spacer was varied to change the thickness of the resulting hydrogel thin film. Photopolymerization was initiated by a UV light source of intensity 15mW/cm^2 for 20 minutes. After polymerization, the film was removed from the glass slide construct and washed to remove unreacted monomer in ultrapure water (Milli-Q Plus, MilliPore).

Films were typically cut into disks using a cork borer for further studies. Disks were first dried at 20°C and atmospheric pressure for 24 hours. These dry disks were then placed in a vacuum oven at 30°C for an additional 24 hours. This two stage drying helps to insure no moisture is entrapped in the disk.

4.2.4 Preparation of Nondegradable Hydrogel Films

pH-Responsive hydrogels composed of poly(methacrylic acid) and a crosslinker, which did not undergo degradation by hydrolysis, were synthesized. Methacrylic acid (Sigma-Aldrich Inc., St. Louis, MO) and poly(ethylene glycol) (MW=400) dimethacrylate (Polysciences, Warrington, PA) were added to a small

glass vial. The two monomers were added in a molar feed ratio of 20% crosslinker to methacrylic acid. A solution of 50% ethanol (Sigma-Aldrich Inc., St. Louis, MO) and 50% ultrapure water was added to reach a solvent percentage of 50% by monomer weight.

The UV-free radical initiator, 2,2-dimethoxy-2-phenylacetophenone (Sigma-Aldrich Inc., St. Louis, MO), was added to the monomer solution at a ratio of 5 percent of monomer weight. A vortex mixer was used to ensure complete dissolution of the initiator. This monomer solution was then photopolymerized and cut into disks as described in Section 4.2.3.

4.2.5 Characterization of Poly(methacrylic acid) by GPC

Gel permeation chromatography was used to obtain the average molecular weight and polydispersity of poly(methacrylic acid) in the hydrogel network. To accomplish this, an uncrosslinked polymer sample was prepared by polymerizing poly(methacrylic acid) without any crosslinker but with all other polymerization conditions mimicked as closely as possible. Approximately 2 mg of poly(methacrylic acid) was dissolved in 1 mL of the aqueous mobile phase which consisted of 4:1 0.1 molar sodium nitrate to acetonitrile solution. Dissolved samples were filtered using a 0.22 micron syringe filter before being run through the GPC.

A Waters 2695 Separations Module and Ultrahydrogel columns at 40°C were used for this separation. An injection volume of 50 µL and a flowrate of 1mL/min for a 60 minute elution time were selected. A total run time of 60

minutes was set. Two poly(ethylene oxide) (PEO) standards were run prior to the samples for molecular weight comparison. EmpowerPro software was used to calculate the PEO equivalent molecular weights of the poly(methacrylic acid) samples.

4.2.6 FTIR of Hydrogel Films

Transmission Fourier Infrared Spectroscopy (FTIR) was used to further understand the chemical structure of the hydrogel. A freeze-dried 10 mg hydrogel sample was crushed with 190 mg of potassium bromide using a mortar and pestle for approximately 2 minutes. This crushing time was minimized to reduce the incorporation of water into the sample. The resulting fine powder was pressed into a 13 mm translucent pellet using 18000 psi on a mechanical press. Pellets were stored in a desiccator until use. Spectra were obtained under nitrogen using a Nicolet Magna IR 560 Spectrometer and analyzed using EssentialFTIR software. Each spectrum was obtained from an average of 100 scans. FTIR was performed on freeze-dried samples of uncrosslinked poly(methacrylic acid) and polycaprolactone diol for comparison.

4.2.7 Mechanical Analysis of Thin Hydrogel Films

An Instron was used to determine the tensile stress-strain properties of these hydrogels. Thin hydrogel films were prepared as described in Section 4.2.3 but with thinner Teflon® spacers than were used to generate disks. This synthesis yielded thin films with an approximate thickness of 50 μm. Films were

swollen in buffers of pH 4 and 7 overnight. Samples were prepared using a "dogbone-shape" in accordance with ASTM D412 and a width of 7 mm. This specimen shape was chosen to ensure a break in the gage length and not in the area being gripped.

The pneumatic grips of the Instron were not used as they generated too great a force for the material. The grips were hand-tightened as not to crush the hydrogel [11]. The specimen was removed from the buffer and coated with light mineral oil to discourage drying while testing. Elongation rates of 0.5 mm/min and 3 mm/min were used. Raw data was collected from the Instron including time, extension, and load.

4.3 Results and Discussion

4.3.1 Analysis of Polycaprolactone Diacrylate by ^{1}H NMR Spectroscopy

The H^1 NMR spectrum of polycaprolactone diol is presented in Figure 4.3. Unique hydrogens are labeled with their corresponding peaks by color. The H^1 NMR spectrum of polycaprolactone diacrylate is presented in Figure 4.4. In both spectra, tetramethylsilane (TMS) labels 0 ppm. The peaks between 5.8 – 6.5 ppm are consistent with the successful synthesis of polycaprolactone diacrylate. Three unique hydrogens are visible from the new vinyl groups, H_2C=CH-, added to each end of polycaprolactone. The NMR spectrum shown in Figure 4.4 is in agreement with those previously reported [12].

NMR spectroscopy is a powerful tool since it enables the quantitative analysis of synthesized molecules. The peaks corresponding to polycaprolactone acrylation between 5.8 - 6.5 ppm were integrated. This value was compared to the integrated value of another unique hydrogen peak in polycaprolactone. The theoretical ratio of these hydrogens was compared to the actual ratio of the peaks, and a 72% extent of reaction was calculated. Consistent extent of reaction and purity of polycaprolactone diacrylate was necessary to synthesize consistently crosslinked hydrogel networks.

4.3.2 Gel Permeation Chromatography (GPC) Results

Uncrosslinked poly(methacrylic acid) was analyzed using gel permeation chromatography. The resulting peak was calibrated to poly(ethylene) oxide standards that contained peaks in the range of 636 and 478000 Daltons. Figure 4.5 shows the molecular weight distribution of uncrosslinked poly(methacrylic acid). This is a reasonable approximation for the chain length of poly(methacrylic acid) within hydrogels crosslinked with polycaprolactone diacrylate because the polymerization conditions were made to mimic the crosslinked systems as closely as possible. The number average molecular weight of poly(methacrylic acid) in the crosslinked gel is needed for the theoretical analysis of the materials using the Flory-Rehnher equation. This analysis enables the calculation of crosslinking density and molecular weight between crosslinks.

The shape of the peak in Figure 4.5 is worthy of note. The slight bimodal distribution is likely due to the formation of shorter chains at the beginning of the

photopolymerization. The hydrogels synthesized in this thesis are not purged with nitrogen to remove residual oxygen in monomer solution. Oxygen is a free-radical scavenger in this type of photopolymerization and would cause the formation of shorter chains. However, once the dissolved oxygen is used up, the formation of longer chains commences.

It is necessary to investigate hydrogel materials which have not been purged with nitrogen for fabricating silicon-based sensors. Existing processing facilities, such as ones for the microfabrication of integrated circuits, are not equipped to perform photolithography in an oxygen-free environment. To overcome the limitations of a free-radical scavenger, a larger quantity of initiator is used in all photopolymerizations in this thesis. The number average molecular weight is approximately 50 kDa (poly(ethylene oxide) equivalent).

4.3.3 FTIR Results

FTIR is a useful tool for analyzing the chemical composition of hydrogels. Figure 4.6 shows the FTIR spectrum of poly(methacrylic acid) crosslinked with 20% polycaprolactone diacrylate. For comparison, the spectra of uncrosslinked poly(methacrylic acid) and polycaprolactone diol are included. It is necessary to compare the C-H stretching vibration of methacrylic acid present in both the hydrogel and uncrosslinked poly(methacrylic acid) spectra at 3000 cm^{-1}. The strong peak at 1725 cm^{-1} corresponds to the C=O bond of the ester group in polycaprolactone. [13] Poly(methacrylic acid) shows a similar C=O absorption peak at a slightly smaller wavenumber. Both C=O peaks appears in the hydrogel

spectrum. The polycaprolactone diol and hydrogel spectra show absorption due to ether stretching at 1110 cm^{-1} [12].

A broad O-H peak at greater than 3200 cm^{-1} is present in both the uncrosslinked poly(methacrylic acid) and the hydrogel. A small O-H peak is seen with the polycaprolactone diol since this functionality exists only on the polymer ends. The small peaks present only in the hydrogel spectrum around 1600 cm^{-1} are attributed to a small quantity of C=C stretching. This suggests a small amount of unreacted, functional ends of the polycaprolactone diacrylate remain after photopolymerization [4]. FTIR shows qualitatively that the hydrogel is chemically composed of both poly(methacrylic acid) and polycaprolactone.

4.3.4 Hydrogel Mechanical Analysis Results

Raw data collected from the Instron included time (sec), extension (mm), and load (kgf). The tensile stress was calculated by dividing the load by the initial cross-sectional area of the hydrogel thin film being tested. The initial dimensions of the swollen film were measured using calipers. The tensile strain (mm/mm), α, was calculated by finding the difference between the current length and the initial length and dividing that by the initial length. By definition, Young's modulus, E_1, is the tensile stress divided by the tensile strain.

To obtain this ratio, tensile stress was plotted versus tensile strain in Figure 4.7. At low stress and strain, a linear fit for the data was obtained. The derivative of the fitted linear equation was taken to find the slope of that data at a tensile strain of zero. This value is the Young's modulus of poly(methacrylic

acid) crosslinked with polycaprolactone diacrylate swollen in pH 3.5 and found to be 2.54 MPa. Young's modulus, E_1, is another term for elastic modulus in tension, and helps describe the material's ability to return to its original shape following deformation as a result of a load [14].

The hydrogel analyzed here and used to fabricate microsensors in this thesis are highly crosslinked. Increased crosslinking results in a stiffer hydrogel and a higher Young's modulus. A higher Young's modulus tends to correspond with a lower equilibrium swelling ratio [15].

Young's modulus is one of several elastic moduli, and should not be confused with G, shear modulus, another important property of hydrogels calculated from the stress-strain behavior. Shear modulus is proportional to the molecular weight between crosslinks in a hydrogel network and found using the Mooney-Rivlin equation. The shear modulus and the mechanical strength of a hydrogel is highly dependent on the amount of crosslinking [16]. Shear modulus can be calculated from the Young's modulus if Poisson's ratio is known.

4.4 Conclusions

Hydrogels have many beneficial properties which make them ideal materials for use in the body. A biodegradable crosslinker was synthesized by functionalizing polycaprolactone with acrylate ends to produce a macromer which could undergo free-radical polymerization. The extent of reaction for this synthesis was determined to be 72% by NMR. This particular crosslinker was

chosen for its very slow hydrolytic degradation deemed ideal for the material's use as a microsensing element.

A novel biodegradable, pH-responsive hydrogel was synthesized by UV-free radical photopolymerization from a monomer solution containing methacrylic acid and polycaprolactone diacrylate. The length of poly(methacrylic acid) chains was analyzed using GPC and found to be approximately 50 kDa. FTIR was conducted on samples of polycaprolactone diol, poly(methacrylic acid), and poly(methacrylic acid) crosslinked with polycaprolactone diacrylate. By comparison, the chemical composition of the hydrogel could be well understood. Finally, an Instron was utilized to conduct mechanical testing with thin hydrogel films in their swollen state. Tensile testing yielded a Young's modulus of 2.5 MPa for poly(methacrylic acid) crosslinked with 20 mol percent polycaprolactone diacrylate. Many of these material properties are utilized later in this thesis for specific theoretical analysis.

FIGURES

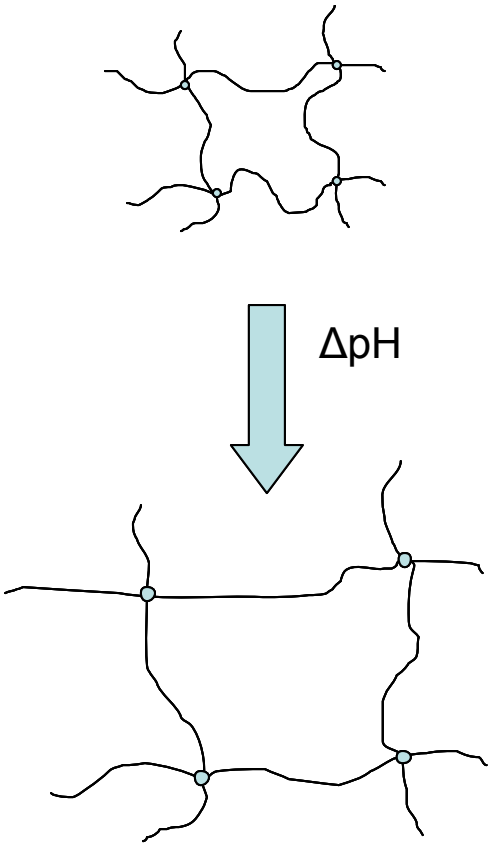

Figure 4.1: Network mesh size change in pH-responsive hydrogels

pH-Responsive hydrogel network where the arrow indicated a pH change across the pK_a of the material. (a) Neutrally charged chains are held together by crosslinking, and (b) like charged chains repel one another to increase the network mesh size

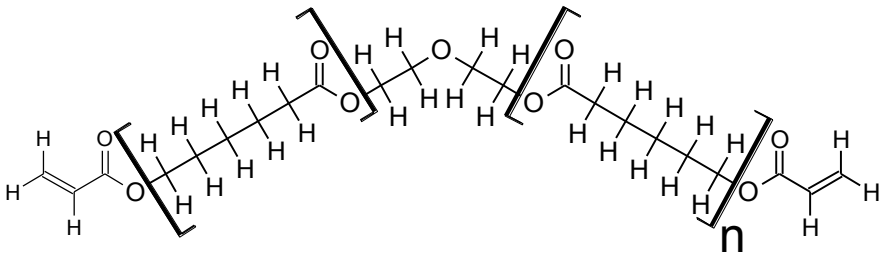

(a)

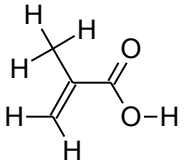

(b)

Figure 4.2: Monomers used in the synthesis of poly(methacrylic acid) crosslinked with polycaprolactone diacrylate hydrogels (a) PCL diacrylate, (b) methacrylic acid

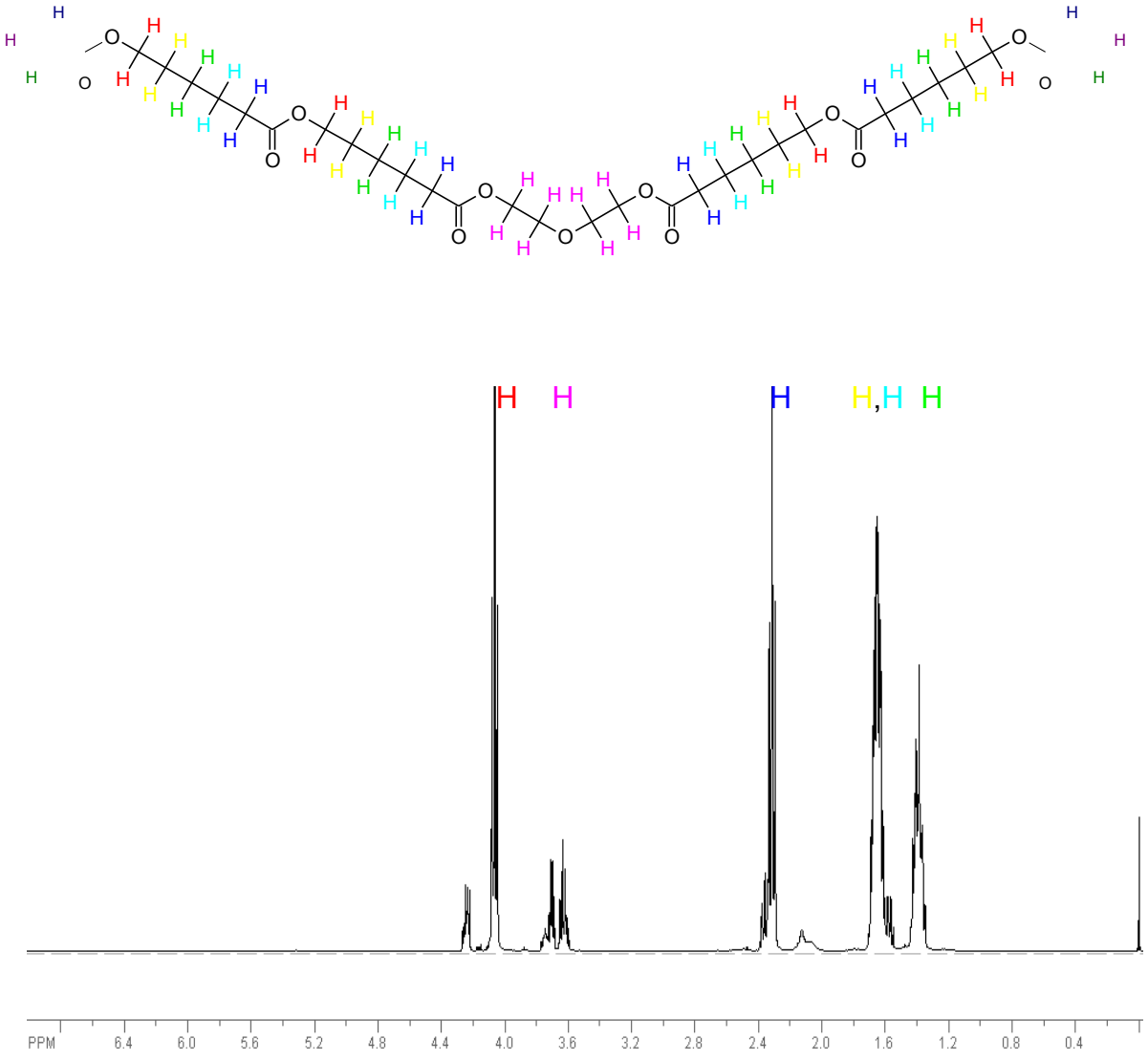

Figure 4.3: H^1 NMR spectrum of polycaprolactone diol (M_n=1250 Da)

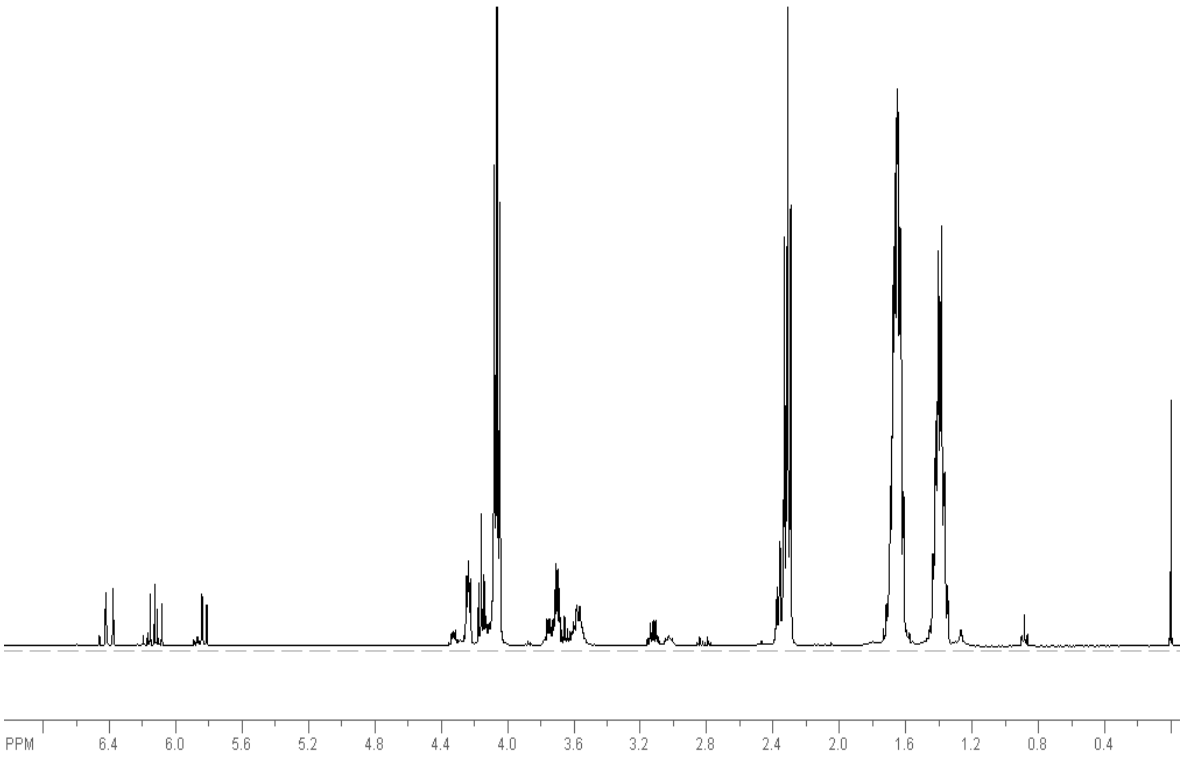

Figure 4.4: H^1 NMR spectrum of synthesized polycaprolactone diacrylate

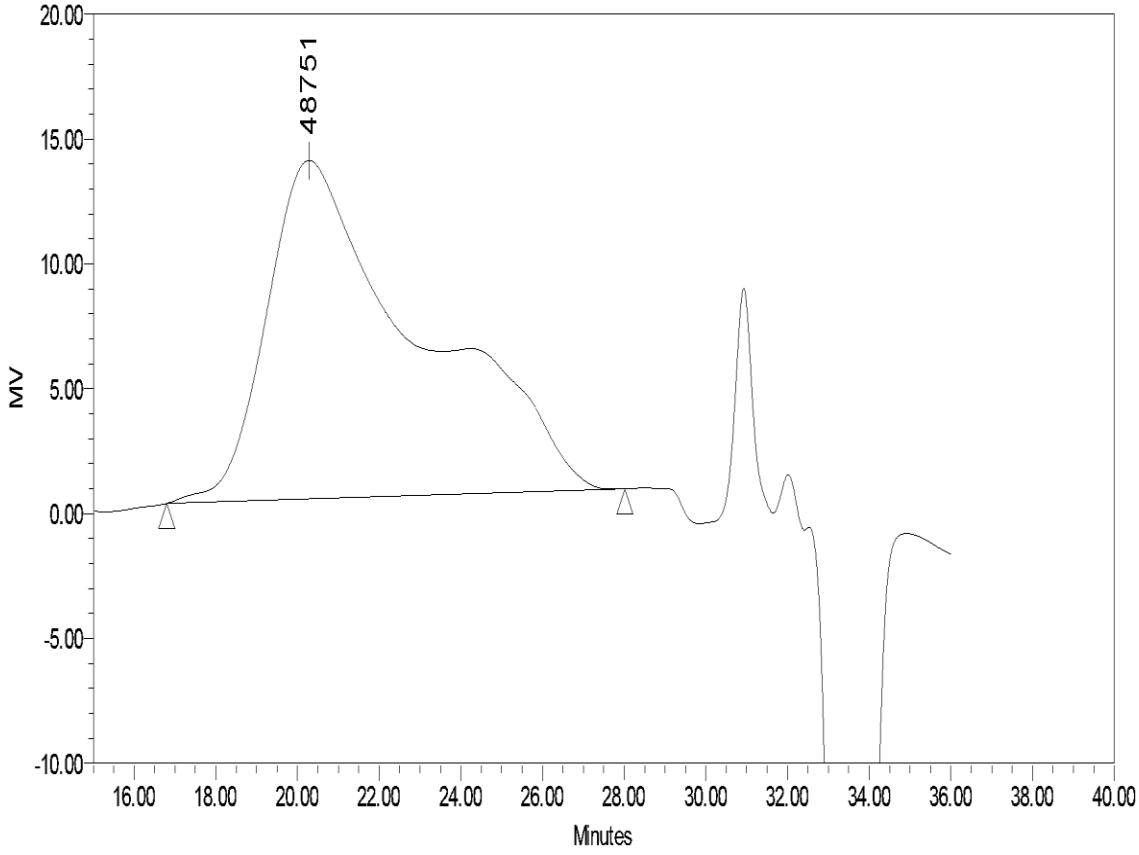

Figure 4.5: GPC of uncrosslinked poly(methacrylic acid) with peak number average molecular weight of approximately 50 kDa.

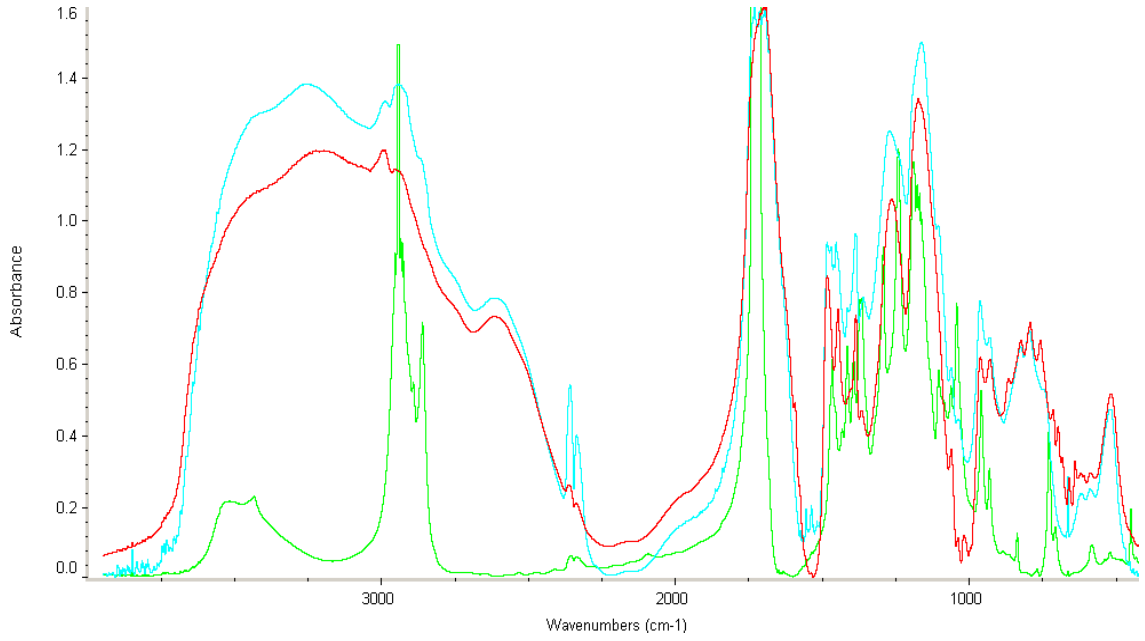

Figure 4.6: FTIR spectra of poly(methacrylic acid) -red-, polycaprolactone diol -green-, and poly(methacrylic acid) crosslinked with polycaprolactone diacrylate -blue-

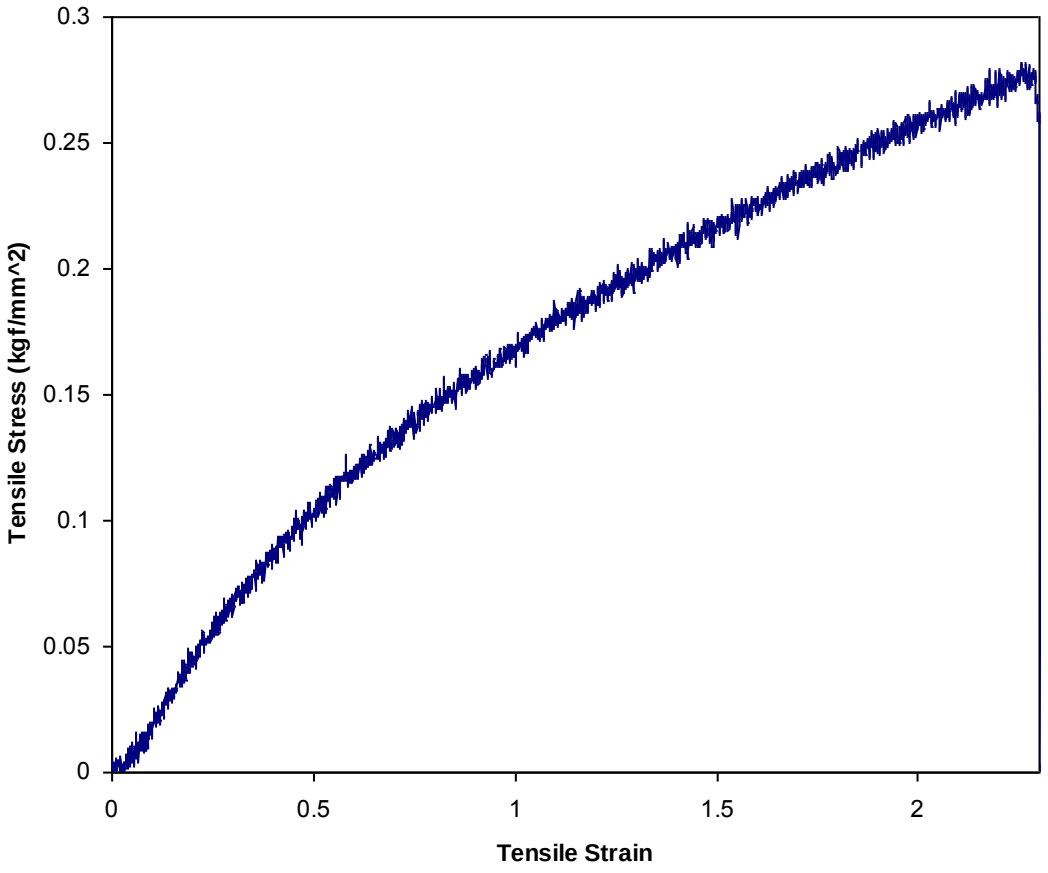

Figure 4.7: Tensile stress versus tensile strain data for poly(methacrylic acid) crosslinked with 20% polycaprolactone diacrylate at pH 3.5.

REFERENCES

1. Peppas, N.A., et al., *Hydrogels in pharmaceutical formulations.* Eur Journal Pharm Biopharm, 2000. **50**(1): p. 27-46.
2. Hull, T.H., *The challenge of contraceptive implant removals in east Nusa Tenggara, Indonesia.* Int Fam Plan Perspec, 1998. **24**(4): p. 176.
3. Lowman, A.M. and N.A. Peppas, *Solute transport analysis in pH-responsive, complexing hydrogels of poly(methacrylic acid-g-ethylene glycol).* J Biomat Sci-Polym E, 1999. **10**(9): p. 999-1009.
4. Chao, G.T., et al., *Synthesis, characterization, and hydrolytic degradation behavior of a novel biodegradable pH-sensitive hydrogel based on polycaprolactone, methacrylic acid, and poly(ethylene glycol).* J Biomed Mater Res A, 2008. **85A**(1): p. 36-46.
5. Siepmann, J. and A. Gopferich, *Mathematical modeling of bioerodible, polymeric drug delivery systems.* Adv Drug Deliver Rev, 2001. **48**(2-3): p. 229-247.
6. Peppas, N.A., et al., *Hydrogels in biology and medicine: From molecular principles to bionanotechnology.* Adv Mater, 2006. **18**(11): p. 1345-1360.
7. Carr, D.A. and Peppas, N.A., *Assessment of poly(methacrylic acid-co-N-vinyl pyrrolidone) as a carrier for the oral delivery of therapeutic proteins using Caco-2 and HT29-MTX cell lines.* J Biomed Mater Res A, 2010. **92A**(2): p. 504-512.

8. Fisher, O.Z., et al., *Enhanced core hydrophobicity, functionalization and cell penetration of polybasic nanomatrices*. Pharm Res, 2009. **26**(1): p. 51-60.
9. Peppas, N.A., *Hydrogels*, in *Biomaterials Science*, A.S.H. Buddy D. Ratner, Frederick J. Shoen, Jack E. Lemons, Editor. 2004, Elsevier: San Diego, California.
10. Lee, W.F. and T.S. Cheng, *Studies on preparation and properties of porous biodegradable poly(NIPAAm) hydrogels.* J Appl Polym Sci, 2008. **109**(3): p. 1982-1992.
11. Instron Material Testing Solutions, Grip Solution for Testing Polymer Hydrogels, 12-14-2009. http://www.instron.us/wa/solutions/Polymer_ Hydrogels_Testing_Grip_Solution.aspx
12. Kweon, H., et al., *A novel degradable polycaprolactone networks for tissue engineering.* Biomaterials, 2003. **24**(5): p. 801-808.
13. Zhu, Y., et al., *Surface modification of polycaprolactone with poly(methacrylic acid) and gelatin covalent immobilization for promoting its cytocompatibility*. Biomaterials, 2002. **23**(24): p. 4889-4895.
14. Green Book, *IUPAC Quantities, Units and Symbols in Physical Chemistry*. Second Edition, 1993. Oxford: Blackwell Scientific Publications.
15. Li, H. and Luo, R., *Modeling and characterization of glucose-sensitive hydrogel: Effect of Young's modulus.* Biosens Bioelectron, 2009. 24(12): p. 3630-3636.

16. Anseth, K.S., et al., *Mechanical properties of hydrogels and their experimental determination*. Biomaterials, 1996. **17**: p.1647-1657.

CHAPTER 5: SWELLING AND DEGRADATION STUDIES OF HYDROGELS COMPOSED OF POLY(METHACRYLIC ACID) AND POLYCAPROLACTONE

5.1 Introduction

A polymer's degradation rate is of paramount importance in biomedical applications. In drug delivery systems, polymeric degradation can control the rate of drug release. Degradation rates are important in tissue engineering applications since it must be matched with the cell growth rate to be effective. Polycaprolactone is an appealing material for biomedical applications because it is biocompatible and its low glass transition temperature makes it flexible at physiological temperatures [1]. Its use has been limited due to very slow hydrolytic degradation rates, reported to be greater than 24 months [2]. To overcome this, polycaprolactone is often copolymerized with other aliphatically degraded esters such as poly(glycolic acid) or poly(lactic acid) to disrupt the crystallinity [1].

It is well known that polycaprolactone degradation by hydrolysis (Figure 5.1) is both acid and base catalyzed. Polycaprolactone does not undergo autocatalysis despite degradation to the acidic reaction product, carboxylic acid, when it undergoes hydrolytic degradation. This is attributed to the high crystallinity of the material and thus very slow reaction times since degradation is restricted to the surface. Crosslinked polycaprolactone systems show

significantly lower crystallinity than linear polycaprolactone chains which have not been polymerized into a three-dimensional network. It is well known that lower crystallinity yields much faster degradation [3].

Another method for accelerated degradation of a polycaprolactone crosslinked hydrogel was reported by Kim and Bae [4]. They showed rapid degradation of a polyoxyethylene/polycaprolactone multiblock copolymer by increasing the temperature. The copolymer formed a physical hydrogel which was disrupted by the additional heat. In vivo studies were performed with this hydrogel implanted in a mouse and the mouse receiving minutes of infrared radiation per day. A significant decrease in the mass of the implant was seen in the mouse which was irradiated. The implants were removed after 60 days, and only 20% of the implant remained versus 60% in the control. This study shows the importance of controlling the crystallinity of polycaprolactone in any hydrogel when the goal is a controlled biodegradation time. Additionally, these results show promise towards hydrogel-based devices in the body whose degradation rate could be tuned after implantation, which would be an important step towards patient-specific medicine.

Degradation of polycaprolactone is also accelerated by enzymes. Anseth et. al. reported accelerated degradation in a hydrogel consisting of poly(ethylene glycol) and polycaprolactone when incubated with lipase [5]. Usually hydrogels are assumed to undergo bulk degradation with cleaved crosslinks present at a uniform concentration throughout the gel (Figure 5.2). Bulk hydrolytic

degradation results in a decrease in the crosslinking density, and thus volume swelling ratio, Q, of the hydrogel. However, in an enzymatic degradation, the large biomolecule must diffuse into the matrix to cleave internal bonds. For this reason, degradation should proceed more rapidly at the surface initially.

Mathematical treatment of enzymatic degradation of hydrogels is more complicated than hydrolytic cleavage. In these hydrogel networks with degradable crosslinks, each crosslink must be cleaved at two points and then the oligomer must diffuse out of the hydrogel matrix to contribute to mass loss. The rate of mass loss was dependent on the percentage of caprolactone in the hydrogel and the amount of lipase in solution. Complete degradation of this hydrogel network was shown in a 1.0 mg/mL lipase solution in less than one week [5].

Chao and Wei recently reported a pH-responsive hydrogel consisting of poly(methacrylic acid) and crosslinked by both poly(ethylene glycol) and polycaprolactone [6]. The swelling ratio of this novel material in aqueous buffers of 1.2 and 7.2 pH was reported as a function of time. The material swelling increases about 12% in the low pH buffer and 250% in the high pH buffer versus a dry gel. A hydrolytic degradation study with the material shows mass losses after 30 days in buffers of pH 1.2 and 12 between 5-14% and 5-38% respectively. The wide ranges in the reported values of mass loss are attributed to different feed ratios of the polycaprolactone, poly(ethylene glycol) and

methacrylic acid. No data from these degradation studies were shown past 30 days.

Mathematical modeling of the degradation profile of biodegradable and bioerodible polymers is quite developed due to their applications in drug delivery and tissue engineering. True biodegradation models are very complicated because they must combine transport phenomena and chemical reaction kinetics. For these reasons, empirical models are often utilized rather than mechanistic ones [7]. Polycaprolactone degradation by hydrolysis using an external acid catalyst was modeled using pseudo-first-order kinetics [8].

To better understand the kinetic response of hydrogel-based sensors, we must first understand the kinetic response of the hydrogel itself. The swelling and shrinking of hydrogels requires first transport of the stimulus into the network and, second, transport of the water into or out of the network [9]. An interesting complexity in this system is that shrinking of the gel can generally occur more rapidly than its swelling. The characteristic time of the response in a hydrogel sensor is dependent on the square of the distance, so the hydrogel thickness should be as small as possible [10]. This is why microfabrication techniques are being enthusiastically investigated with hydrogels.

It is interesting to note that the type of transducer can further slow the kinetics of the sensor. If the method of transduction is based on measurement of the changes of the optical transparency or conductivity of the material, then free swelling kinetics can apply. If the volume change of the gel must be transduced

mechanically, such as by the use of microcantilevers, then the sensor will be inherently slower. The external force required slows the sensor performance versus our free swelling models [10].

Within this thesis, the proposed strategy for generating pH-responsive hydrogel networks which are also biodegradable is to utilize hydrolytically cleavable polycaprolactone diacrylate crosslinkers. The choice of polycaprolactone was due to its very slow degradation rate and previous FDA approval in implantable devices. In this chapter, it is shown how the degradation of the crosslinks changes the volume swelling ratio, Q, of the hydrogel. Since the Q is a characteristic parameter of these materials that is later transduced by microcantilever beams to generate novel pH microsensors as shown in this dissertation, it is essential that we understand the change of Q with time. Another important aspect of studying the degradation of these materials is the analysis of resulting byproducts. If these materials are to be utilized as sensing element for *in vivo* microsensors, it is necessary to evaluate the degradation products and understand how these polymers can be cleared from the body.

The primary purpose of studying the swelling of hydrogel disks is to anticipate their behavior as microsensing components. For instance, the pH sensing range expected from a microsensor with a hydrogel sensing element can be estimated by the pH range over which a disk of that hydrogel changes in volume. While the equilibrium swollen volume of a hydrogel disk is certainly different than the same hydrogel as a thin film covalently bound to a silicon

surface, it is useful to study both to anticipate and model sensor performance. Perhaps the least useful of these bulk hydrogel studies concern the kinetic swelling behavior. These studies were only used to provide conservative equilibration times for studying sensor behavior at equilibrium.

Polycaprolactone is biodegraded and utilized as a carbon source by a multitude of microorganisms present throughout the natural world. Enzymes which occur naturally to degrade cutin and lipids can cleave polycaprolactone [11]. Examples of such enzymes include cutinases, which enable fungal phytopathogens to break through the protective layer, cutin, of plants [12]. Currently, research is being conducted to engineer better enzymes to hydrolyze polycaprolactone. A bacteria known to degrade polycaprolactone underwent UV irradiation and a mutant was selected to hyper-produce polycaprolactone depolymerase [13].

5.2 Materials and Methods

5.2.1 Equilibrium Swelling Studies

Dry hydrogel disks were weighed. Each disk was placed in a separate 50 mL centrifuge tube. To the tube, approximately 45mL of phosphate-citrate buffer solution was added. This buffer system was chosen for its wide pH range of 2.2 to 8.0 [14]. Stock solutions were prepared of 0.2M dibasic sodium phosphate (Sigma-Aldrich Inc., St. Louis, MO) and 0.1M citric acid (Sigma-Aldrich Inc., St.

Louis, MO). Potassium chloride was added to control the ionic strength of all buffers to be a constant 0.5 M. The pH of each buffer was measured using a pH probe.

Disks were allowed to equilibrate with the buffer solution for 24 hours at 20°C. Disks were removed, blotted with a Kimwipe, and massed to obtain their swollen weight. Equilibrium swelling studies were conducted in triplicate.

5.2.2 Dynamic Swelling Studies

5.2.2.1 From Dry State

Dry hydrogel disks were weighed. Each disk was placed in a separate 50 mL centrifuge tube. To the tube, approximately 45 mL of phosphate-citrate buffer solution was added. Buffers were prepared as described in Section 5.2.1. Disks were left to swell for a set amount of time, typically 15 - 30 minutes at 20°C. Disks were removed, blotted with a Kimwipe, and massed to obtain their swollen weight. Then disks were replaced in the buffer to continue with the swelling study. Dynamic swelling studies were conducted in triplicate.

5.2.2.2 From Swollen State

Dry hydrogel disks were weighed. Each disk was placed in a separate 50 mL centrifuge tube. To the tube, approximately 45 mL of pH 7.4 phosphate-citrate buffer solution (I = 0.5 M) was added. Disks were swollen in buffer for 24 hours to ensure they reached their equilibrium swollen volume. The buffer in each test tube was changed to a pH 4.8 buffer at time zero. Disks were

removed, blotted with a Kimwipe, and weighed to obtain their swollen weight at set intervals. Disks were replaced in the buffer to continue with the swelling study after weighing.

5.2.3 Hydrogel Degradation Studied Gravimetricaly

Dry hydrogel disks were massed. Each disk was placed in a separate 15 mL centrifuge tube. To the tube, approximately 14 mL of phosphate buffered saline (PBS) solution (Sigma-Aldrich Inc., St. Louis, MO) was added. Centrifuge tubes were placed in a 37°C shaken bath. The solution in each centrifuge tube was replaced weekly with fresh PBS. Before discarding, the pH of the PBS was measured to ensure it had provided adequate buffering to maintain the environmental pH of the degrading material at pH 7.4 for the previous week. At predetermined time intervals, disks were removed from the buffer, blotted with a KimWipe, massed, and returned to the centrifuge tube to continue with the degradation study.

Hydrogel disks were prepared with a nondegradable, PEG-based crosslinker for comparison in this study. Swollen volumes of all disks were measured periodically over the course of 6 months. After 6 months, the disks no longer had the mechanical integrity to continue with this type of study.

5.2.4 Hydrogel Degradation using Gel Permeation Chromatography

Hydrogel disks composed of poly(methacrylic acid) crosslinked with 2.5 mole percentage polycaprolactone diacrylate were swollen in phosphate-citrate

buffer solution of pH 2.9 and 20°C for approximately one year. This acidic buffer was chosen to accelerate degradation due to the fact that cleavage of polycaprolactone by hydrolysis is an acid catalyzed reaction. After one year, the hydrogel disk was no longer visible within the solution indicating that the crosslinkers had been cleaved by hydrolysis and that what remained of the hydrogel network now existed as polymer chains dissolved in the buffer solution.

The buffer with dissolved polymer chains was then lyophilized. A white powder composed primarily of salts from the buffer remained. This powder was washed with acetonitrile to selectively remove the polymer chains for further analysis. The polymer chains obtained from this extraction were analyzed using Gel Permeation Chromatography. The conditions and columns for this analysis are as describe in Section 4.2.4.

5.3 Results and Discussion

5.3.1 Equilibrium Swelling Results

The swelling behavior of hydrogels composed of poly(methacrylic acid) crosslinked with varying mole percentages of polycaprolactone diacrylate was studied gravimetrically. This method allowed a 24 hour equilibration time for hydrogel disks with phosphate-citrate buffer solutions of varying pH and consistent ionic strength. The weight swelling ratio, q, was found for hydrogels

over the range of 3.2 to 7.8 pH (Figure 5.3). The weight swelling ratio was found by dividing the swollen weight by the dry weight of thin hydrogel disks.

The weight swelling ratio of poly(methacrylic acid) hydrogels crosslinked with 5, 10, and 20% polycaprolactone diacrylate did not differ significantly at pH 4 and below. The 2.5% crosslinked hydrogel was found to swell about 50% more at these low pHs. At pH 7.4, the weight swelling ratio of the hydrogels varied from 6.2 to 2.4 (Table 5.1). Lower percent crosslinking always resulted in a higher q at pH 6 and above. Table 1 also compares $q_{7.4}/q_{3.2}$, the ratio of the weight swelling ratio,q, at pH 7.4 to that at pH 3.2. The highest $q_{7.4}/q_{3.2}$ was 4.5 for poly(methacrylic acid) crosslinked with 5 mol percent polycaprolactone diacrylate.

The swelling ratio of a material is a very important parameter for the use of hydrogel sensing components in silicon-based devices. In the case of a hydrogel thin film adhered to a silicon substrate with a self assembled monolayer (SAM), a q that is too high will result in delamination of the thin film. Based on previous work [15] and the results presented in Chapter 6, a q at pH 7.4 of around 2.5 is desirable with microcantilever sensors.

Table 5.1 not only compared different crosslinking percentages but also different crosslinker lengths. While it might seem intuitive that a shorter crosslinker would yield a lower q at pH 7.4 if percent crosslinking were kept constant, that was not the case here. This is likely a result of polycaprolactone diacrylate being less hydrophilic than poly(methacrylic acid). While the

crosslinking percent was kept constant at 20%, the incorporation of crosslinkers with polycaprolactone of 1250 Dalton molecular weight resulted in more of the hydrophobic crosslinker by weight in the hydrogel, and thus less swelling in aqueous solutions. If a more hydrophilic crosslinker were used in the synthesis of a similar array of hydrogels, it is expected that a shorter crosslinker would yield a lower weight swelling ratio, q, at pHs above the pK_a of the material.

It is known that by incorporating hydrophobic or hydrophilic monomers into pH-responsive hydrogels the pK_a of the material can be shifted. In an anionic, pH-responsive material, the incorporation of a more hydrophobic crosslinker, such as PCL diacrylate would cause the pK_a to shift higher. In a cationic, pH-responsive hydrogel, the opposite is true. A PCL diacrylate crosslinker would shift the pK_a lower. The hydrophilicity of the crosslinkers of a hydrogel network can shift the thermodynamic equilibrium of the material.

A shift in the pK_a of hydrogels is often desirable. In this thesis, pH-responsive hydrogel thin films are utilized as sensing components in silicon-based microsensors. The range over which hydrogels can provide sensing corresponds with the pH range over which the degree of ionization of the carboxylic acid groups, and thus overall negative charge of the polymer chains, is changing [16]. Since pH-responsive hydrogels experience a dramatic change in their swollen volume around the pK_a of the material, the ability to shift the pK_a of the hydrogel corresponds with the ability to shift the sensing range of a resulting sensor.

A potential application for biodegradable, pH-microsensors *in vivo* is to diagnose acidosis in transplanted tissues. Research has shown that a drop in pH is one of the first indications that a transplanted tissue is not being sufficiently profused with blood [17]. Without a sufficient blood supply, acidic products of cell metabolism such as lactic acid accumulate and cause a drop in pH in this microenvironment. If this condition were diagnosed quickly, a follow-up surgery could be conducted to remedy the problem. Since human tissues are of a very limited in supply, it is desirable to monitor transplanted tissues and ensure they survive. A biodegradable, hydrogel-based microsensor to detect tissue acidosis would need a sensing range to detect small pH changes just below the biological pH of 7.4.

Since it was desired to create a sensor which would have its maximum sensitivity just below pH 7.4, hydrophobic crosslinkers were incorporated with poly(methacrylic acid) to shift the pK_a higher. The pK_a of the hydrogel was found by fitting the swelling data versus pH (Figure 5.3) with a hyperbolic tangent. The inflection point was found by setting the second derivative of the fitted equation equal to zero. As predicted, the pK_a was found to increase with polycaprolactone diacrylate crosslinking. The shift in pK_a was approximately 0.3 pH units from pH 5.7 for poly(methacrylic acid) crosslinked with 2.5 mol percent polycaprolactone diacrylate to pH 6.0 for 20 mol percent crosslinking. This shift is shown in Figure 5.3 by labeling the pK_a of hydrogels with 2.5% and 20% crosslinked with vertical lines.

5.3.2 Dynamic Swelling Results

The dynamic behavior of pH-responsive hydrogels composed of poly(methacrylic acid) crosslinked with polycaprolactone diacrylate was studied. Figure 5.4 shows the change of the weight swelling ratio, q, when hydrogel disks swollen to equilibrium in phosphate-citrate buffer of pH 7.4 (I=0.5M) were placed in pH 4.8 buffer. As with the results presented in Figure 5.3, we observed that samples with higher initial crosslinking ratio exhibited the lowest value of q. Hydrogel samples with a 2.5% nominal crosslinking ratio exhibited the greatest change in weight swelling ratio with the pH change tested.

Poly(methacrylic acid) crosslinked with 20 mol% polycaprolactone diacrylate reached its equilibrium weight swelling ratio approximately 45 minutes after the buffer change. The poly(methacrylic acid) crosslinked with 2.5% and 5% polycaprolactone diacrylate did not reach equilibrium values in the timescale of this experiment. The time required to reach equilibrium is an important parameter if these hydrogels will be used in sensors. While the time to equilibrium of a hydrogel thin film is largely dependent on the thickness, this study was conducted to better understand a trend among these materials. The hydrogel with the smallest weight swelling ratio reached a new equilibrium swelling ratio most rapidly due to the smallest quantity of water needing to be expelled from the material. Molecules must diffuse out of the hydrogel network and thus the process is limited by diffusion.

Another dynamic swelling was conducted on hydrogel disks that were dry at time zero (q=1). The weight swelling ratio was plotted versus time in Figure 5.5. The dynamic swelling behavior of poly(methacrylic acid) crosslinked with polycaprolactone (M_n=520 Da) diacrylate was compared at pH 2.9 and 7.4. The dynamic swelling behavior of a nondegradable hydrogel network crosslinked with the same mol percentage of poly(ethylene glycol) dimethacrylate was included for comparison.

Overall, these two materials show comparable dynamic behavior at high and low pH. The PEG-crosslinked material reached equilibrium swelling at pH 2.9 more rapidly then the PCL-crosslinked one. At 2 hours, the PCL-crosslinked hydrogel had both a higher weight swelling ratio at pH 7.4 and a lower weight swelling ratio at pH 2.9. Since this PEG-crosslinked hydrogel has previous been incorporated into a hydrogel-based microcantilever sensors, this study showed promise that the PCL-crosslinked material could successfully function in a sensor as well.

5.3.3 Study of the Degradation Process Gravimetrically

The hydrolytic degradation of poly(methacrylic acid) crosslinked with 20 mol% polycaprolactone diacrylate was studied gravimetrically. Disks were swollen in PBS at 37°C and degradation measured by removing the disks at predetermined times and obtaining the mass of the swollen disk. This study of hydrogel degradation was stopped after 90 days because the materials no longer possessed the mechanical integrity for this experimental method. Figure 5.6

shows the results of this study. The weight swelling ratio, q, was plotted on the y axis over q_o, which is the first equilibrium weight swelling ratio found at 1 day. For this degradation study, poly(methacrylic acid) crosslinkd with polyethylene glycol dimethacrylate was tested in parallel as a control.

The q/q_o of the poly(methacrylic acid) crosslinked with polycaprolactone diacrylate increased linearly over the timeframe of this experiment. A linear fit of the data yields Equation 5.1 where t is in days. The R^2 value is 0.992. This fitted equation is used to predict the change in equilibrium swelling of this degradable hydrogel for the microsensing applications presented later in this thesis.

$$\frac{q}{q_0} = 0.012 * t + 1.012 \qquad \text{Equation 5.1}$$

The q/q_o of the sampled used as a control did not change within error between 7 and 90 days. The linear increase in q/q_o is consistent with the loss of crosslinking by hydrolytic cleavage of the polycaprolactone. A more detailed analysis of the hydrogel structure with degradation was desired, and so the Flory-Rehner equation was utilized in Section 5.3.3 for this purpose.

5.3.4 Application of Flory-Rehner Equilibrium Swelling Theory

Hydrogels which underwent bulk polymerization and exhibit Gaussian chain distribution can be described by the Flory-Rehner equation (Equation 5.2). Flory-Rehner theory recognizes three thermodynamic contributions that together determine the equilibrium swelling of a hydrogel. The first is entropy of mixing between the polymer chains and solvent. Mixing increases entropy in the system

and thus favors swelling. The second is a loss of entropy as the quantity of chain conformations possible for each chain is reduced. This restriction to the chains decreases entropy. Finally, there is a heat of mixing between the polymer and solvent which can be positive or negative. Together, these determine the amount of swelling a hydrogel will undergo. It is also important to note that Flory-Rehner theory can only describe hydrogel swelling behavior at equilibrium [18].

Gel permeation chromatography (GPC) was used in Section 4.3.2 to determine the average molecular weight of polymethacrylic acid (PMAA) in the synthesized hydrogel network. The number average molecular weight is needed to calculate the distance between crosslinks in the hydrogel using the Flory-Rehner equation (Equation 5.2).

$$\frac{1}{\overline{M}_c} = \frac{2}{\overline{M}_n} - \frac{(\upsilon / V_1)[\ln(1-\upsilon_{2,s}) + \upsilon_{2,s} + \chi_1 \upsilon_{2,s}^2]}{(\upsilon_{2,s}^{1/3} - \frac{\upsilon_{2,s}}{2})} \qquad \text{Equation 5.2}$$

Here, $\overline{M}_c$ is the molecular weight between crosslinks, $\overline{M}_n$ is the number average molecular weight of the polymethacrylic acid chains, $\overline{\upsilon}$ is the polymer specific volume, V_1 is the molar volume of water, χ_1 is a Flory-Huggins Interaction parameter of the material [19] [20] [21], and $\upsilon_{2,s}$ is the equilibrium polymer volume fraction, i.e. the volume of the dry polymer sample divided by the volume of the swollen gel [21]. This calculation is highly dependent on the Flory-Huggins Interaction parameter, which varies with swollen volume content and can be estimated by Equation 5.3 if not previously determined.

$\chi_1 = 0.44 + 0.6\upsilon_{2,s}$ Equation 5.3

Using the Flory-Rehner equation (Equation 5.2), equilibrium swelling data were used to calculate the average molecular weight between crosslinks, M_c, versus time. This parameter is meaningful to the understanding of our degrading hydrogel since each hydrolytic cleavage of a crosslink results in an increase in the molecular weight between crosslinks. The greater the number of crosslinks that have degraded, the higher the average molecular weight between crosslinks becomes. This data are presented in Figure 5.7. A linear fit of the data yields Equation 5.4 where time, t, is in days. The R^2 value is 0.991.

$$M_c = 49.4 * t + 11117$$ Equation 5.4

An estimate of the total degradation time of the hydrogel can be obtained by setting M_c equal to M_n and solving for time using Equation 5.4. Complete degradation of the hydrogel network is predicted to occur at 565 days, or approximately 1.5 years. This estimate is consistent with degradation times of polycaprolactone previously reported in the literature.

Similarly, a decrease in the crosslinking density of the hydrogel is presented in Figure 5.8. The crosslinking density was found to decrease from approximately 95 to 75 micromols/mL over the first 60 days of degradation in PBS. It was also important to consider the number of polymer repeat units between crosslinks, and analyze how this quantity would change with time. The

Flory-Rehner theory used above assumes a gaussian distribution of polymer chains, and thus the number of polymer units between crosslinks is important. This value, shown in Figure 5.9, was calculated by dividing the molecular weight between crosslinks by the molecular weight of the repeat unit. Polymer repeating units between crosslinks increases from approximately 125 to 165 units over the first 60 days of degradation.

5.3.5 Hydrogel Degradation Evaluated by Gel Permeation Chromatography

Hydrogels composed of poly(methacrylic acid) crosslinked with 2.5 mol% polycaprolactone diacrylate were degraded in a phosphate-citrate buffer solution at room temperature. Gel permeation chromatography was performed of the polymer chains which remained in the buffer after the hydrogel network had been degraded by hydrolysis. Two peaks were found corresponding to poly(ethylene oxide) equivalent number average molecular weights of 555 and 1035 Daltons. The M_n peak of 555 Daltons is as one might expect given the biodegradable crosslinks had been originally synthesized from 1250 Dalton polycaprolactone. For the polycaprolactone crosslinkers to escape the hydrogel network, they would need to be cleaved twice, on average, by hydrolysis. Thus, an approximate average molecular weight of 555 Daltons is consistent with the degradation of this hydrogel network that was expected.

The molecular weight peak corresponding to 1035 Daltons is likely the result of polycaprolactone chains which never became covalently adhered to the hydrogel network. These could readily escape the hydrogel network by diffusion.

It was expected that poly(methacrylic acid) chains of approximately 50 kDa would correspond to a peak in GPC. Several explanations are possible for their absence. First, since solubility of a polymer decreases with increasing molecular weight, the extraction conducted with acetonitrile may not have been sufficient to dissolve the longer chains. Second, it is possible that the dissolved components remaining after the hydrogel disks had disappeared existed not of single poly(methacrylic acid) chains but a more complex structure. Perhaps these larger structures were removed during sample filtration prior to performing GPC. Nevertheless, the appearance of two distinct polycaprolactone peaks and the dissolution of the hydrogel disks over the course of one year, support the conclusion drawn by the author that hydrolysis of the crosslinks occurred.

5.4 Conclusions

In conclusion, these studies together provide critical knowledge of the swelling and degradation properties of hydrogels composed of poly(methacrylic acid) crosslinked with varying amounts of polycaprolactone diacrylate. By varying the crosslinking density, the weight swelling ratio,q, at high pH (above the pKa) was shown to increase 3-fold. The q at low pH varied little with crosslinking density. The dynamic swelling behavior was studied with varying crosslinking density. The highest crosslinked material reached equilibrium swelling most rapidly. As the intended application of these materials is in sensing, a shorter time to equilibrium is desirable.

A slowly degrading hydrogel is needed if these materials are to be utilized as sensing elements for *in vivo* microsensors. Degradation studies conducted on poly(methacrylic acid) crosslinked with 20 mol% polycaprolactone diacrylate in phosphate buffered saline solution at 37°C predict a complete degradation time of 1.5 years. Up to 3 months, the ratio of weight swelling ratio, q/q_0, increased linearly with time for this biodegradable hydrogel while a similar hydrogel with nondegradable crosslinks showed no change.

This knowledge makes it possible to approximate the performance of these hydrogels as sensing elements in certain types of microsensors. The microcantilever-based sensors reported in Chapter 6 rely on changes to the swollen volume of these hydrogels with pH. It is known that very thin hydrogel films which are covalently adhered to a substrate, such as silicon or glass, will not swell in the same way as unconstrained materials which are free to swell in all three dimensions. However, it is still important to understand the swelling potential of these materials in the bulk to help predict their performance when utilized as thin films in sensing applications.

A primary goal of this dissertation was to integrate hydrogels as sensing elements that were also biodegradable. This goal might at first seem counterintuitive. Traditionally sensors are engineer to increase the sensing lifetime of the device. However, for certain *in vivo* applications, a longer lifetime of the sensor is not needed. One such example is diagnosing ischemia in transplanted tissue. The need to monitor sufficient blood supply to a newly

transplanted tissue is short, on the order of days. Thus a microsensor that would be implanted along with a tissue as it was transplanted would need only sense the pH of its microenvironment reliably for a short time. Then it would be ideal if this microsensor simply biodegraded and was cleared from the body. This would eliminate the need for a second surgery for sensor removal. Ideally, a sensing element would be designed such that it exhibited a useable lifetime in the body, followed by a tunable degradation and clearance from the body. In Chapter 8, the biodegradable, pH responsive hydrogels studied in this chapter are incorporated with a degradable transducer to yield a completely biodegradable pH microsensor.

TABLES

Table 5.1: Summary of equilibrium weight swelling ratios of poly(methacrylic acid) crosslinked with varying mol percentages of polycaprolactone diacrylate

Code	Crosslinking Mol %	PCL (MW)	q pH 3.2	q pH 7.4	q_pH7.4 / q_pH3.2
PMAA_2.5%PCL(1250)DA	2.5	1250	1.5	6.2	4.1
PMAA_5%PCL(1250)DA	5	1250	1.1	4.9	4.5
PMAA_10%PCL(1250)DA	10	1250	1.1	3.3	3
PMAA_20%PCL(1250)DA	20	1250	1.1	2.4	2.2
PMAA_20%PCL(520)DA	20	520	1.2	3.2	2.7

FIGURES

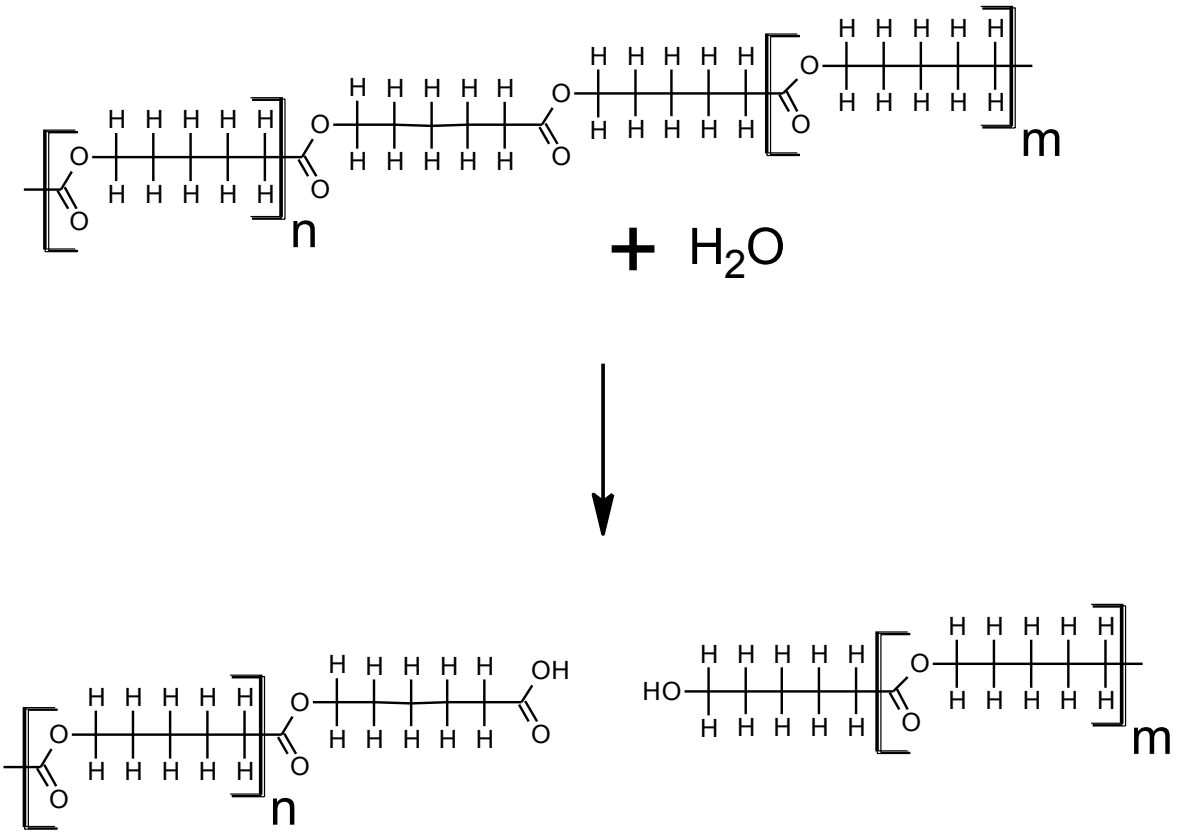

Figure 5.1: Polycaprolactone hydrolytic degradation mechanism

Polycaprolactone degrades by hydrolytic cleavages of its aliphatic ester.

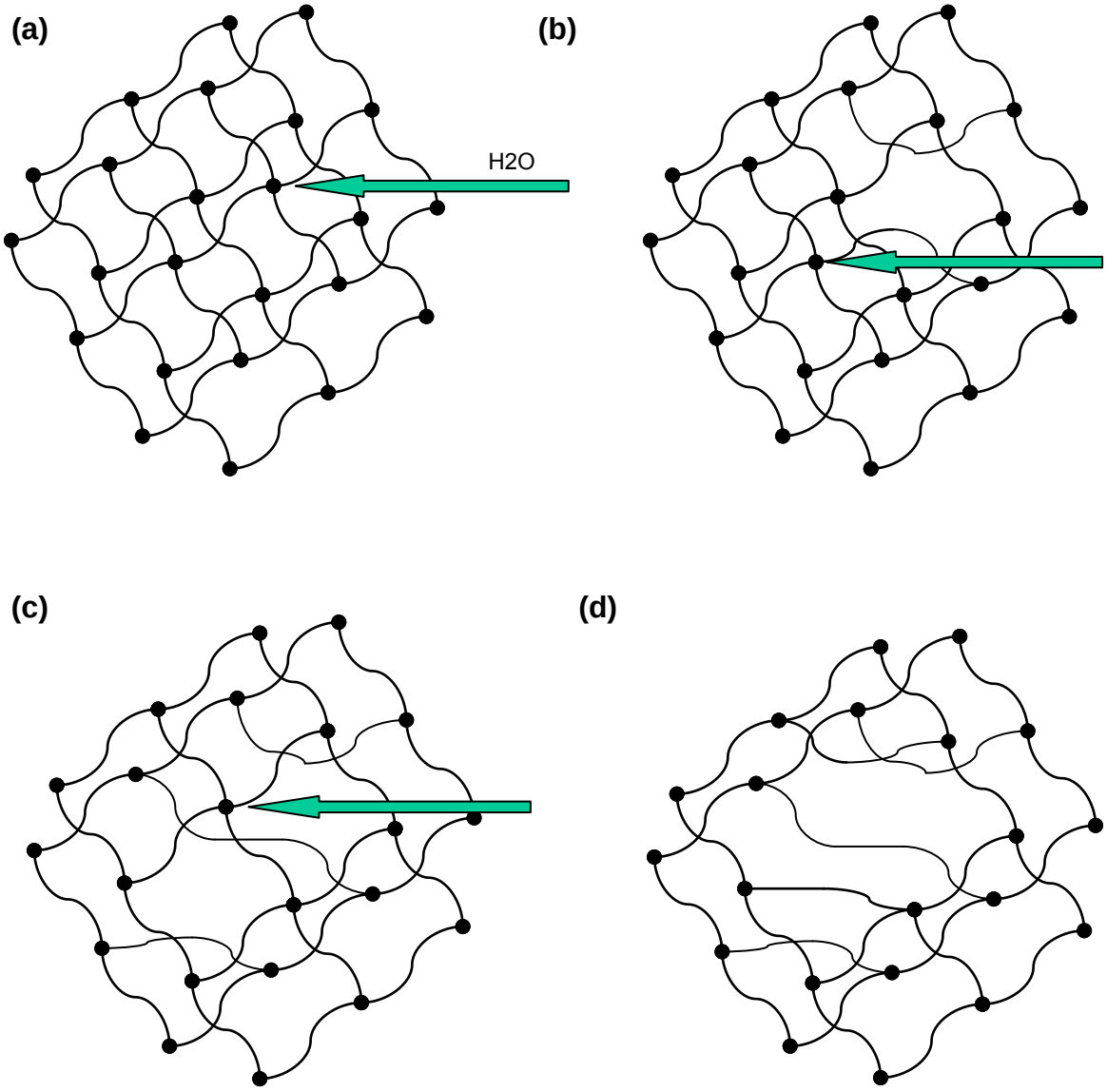

Figure 5.2: Bulk hydrolytic degradation of polycaprolactone crosslinks reduces crosslinking density of the hydrogel

(a) - (c) The sequential cleavage of polycaprolactone diacrylate crosslinks by hydrolysis results in a less densely crosslinked hydrogel (d).

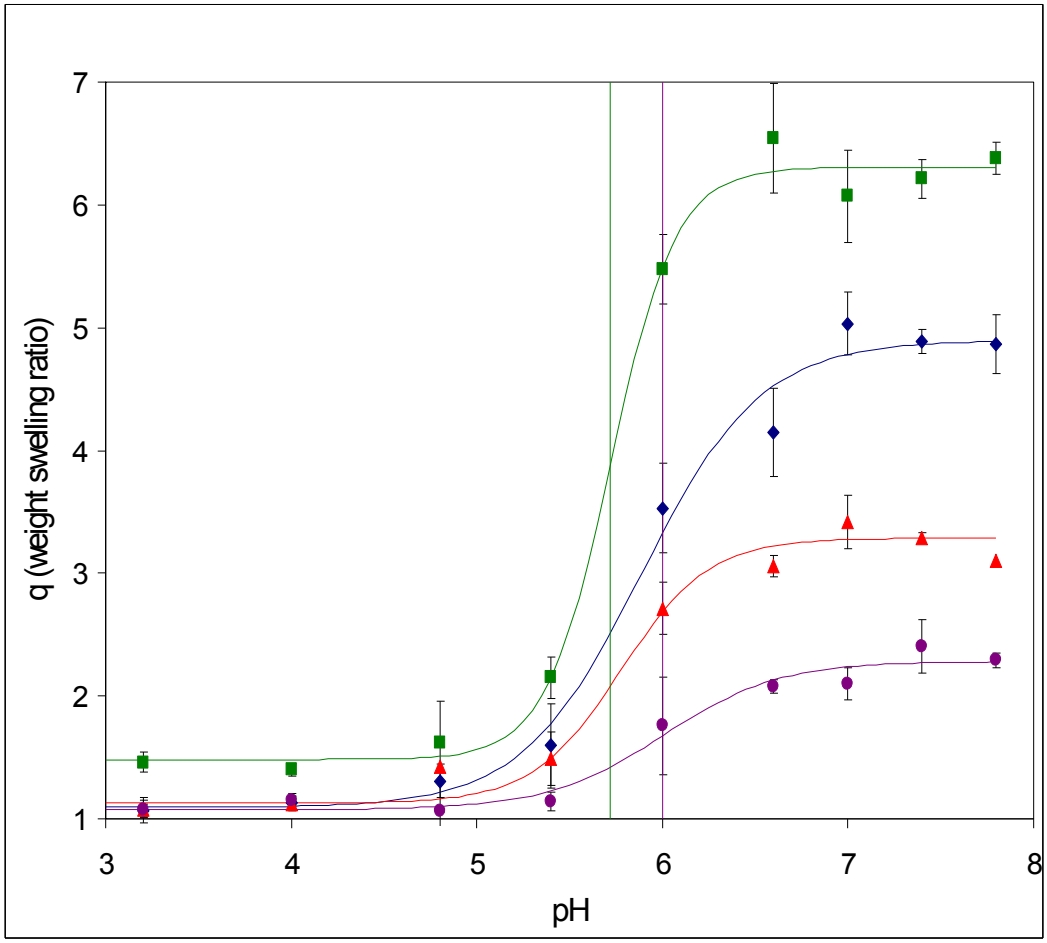

Figure 5.3: Weight swelling ratio versus swelling pH of poly(methacrylic acid) hydrogels crosslinked with varying amounts of polycaprolactone diacrylate (n=3)

Investigation of (-■-) PMAA crosslinked with 2.5 mol% PCLDA, (-♦-) PMAA crosslinked with 5 mol% PCLDA, (-▲-) PMAA crosslinked with 10 mol% PCLDA, (-●-) PMAA crosslinked with 20 mol% PCLDA. The vertical green line labels the pKa of PMAA crosslinked with 2.5 mol% PCLDA. The vertical purple line labels the pKa of PMAA crosslinked with 20 mol% PCLDA.

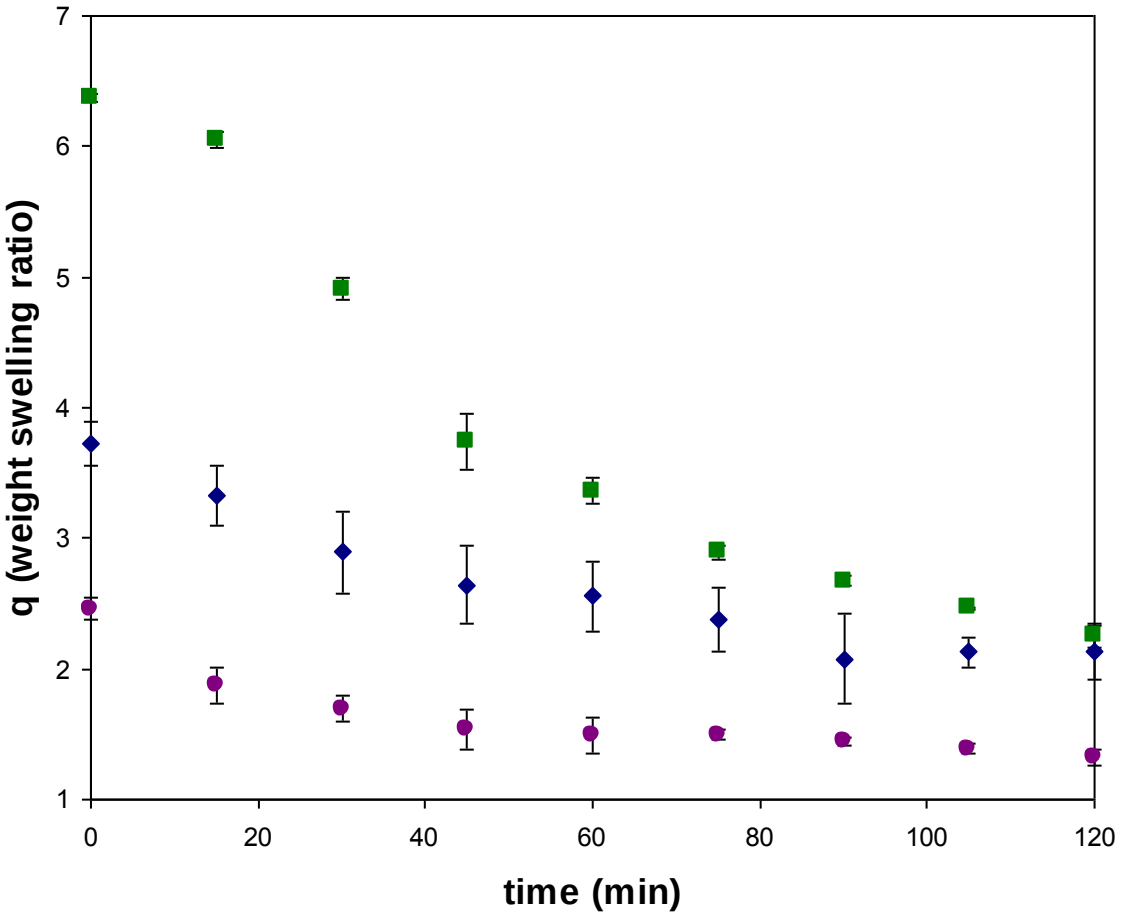

Figure 5.4: Weight swelling ratio versus time of PMAA crosslinked with varying amounts of polycaprolactone diacrylate following a pH change from 7.4 to 4.8 (n=3)

Weight swelling ratio of (-■-) PMAA crosslinked with 2.5 mol% PCLDA, (-♦-) PMAA crosslinked with 5 mol% PCLDA, and (-●-) PMAA crosslinked with 20 mol% PCLDA decreases after pH drop.

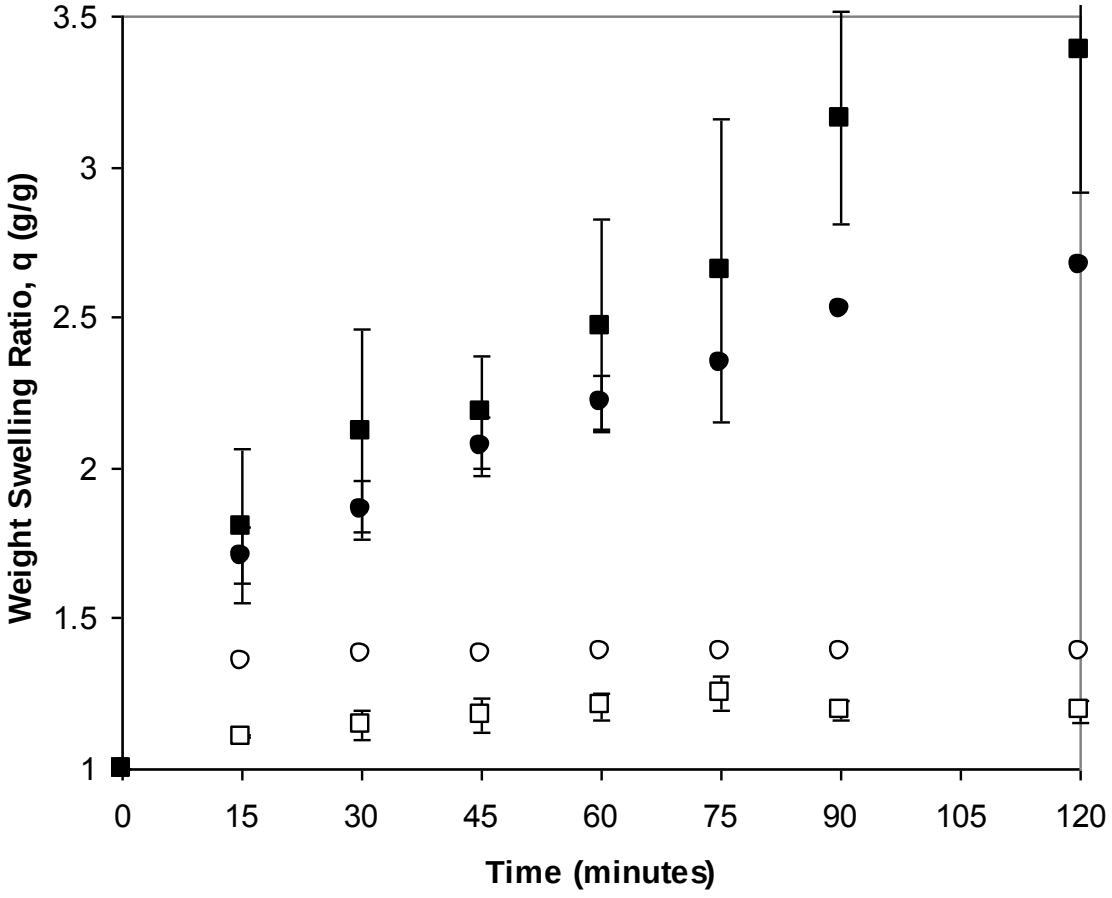

Figure 5.5: Kinetic, pH-responsive swelling comparison of PCL versus PEG crosslinked PMAA systems. PMAA with 20%PCL in pH=7.4 (■), PMAA with 20%PCL in pH=2.9 (□), PMAA with 20%PEG in pH=7.4 (●), and PMAA with 20%PEG in pH=2.9 (○).

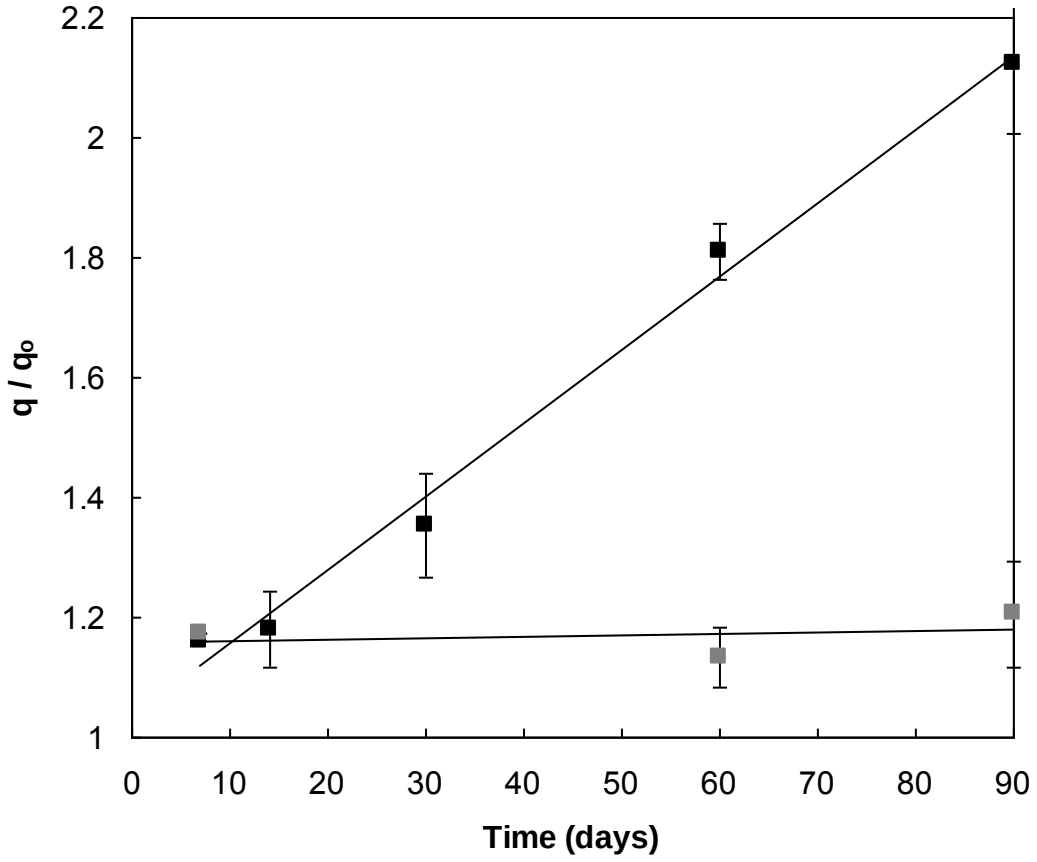

Figure 5.6: Weight swelling ratio, q, divided by the weight swelling ratio at 24 hours, q_0, versus time for PMAA crosslinked with 20 mol% PCL (■) and PMAA crosslinked with 20 mol%PEG (■). (n=5)

The weight swelling ratio of PMAA crosslinked with 20 mol% PCL increased while the PMAA crosslinked with 20 mol% PEG does not. This increase in swelling is attributed to a loss of polycaprolactone crosslinks by hydrolysis.

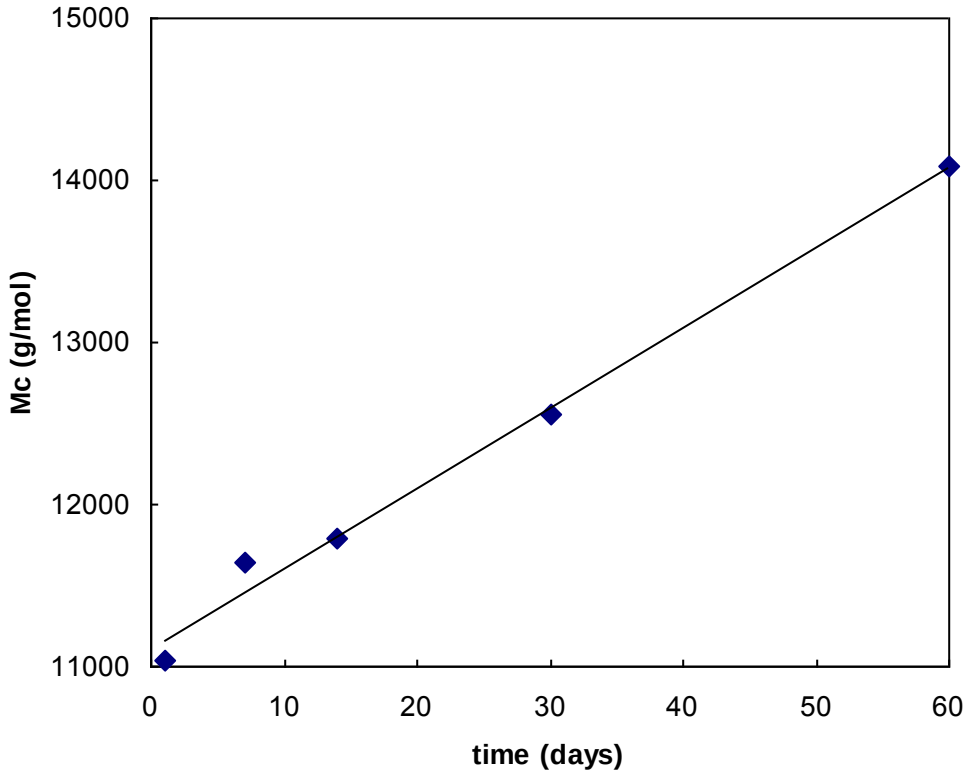

Figure 5.7: Molecular weight between crosslinks versus time for poly(methacrylic acid) crosslinked with 20 mol% PCLDA

The molecular weight between crosslinks was calculated from weight swelling data using the Flory-Rehner equation.

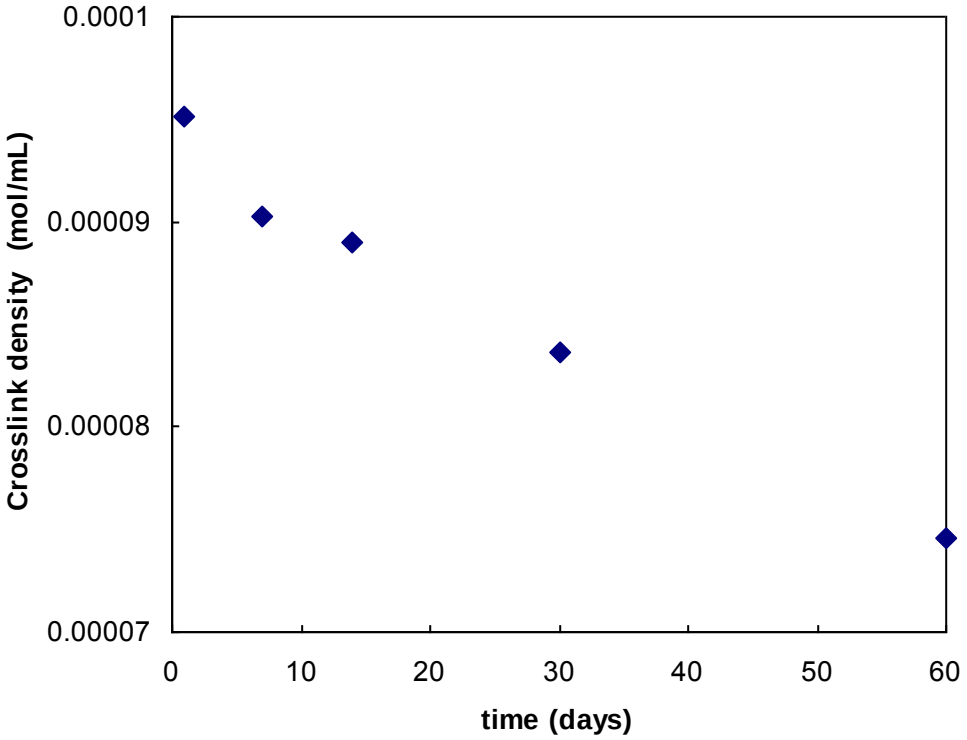

Figure 5.8: Crosslinking density versus time for PMAA crosslinked with 20 mol% PCL

The crosslinking density was calculated from weight swelling data using the Flory-Rehner equation.

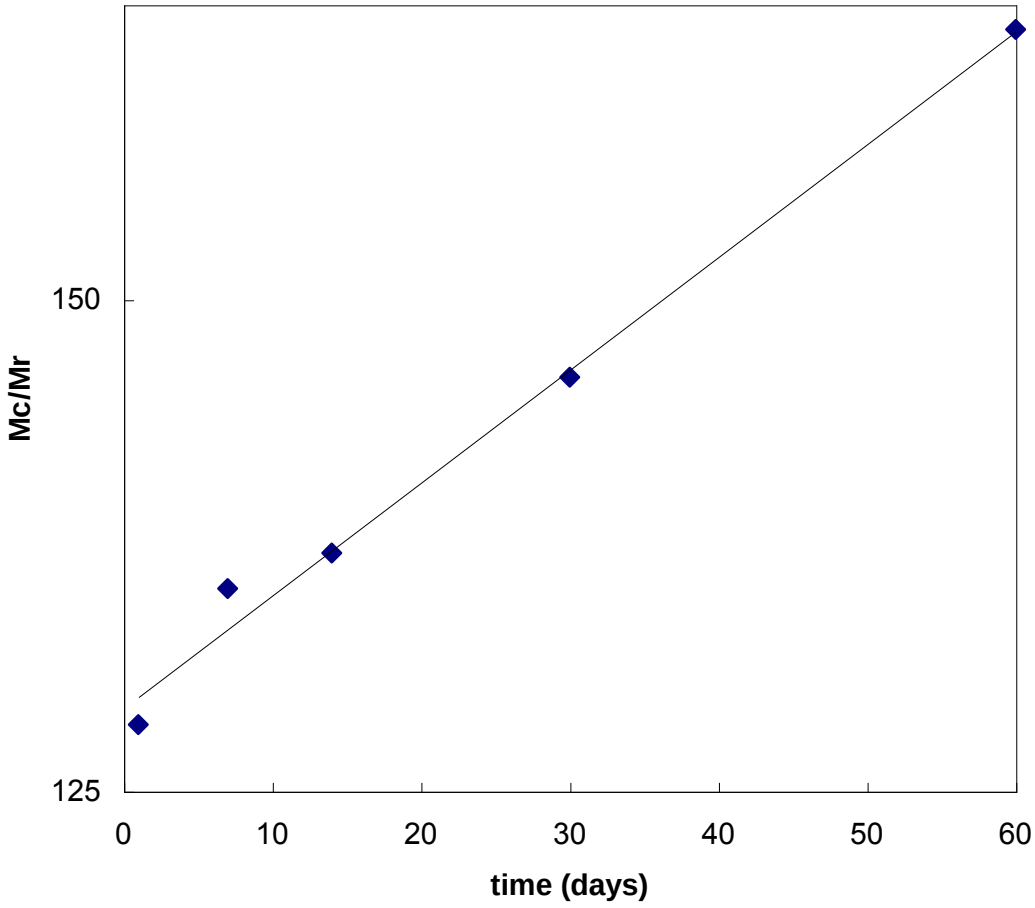

Figure 5.9: Polymer repeating units between crosslinks versus time for PMAA crosslinked with 20 mol% PCL

The number of polymer repeating units between crosslinks was calculated from weight swelling data using the Flory-Rehner equation.

REFERENCES

1. Bramfeldt, H., P. Sarazin, and P. Vermette, *Characterization, degradation, and mechanical strength of poly(D,L-lactide-co-epsilon-caprolactone)-poly(ethylene glycol)-poly(D,L-lactide-co-epsilon-caprolactone).* J Biomed Mater Res A, 2007. **83A**: p. 503-511.
2. Webb, A.R., J. Yang, and G.A. Ameer, *Biodegradable polyester elastomers in tissue engineering.* Expert Opin On Biol Th, 2004. **4**(6): p. 801-812.
3. Kweon, H., et al., *A novel degradable polycaprolactone networks for tissue engineering.* Biomaterials, 2003. **24**(5): p. 801-808.
4. Kim, J.H., S.K. Park, and Y.H. Bae, *In situ accelerated degradation of polyoxyethylene/poly(epsilon-caprolactone) multiblock copolymer by moderate thermal treatment.* J Biomat Sci-Polym E, 2003. **14**(9): p. 903-916.
5. Rice, M.A., J. Sanchez-Adams, and K.S. Anseth, *Exogenously triggered, enzymatic degradation of photopolymerized hydrogels with polycaprolactone subunits: Experimental observation and modeling of mass loss behavior.* Biomacromolecules, 2006. **7**(6): p. 1968-1975.
6. Chao, G.T., et al., *Synthesis, characterization, and hydrolytic degradation behavior of a novel biodegradable pH-sensitive hydrogel based on*

polycaprolactone, methacrylic acid, and poly(ethylene glycol). J Biomed Mater Res A, 2008. **85A**(1): p. 36-46.

7. Siepmann, J. and A. Gopferich, *Mathematical modeling of bioerodible, polymeric drug delivery systems.* Adv Drug Deliver Rev, 2001. **48**(2-3): p. 229-247.
8. Siparsky, G.L., K.J. Voorhees, and F.D. Miao, *Hydrolysis of polylactic acid (PLA) and polycaprolactone (PCL) in aqueous acetonitrile solutions: Autocatalysis.* J Environ Polym Degr, 1998. **6**(1): p. 31-41.
9. De, S.K., et al., *Equilibrium swelling and kinetics of pH-responsive hydrogels: Models, experiments, and simulations.* J Microelectromech S, 2002. **11**(5): p. 544-555.
10. Richter, A., et al., *Review on hydrogel-based pH sensors and microsensors.* Sensors, 2008. **8**: p. 561-581.
11. Karlsson, S., Albertsson, A.-C., *Biodegradable polymers and environmental interaction.* Polym Eng Sci**, 38**(8): p. 1251-1253.
12. Liu, Z., et al., *Structural and functional studies of aspergillus oryzae cutinase: enhanced thermostability and hydrolytic activity of synthetic ester and polyester degradation,* J Am Chem Soc, 2009. **131**(43): p. 15711–15716.
13. Oda, Y., et al., *Polycaprolactone depolymerase produced by the bacterium Alcaligenes faecalis,* FEMS Microbiol Lett, 1997. **152**: p. 339-343.

14. Ruzin, *Plant Microtechnique and Microscopy.* 1999, Oxford University Press.

15. Hilt, J.Z., *Novel micro- and nanoscale diagnostic and therapeutic devices based on intelligent polymer networks*, in *Chemical Engineering*. 2004, The University of Texas: Austin, TX.

16. Guo, W., Hu, N., *Interaction of myoglobin with poly(methacrylic acid) at different pH in their layer-by-layer assembly films: an electrochemical study* Biophys Chem, 2007. **129**(2-3): p. 163-71.

17. Gumbrell, G.P., et al., *Evaluation of a minimally invasive pH based microvascular ischemial monitor*. J Clin Eng, 1998. **23**: p. 344-353.

18. Sperling, L.H., *Introduction to Physical Polymer Science*, 3rd Edition. p. 428.

19. Eichenbaum, G.M., et al., *Investigation of the swelling response and loading of ionic microgels with drugs and proteins: The dependence on cross-link density.* Macromolecules, 2001. **34**(18): p. 6526-6526.

20. Mikos, A.G. and N.A. Peppas, *Flory Interaction Parameter-Chi For Hydrophilic Copolymers With Water.* Biomaterials, 1988. **9**(5): p. 419-423.

21. Flory, P.J. and J. Rehner, *Statistical mechanics of cross-linked polymer networks.* J Chem Phys, 1943. **11**(11): p. 521-526.

CHAPTER 6: MICROSENSORS BASED ON SILICON MICROCANTILEVERS AND BIODEGRADABLE, PH-RESPONSIVE HYDROGEL NETWORKS

6.1 Introduction

Primarily due to the popularity of atomic force microscopy (AFM), microfabricated silicon cantilevers have become inexpensive and readily available [1]. Microcantilevers are shaped like tiny diving boards with one end of a thin beam anchored to a substrate. Typical dimensions of microcantilevers are 100 μm in length by 20 μm in width and 1 μm in thickness. Silicon microcantilevers of these dimensions are sensitive enough to detect molecular adsorption [2]. As a result, there has been an increased interest in their use as transducers in novel biosensors. Small size and the precision with which microcantilever deflection can be detected lend these transducers naturally to biological applications. Microcantilevers have been used to measure a wide variety of biological phenomena from the presence of specific proteins such as cholesterol in solution [3] to biological interactions such as biotin-streptavidin [4] and the hydrogen bonding of DNA base pairs [5].

Notably, microcantilevers are also advantageous as sensor components because they have the flexibility to work in both gaseous and liquid environments [6]. Physical, chemical, or biological stimuli can result in an electrical or optical signal when a microcantilever is used as the transducer. Cantilevers generate these signals by changes in their deflection or resonance frequency. The

simplest example of cantilever deflection for sensing is the case of bimetallic thermostats. These are theoretically well understood and the deflection's dependence on various parameters is quantified [7,8]. The resonance frequency mode of operation for chemical sensors is limited to gaseous media [9].

An often-overlooked aspect of creating microcantilever sensors for biological applications is the application and evaluation of the thin polymer coating. Ways to characterize the coating include: comparing the resonance frequency of the bare and coated microcantilevers, SEM imaging and SFM tip-scratch tests [10]. Methods to produce micropatterned polymers on a surface include microcontact printing, laser ablation, photolithography, inkjet printing, and microscale self-assembly [11]. One method of photolithography that does not require the use of expensive photomasks uses a commercial liquid-crystal-display projector to initiate pattern surfaces [12, 13]. The most recent generation of this device gives a resolution of 2 μm and can pattern over an area of 25 cm^2 [14].

Hydrogel-based microcantilever sensors offer the opportunity for diverse sensing. A thin layer of a responsive hydrogel can be photopolymerized atop a microcantilever beam or a variety of responsive hydrogels photopolymerized atop the various microcantilevers in an array using a photolithographic technique. As the hydrogel responds to changes in its environment by changing its swollen volume, stress is generated at the surface between the hydrogel and the silicon.

This stress results in a deflection of the beam that is both repeatable and easy to measure.

The most common method of measuring cantilever deflection is the optical method. This method uses a laser beam's deflection near the tip of the cantilever. Deflection is measured by a photodetector placed away from the cantilever. This is a preferred method of measuring deflection since it doesn't require any electrical connections and provides a linear response curve. This is widely considered a "simpler" method than utilizing piezoresistive readouts. Piezoresistive cantilevers have a doped region in the beam where resistivity is changed with the stress of bending. These regions are incorporated into a Wheatstone bridge so that the changes in resistivity can be measured. Other methods of producing measurable outputs include piezoelectric, capacitance and electron tunneling [9].

Microcantilever deflections can be detected to less than 1 Angstrom; however, a limit exists due to thermal noise [15]. At present, even high speed methods of AFM maintain nanometer resolution [16]. Angstrom resolution is possible when microcantilever deflection is measured using a laser beam reflected off the top of the microcantilever and onto a photodiode. Other methods that measure microcantilever deflection, such as piezoresistive cantilevers used in combination with a wheatstone bridge as a strain gage, are not as sensitive.

The sensitivity of environmentally responsive hydrogel based sensors can be ultrahigh. This is due to the fact that pH-responsive hydrogels experience a very large change in volume over a very small change in pH. However, the working range of these sensors is limited. They are only highly sensitive over the range where the material is partially ionized. This limited working range makes hydrogel sensors particularly well suited to biological systems since they are generally static systems where very small changes would correspond to disease states. Another advantage of these materials with regard to their sensitivity and towards their application in microscale sensors is that a 2-point calibration is all that is required. These materials generally swell linearly in their working range.

pH-Responsive hydrogels exhibit hysteresis phenomena with respect to swelling which results in sensors that are more sensitive than they are accurate. Accuracy is difficult with these sensors because at a particular pH value, the swollen volume can be different whether the pH was arrived at by a rise in pH or a fall. This behavior is a result of the unique thermodynamics intrinsic to these materials. The narrower the pH fluctuations, the more accurate the value will be. This is again well suited to biological applications that would fluctuate narrowly.

The range of a hydrogel-based pH sensor is determined by the type of hydrogel employed in the device and its pK_a. The highly sensitive region of these pH sensors is restricted to the hydrogel phase transition range. For this reason, microscale pH sensors might best be employed in a microarray of similar microcantilever sensors patterned with different hydrogels. Since the pK_a of a

hydrogel can be tuned by the monomer choice for the gel, custom arrays are not difficult to imagine and open the field for a variety of sensing applications.

Peppas and Hilt developed a microscale pH sensor by micropatterning poly(methacrylic acid) (PMAA) crosslinked with poly(ethylene glycol) dimethacrylate onto a silicon microcantilever. This novel sensor demonstrated a maximum sensitivity of 18.3 μm/pH units deflection [17]. The pH range of the sensor was approximately 5.5-7 [18]. Another type of hydrogel-based microcantilever sensor locates the responsive hydrogel between the beam and the substrate. One advantage of this design is a greater force transfer to the beam [19]. This sensor demonstrated a sensitivity of 7.2μm/pH units over a range of 3-6 pH units. Another advantage is that the pH range would not be restricted by the beam colliding with the silicon substrate. However, one notable disadvantage of this design is that polymerization with photolithography would be limited when the hydrogel is polymerized beneath a silicon beam.

Some heterogeneities were observed in another study of a hydrogel-based microcantilever pH sensor. This sensor employed a copolymer of poly(acrylic acid) and poly(vinyl alcohol). This hydrogel exhibited the same swelling characteristics as PMAA hydrogels, because of the dissociation of the carboxylic acid to the negatively charged carboxylate ion. The like charged chains repelled each other and the resulting electrostatic force caused swelling [20]. Piezoresistive silicon pressure sensor chips were used as they are highly stable and reliable. This approach simplified the study such that all performance

and lifetime issues of the sensor were entirely dependent on the hydrogel's behavior. Sorber et al. [20] found volume spikes which occurred systematically during swelling and before shrinking began. The author used FTIR to verify that these discontinuities occurred on the molecular level as well. The spectroscopy data showed times of lower carboxylate concentrations which caused a reduction in the driving force for swelling. When developing and optimizing a novel hydrogel-based sensor, one needs to be aware of these discontinuities in volume change.

With cantilever sensors, smaller is not always better, as the size of the sensor must be chosen based on the output desired. Nanocantilevers can translate extremely small changes in mass into large changes in their frequency. While nanocantilevers have the advantage of measuring very small mass changes, these are not usually necessary in hydrogel-based sensors because hydrogels experience a very large volume and thus mass change over a small pH range. Another way to engineer these systems is by utilizing analogous microstructures such as bridges and cantilever-like structures with more than one anchor point, rather than the standard cantilever beam.

The objective of this section of the thesis was to fabricate and test microsensors composed of microcantilever arrays and biodegradable, pH-responsive hydrogels with the ultimate goal of producing an ultrahigh sensitivity microsensor. Variables for optimization were presented both for the microcantilever component and the hydrogel component. Silicon

microcantilevers of varying length, width, thickness, and force constant were tested. Hydrogels of different crosslinking ratios were utilized which provided varying Q, or volume swelling ratio, and varied thickness of the hydrogel sensing element. Microsensors were tested in biologically mimicking solutions for their maximum deflection and pH-sensing range.

The theory which exists to predict composite cantilever beam deflection caused by a volume change in one layer was evaluated. A development of this theory is presented herein. Finally, the predicted deflection of these composite microcantilevers was compared to the actual deflections measured experimentally.

6.2 Materials and Methods

6.2.1 Preparation of Silicon Microcantilever Arrays for Hydrogel

Silicon microcantilever arrays (NanoWorld AG, Neuchatel, Switzerland) were purchased with cantilevers of varying lengths, thicknesses, and force constants as indicated in Table 6.1. The top surface of all microcantilevers was bare silicon. First, silicon microcantilever arrays were cleaned with a series of solvents. This step was necessary to remove any grease or oils that might have been deposited on the array during manufacture. Briefly, arrays were rinsed with the following solvents each for 5 minutes: acetone, toluene, acetone, and methanol. Following this cleaning process, arrays were rinsed several times with ultrapure DI water to remove all residual solvents.

A Piranha clean was conducted on the arrays to remove any remaining organic contaminants from the silicon surface. A 3:1 solution of sulfuric acid and hydrogen peroxide was prepared and allowed to react for 5 minutes. The Piranha solution was poured over the silicon microcantilever arrays and allowed to react. After 20 minutes, the piranha solution was removed and the microcantilever arrays were rinsed with ultrapure DI water to remove all residual acid.

An organosilane treatment was performed on the silicon microcantilever arrays to promote covalent adhesion of the hydrogel to the silicon surface (Figure 6.1). A solution of 10% by weight 3-methacryloxypropyltrimethoxysilane (3-MPS, Sigma-Aldrich, St. Louis, MO) in acetone was prepared. Microcantilever arrays were placed in the 3-MPS solution for 2 hours to allow formation of the self assembled monolayer. Arrays were removed from the solution and rinsed with methanol and acetone, then dried with nitrogen and placed in a 100°C oven for 12 hours.

6.2.2 Photopolymerization of hydrogel atop microcantilever beams

Monomer solutions were prepared as described for hydrogel films in Section 4.2.3. Microcantilever arrays which had undergone organosilane treatment were dipcoated in monomer solution and then exposed to UV light of 15mW/cm^2 for 15 minutes. Figure 6.2 provides a pictorial description of the overall sensor fabrication process. The array was placed in phosphate-citrate buffer of pH 7.4 (I=0.5M) to swell the hydrogel. Hydrogel that had

photopolymerized on top of the array (but not on the beams) was removed to leave only hydrogel material on the beams. The hydrogel not located on the beams became detached when swollen due to a lack of covalent adhesion to the silicon substrate. When a thicker layer of hydrogel was desired atop the microcantilever beam, this process was repeated.

6.2.3 Imaging hydrogel atop microcantilever beams using fluorescence

A monomer solution was prepared as described for hydrogel films in Section 4.2.3, but with the addition of 1% by weight of a fluorescent monomer. Microcantilever arrays which had undergone organosilane treatment were dipcoated in monomer solution and then exposed to UV light of 15mW/cm^2 for 15 minutes. Arrays were swollen in phosphate-citrate buffer of pH 7.4 (I=0.5M). Images were obtained with a CoolSnap digital camera attached to the Nikon Eclipse ME600 fluorescent microscope operating with a FITC filter. Microcantilever arrays were stored protected from direct light to avoid photobleaching of the sample.

6.2.4 Microcantilever Deflection Studies

A change in the swollen volume of a pH-responsive hydrogel atop a silicon microcantilever beam causes the beam to deflect differently in varying pH buffers enabling this device to be used as a pH sensors (Figure 6.3). A Nikon Eclipse ME600 microscope was used to measure the deflection of the microcantilevers. First, microcantilever arrays were placed in a 20 µL glass swelling chamber and

filled with a buffer of desired pH. This swelling chamber was placed on the microscope stage so that microcantilever deflection could be measured while the array was submerged. A 50x objective was utilized in all deflection studies. The fine focus knob of the microscope was adjusted and recorded to obtain the difference in focus height of the microcantilever's base and tip. This difference in height was defined as deflection.

6.2.5 Sensor testing in biologically relevant solution

Since the ultimate goal of producing a biodegradable, pH-responsive sensing element would be placement *in vivo*, a preliminary study was performed to better understand the effects of a protein-rich solution on the hydrogel-based sensor. Fetal bovine serum (FBS, Sigma-Aldrich, St. Louis, MO) was added to phosphate-citrate buffers to prepare a variety of buffers containing 10% FBS over the pH range desired. The serum is the portion of plasma remaining after coagulation of blood, so lacking fibrinogen left behind in the clot. Fetal bovine serum is commonly used to maintain cultured cells in a medium in which they can survive, grow, and divide. FBS is composed of a rich variety of proteins, with the most prevalent protein being bovine serum albumin (BSA).

The hydrogel-based microcantilever sensor was placed in contact with a 10% BSA solution at pH 7.4 and 22ºC for 2 hours, and the deflection measured. Thereafter 20-minute equilibration times were allotted after pH buffer changes and before cantilever deflection was measured. This study was conducted in order of decreasing pH.

6.3 Results and Discussion

6.3.1 Imaging hydrogel atop microcantilever arrays

The photopolymerization of hydrogel atop silicon microcantilever arrays was confirmed by optical microscopy. Consistent deposition of hydrogel across a microcantilever array is desirable in the fabrication of sensing arrays. The method of fabrication chosen for these arrays gave reasonably consistent placement of hydrogel across the beam (Figure 6.4). Shrinkage occurs during the photopolymerization of hydrogels that generates force at the surface between the silicon microcantilever and the hydrogel thin film. The hydrogel thin films polymerized on the beams were 2 – 4 microns in thickness. This force causes the microcantilevers to bend upwards. This unique phenomenon is displayed in image b of Figure 6.5. Image (a) in Figure 6.5 is of a bare microcantilever and is provided for comparison.

Microcantilever arrays submerged in buffer result in swelling of the thin layer of hydrogel atop the microcantilever beam. This swollen hydrogel generates force at the surface between the hydrogel and the silicon causing the beam to deflect downward. Figure 6.6 depicts two beams from the same array deflected downward due to swelling of the hydrogel. Due to the angled side view chosen to image this phenomenon, only one microcantilever in the array can exist in focus at once.

6.3.2 Fluorescent imaging of hydrogel on microcantilever array

Qualitative analysis of microcantilever surface coverage was accomplished by means of photopolymerizing fluorescently-labeled monomers to form hydrogels atop the beams of a microcantilever array. A fluorescently-labeled hydrogel was used since it can be difficult to image thin hydrogel films on silicon. Figure 6.7 is a top-view image of an eight microcantilever array photopolymerized with fluorescently-labeled hydrogel. The surface coverage of microcantilevers in the array with hydrogel was relatively consistent. This image was captured in black-and-white due to the limitations of the CoolSnap digital camera used.

6.3.3 Single microcantilever deflection studies

Microcantilever arrays which contained one each of cantilevers 1, 2, 3, and 4 (Table 6.1) were micropatterned with poly(methacrylic acid) crosslinked with polycaprolactone diacrylate. Cantilevers 1, 2, and 3 demonstrated no significant and repeatable deflection by submerging the array in a range of pH buffers. Those three cantilevers could not transduce the volume change of the pH-responsive material. The reason for this is likely two-fold. First, cantilevers 1, 2, and 3 have a higher force constant relative to cantilever 4,. Thus, a greater force must be exerted on the beam to generate an equivalent deflection. Second, cantilevers 1, 2, and 3 all have smaller surface areas over which the hydrogel could be photopolymerized. The force that can be applied on the beam by the hydrogel is in part due to the surface over which it is adhered.

Figure 6.8 shows the deflection of cantilever 4 in a phosphate-citrate buffer solution over the pH range of 3 to 7 (constant ionic strength of 0.5M). A difference in tip deflection of 50 microns was measured between the high pH and low pH environment for this microcantilever. It is important to note that the standard deviation displayed in Figure 6.8 is a result of the repeated measurement of the same hydrogel-coated microcantilever beam (n=3). Thus this error most accurately demonstrates the error in measuring microcantilever deflection with the optical microscope. For future studies, microcantilever arrays were purchased to allow the measurement of the deflection of many of the same cantilevers on one array.

6.3.4 Microcantilever array deflection studies

Sensing arrays composed of 8 microcantilevers of type 5 (Table 6.1) photopolymerized with poly(methacrylic acid) crosslinked with polycaprolactone diacrylate were tested in a range of phosphate-citrate buffer solutions of constant ionic strength (0.5M). In one study, the average deflection of all cantilevers in the array was measured in order of high to low pH with 2 hour equilibration times (Figure 6.9). The difference in tip deflection between pH 4 and pH 7.5 was approximately 40 microns.

It was shown by Hilt et al. [21] that a histeresis exists with pH-responsive hydrogel coated cantilever beams – namely that the equilibrium swollen volume at a particular pH, thus the deflection, is dependent upon the pH direction by which it was arrived. Therefore, it was important to measure the average

deflection also from low to high pH. Figure 6.10 displays the average deflection of the sensing array when measured from low to high pH. As anticipated, the average cantilever deflections are lower at many pH values than the previous study. At sufficiently high pHs above the pK_a of the material, the average deflections do not differ significantly within error.

It was desirable to better understand the kinetic behavior of these composite cantilevers as response time can be critical in certain sensing applications. Due to the method by which microcantilever deflection was measured, the shortest equilibration time possible was 5 minutes. Figure 6.11 displays the average deflection of microcantilevers allowed just 5 minutes equilibration time in each new buffer. This study was conducted from high pH to low pH. For comparison, a study conducted with 2 hours of equilibration time is also displayed in this figure. The average deflection at 5 minutes and 2 hours of equilibration time do not differ significantly within error. As a result, it is concluded that the time to equilibrium for this type of sensors will be less than 5 minutes.

Microcantilever sensing arrays photopolymerized with pH-responsive hydrogel offer maximum sensing around the pK_a of the hydrogel. A simple method was used to determine the sensitivity of this microsensor. A linear fit of the data contained in the active sensing region of the device was obtained. This linear fit is described by an R^2 value of 0.992. The slope of that data was 1nm/4.5e-5ΔpH. Figure 6.12 depicts this fit over the most active sensing region of the device.

6.3.5 Theoretical analysis of microcantilever deflection

It was desired to develop a broader understanding of silicon microcantilever deflection caused by the swelling and deswelling of thin layers of responsive hydrogels photopolymerized atop the cantilever. Because environmentally-responsive hydrogels respond to a wide variety of stimuli such as temperature and ionic strength, an opportunity exists to generate novel sensors of this type for a variety of biologically relevant conditions beyond just the pH demonstrated in this thesis.

Two key characteristics of a responsive hydrogel were identified which help predict the sensitivity of a resulting microcantilever sensor. Volume swelling ratio, Q, is an important hydrogel characteristic that determines sensor sensitivity. Following the theory, a larger Q generates a greater deflection and thus sensitivity. However, there exists a limit to which Q improves sensitivity. At sufficiently high Q, swelling will result in delamination of the hydrogel thin film instead of deflection of the beam. The volume-swelling ratio of hydrogel thin films is easily obtained gravimetrically (Section 5.2.1). Another property of the hydrogel that affects sensitivity is Young's modulus. This is a mechanical property of hydrogel thin films, which is easily measured using an Instron (Section 4.1.6).

This analysis sought to understand if the microcantilever deflections obtained experimentally, and presented previously in this chapter, fit with the

theory currently available to describe composite cantilevers. And if not, could the existing theory be expanded to better describe these unique sensing devices.

The theory to describe the deflection of a bimetallic cantilever was presented by Timoshenko [7,8]. Equation 6.1 predicts the radius of curvature of the bimetallic cantilever beam,

$$\frac{1}{\rho} = \frac{6E_1E_2t_1t_2(t_1+t_2)\Delta\varepsilon}{(E_1t_1)^2+(E_2t_2)^2+2E_1E_2t_1t_2(2t_1^{\,2}+3t_1t_2+2t_2^{\,2})} \qquad \text{Equation 6.1}$$

where ρ is the radius of curvature of the beam, E_1 is the Young's modulus of layer 1, E_2 is the Young's modulus of layer 2, t_1 is the thickness of layer 1, t_2 is the thickness of layer 2, and Δε is the differential layer strain. In Timoshenko's presentation, this layer stain is a result of volume changes to the metal layers caused by change in temperature. A few modifications make this classic equation more useful in the treatment of composite cantilevers composed of hydrogels and silicon.

First, it is useful to relate differential layers strain, Δε, to the volume swelling ratio of the hydrogel. Volume swelling ratios of hydrogels are easy to measure and widely published in the literature. Q is the swollen volume divided by the dry volume of a hydrogel. In the case of bimetallic cantilevers, the volume change of both layers must be accounted for in the calculation of strain. The treatment of Δε is simpler in the case of the composite cantilevers because only the hydrogel layer experiences a change in volume with pH. While the volume change of the hydrogel captured in Q represents a three-dimensional change in

the hydrogel, only one of those dimensions, that which exists in the lengthwise direction of the cantilever, contributes to the deflection of the cantilever. The Q of a dry, unswollen hydrogel is 1. Thus, Equation 6.2 will describe the driving force of composite cantilever deflection. [21]

$$\Delta\varepsilon = Q^{1/3} - 1 \qquad \text{Equation 6.2}$$

All experimental data presented in this thesis measured deflection of the microcantilever beam, D, not radius of curvature. For this reason, it is convenient to modify Equation 6.1 further to calculate deflection. From geometry, we know that beam deflection, D, and radius of curvature, ρ, are related by Equation 6.3

$$D = \rho\left(1 - \cos\left(\frac{l}{\rho}\right)\right) \qquad \text{Equation 6.3}$$

when the length of the cantilever, *l*, is known. With Equation 6.3 and Equation 6.4, a series of equations exists to calculate the deflection of a composite cantilever beam based on the Q of the hydrogel.

$$\frac{1}{\rho} = \frac{6E_1E_2t_1t_2(t_1+t_2)\Delta\varepsilon}{(E_1t_1)^2 + (E_2t_2)^2 + 2E_1E_2t_1t_2(2t_1^{\,2} + 3t_1t_2 + 2t_2^{\,2})} \qquad \text{Equation 6.4}$$

It would be convenient to have just one equation to relate cantilever deflection and hydrogel volume swelling ratio. To accomplish this, a Taylor Series approximation is used to simplify Equation 6.3 to Equation 6.5,

$$D = \frac{l^2}{2\rho} \qquad \text{Equation 6.5}$$

However, this Taylor Series approximation is only valid at small deflection of the cantilever beam. Combining Equation 6.4 and 6.5, Equation 6.6 is obtained [34].

$$D = \frac{3l^2 E_1 E_2 t_1 t_2 (t_1 + t_2)(Q^{1/3} - 1)}{(E_1 t_1)^2 + (E_2 t_2)^2 + 2E_1 E_2 t_1 t_2 (2t_1^{\,2} + 3t_1 t_2 + 2t_2^{\,2})} \qquad \text{Equation 6.6}$$

The limitations of this small deflection assumption were tested with the parameters of the sensors fabricated in this dissertation. These sensors were fabricated with silicon microcantilevers of length, *l*, 500 μm; thickness, t_1, 1 μm; and Young's modulus of Silicon, E_1, 150 GPa. The hydrogel layer of poly(methacrylic acid) crosslinked with 20 mol percent polycaprolactone diacrylate has a Young's modulus of 2 MPa and a thickness of approximately 3 microns. When the volume swelling ratio, Q, is allowed to vary, the tip deflection changes as shown in Figure 6.13.

Both Equation 6.6, and the series of Equations 6.3 and 6.4, were used to calculate the microcantilever deflection. For the cantilever sensors presented in this dissertation, the assumption in Equation 6.6 results in less than 1% error in tip deflections of less than 85 microns. Since no data is presented for deflections of greater than 85 microns in this thesis, Equation 6.6 was deemed adequate to describe the composite cantilever sensors presented here.

In Figure 6.14, the composite cantilever deflection predicted by Equation 6.6 was compared to experimental data. Here, volume swelling ratios, Q, are the result of a hyperbolic tangent fit of the equilibrium swelling study conducted on hydrogel thin films and presented in Figure 5.2. Sensors were fabricated with

silicon microcantilevers of length, *l*, 500 μm; thickness, t_1, 1 μm; and Young's modulus of Silicon, E_1, 150 GPa. The hydrogel layer of poly(methacrylic acid) crosslinked with 20 mol percent polycaprolactone diacrylate has a Young's modulus of 2 MPa and a thickness of approximately 3 microns. The thickness of the hydrogel thin film was approximated by imaging the composite beam. Equation 6.6 accurately predicts the deflection of the cantilever within the error of these experiments. The existing theory available to describe composite cantilevers appears adequate to describe the microcantilever pH sensors fabricated and tested in this thesis.

6.3.6 Microcantilever deflection versus pH in serum

The sensitivity of novel pH microsensors was tested in 10% FBS pH buffer solutions of constant ionic strength. It was hypothesized that proteins might disrupt the sensitivity of this type of sensor. Due to the sensing element being composed of responsive hydrogel, proteins might diffuse into the network and change the equilibrium deflection of the beam. It is necessary for these sensors to retain their sensitivity in protein-rich solutions if they are ever to be useful *in vivo*. The average deflection of the microcantilevers in the array versus pH is shown in Figure 6.15. A hyperbolic tangent fit of the data produced the dotted line in the figure. From this data, we observe a reduction in the maximum deflection of the cantilevers observed at high pH. An approximately 25% reduction in the sensitivity of these sensors was observed, but overall the

presence of proteins in solution did not compromise the function of the sensing element.

6.4 Conclusions

Biodegradable, pH-responsive hydrogel networks composed of poly(methacrylic acid) crosslinked with polycaprolactone diacrylate were photopolymerized atop microcantilever arrays. Microcantilever beams of varying force constant were tested and the crosslinking ratio of the hydrogel was varied to generate the highest sensitivity sensor. In general, a lower force constant silicon microcantilever and a thicker hydrogel thin film resulted in higher sensitivity sensors. It was determined that a microcantilever of force constant 0.03 N/m and a 20% crosslinked hydrogel allowed the fabrication of the highest sensitivity sensor, 1nm/4.5e-5ΔpH. These sensors were tested in a variety of biologically mimicking solutions of varying pH, including protein-rich solutions, which did not significantly interfere with the function of the sensor.

Imaging the hydrogel atop the cantilever was undertaken with an optical microscope and satisfactory images were obtained using a fluorescently labeled hydrogel. These images were used to evaluate the consistency of hydrogel deposition across an array. A composite cantilever deflection equation, based on the bimetallic cantilever deflection equation first presented by Timoshenko in 1925, was evaluated for the microcantilever sensors fabricated and tested in this thesis. A “small deflection” assumption present in this composite cantilever deflection equation was tested for the sensors and tip deflections presented here.

Given the parameters of these microcantilever pH sensors, the composite cantilever equation agrees with experimentally obtained deflection data within the error of those experiments. This theory appears sufficient to describe the microcantilever pH sensors fabricated and tested in this thesis.

TABLES

Table 6.1: Dimensions, force constant, and resonant frequencies of all silicon microcantilevers tested

Cant #	Length	Width	Thickness	Force Constant	Resonant Frequency
1	100 μm	50 μm	2.7 μm	40 N/m	350 kHz
2	150 μm	30 μm	2.7 μm	7.4 N/m	150 kHz
3	210 μm	30 μm	2.7 μm	2.7 N/m	80 kHz
4	500 μm	30 μm	2.7 μm	0.2 N/m	15 kHz
5	500 μm	100	1 μm	0.03 N/m	6 kHz

FIGURES

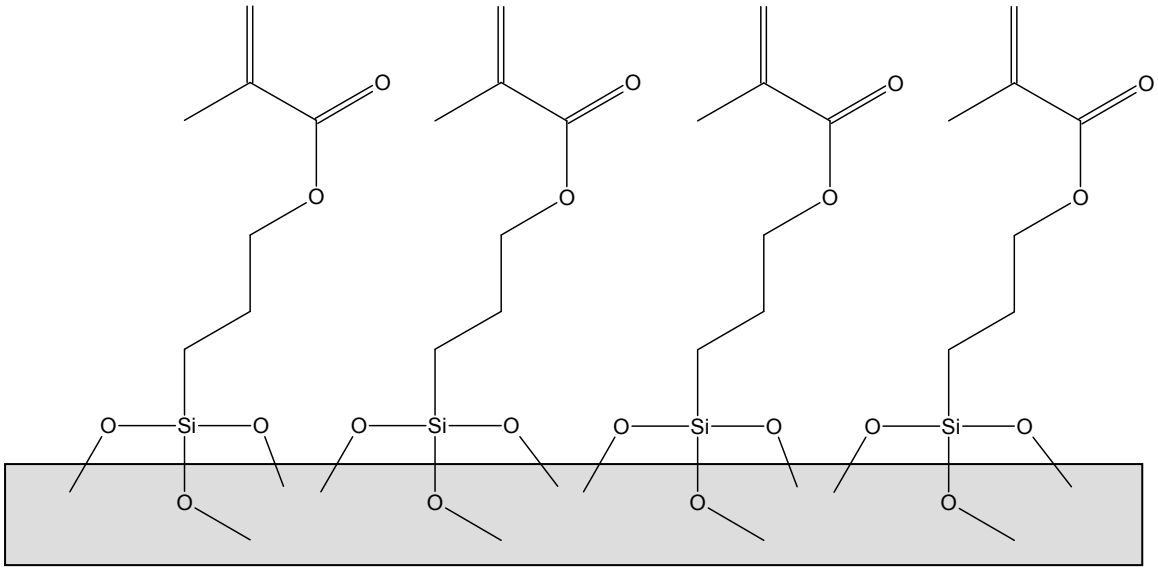

Figure 6.1: Self Assembled Monolayer of 3-MPS on Silicon

3-Methacryloxypropyltrimethoxysilane self-assembled on silicon provides functional groups (methacrylates) anchored to the surface. This chemistry allows the covalent adhesion of hydrogel to silicon microcantilevers.

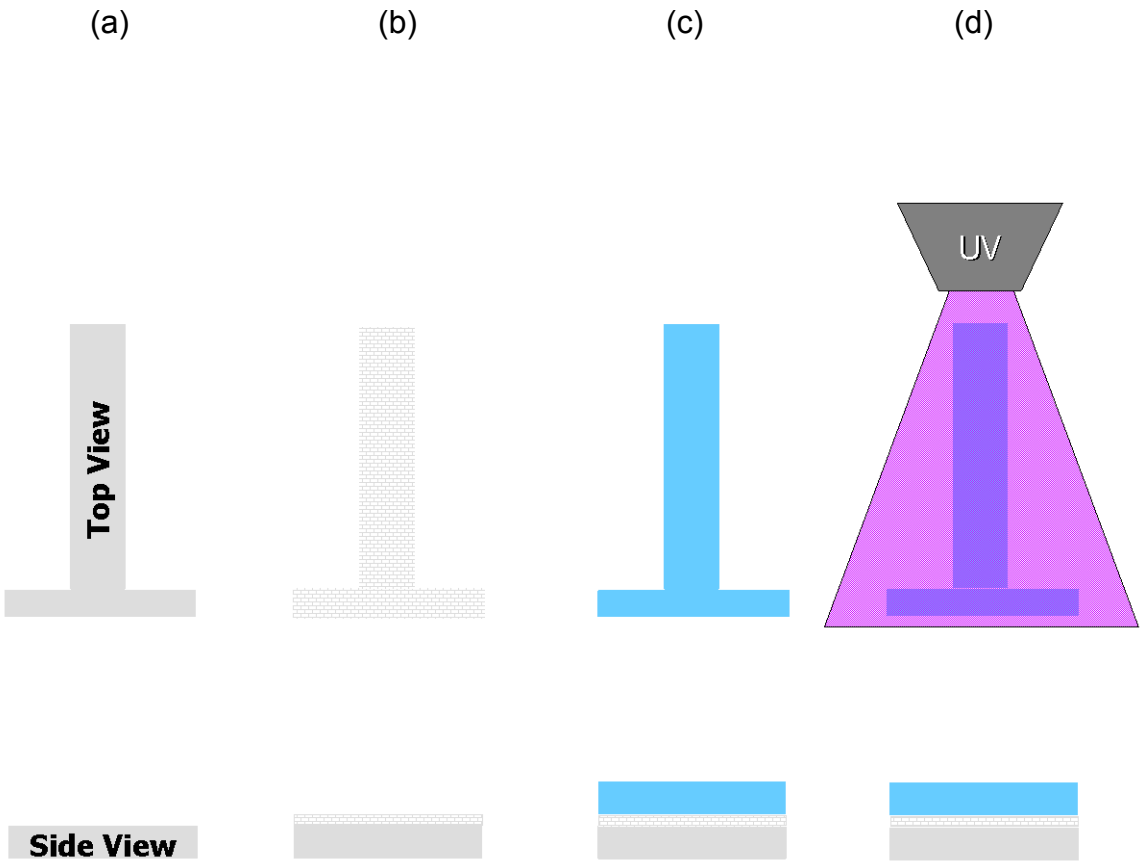

Figure 6.2: Microcantilever sensor fabrication procedure

(a) Silicon microcantilevers are cleaned with solvents and Piranha, (b) Organosilane treatment of the microcantilever yields functional groups anchored to the surface, (c) A thin layer of monomer solution is deposited on the microcantilever, and (d) Photopolymerization is initiated with UV light

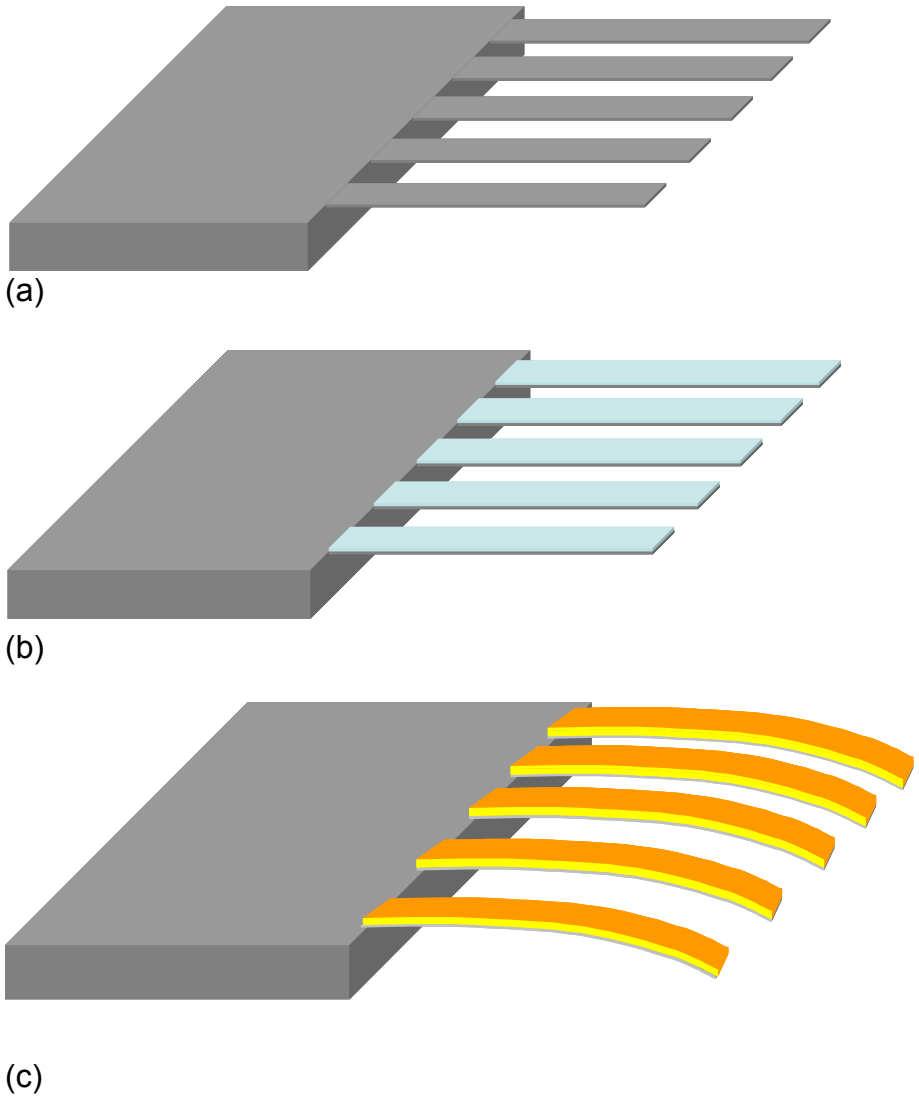

Figure 6.3: Microcantilever arrays with responsive hydrogel

Microcantilever arrays serve as transducers for pH-responsive hydrogel. (a) bare silicon microcantilever array; (b) microcantilever array with thin layer of hydrogel photopolymerized atop the beams; (c) microcantilever array with swollen hydrogel causing the beam to deflect downward

(a)

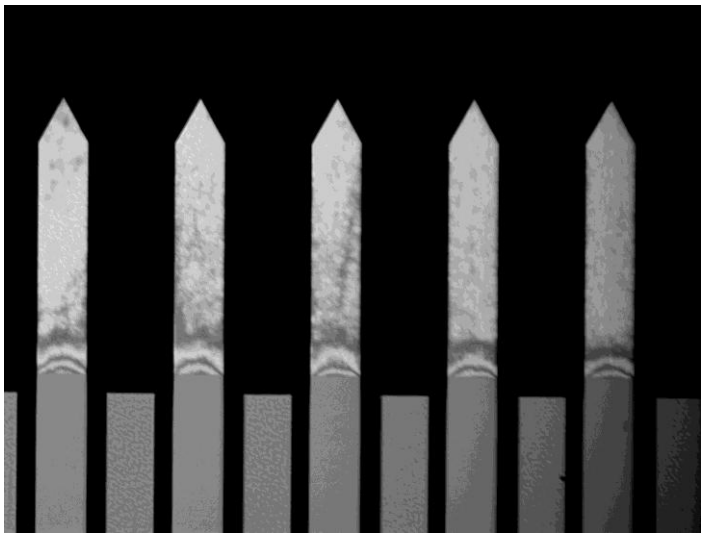

(b)

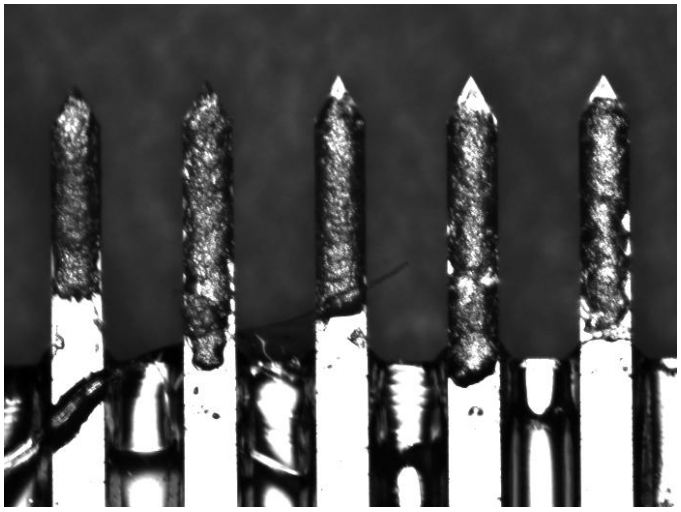

Figure 6.4: Top-view images of microcantilever array

Poly(methacrylic acid) crosslinked with 20 mol% polycaprolactone diacrylate photopolymerized atop 8 microcantilever array. Images of (a) bare silicon array and (b) array with hydrogel photopolymerized atop beams

(a)

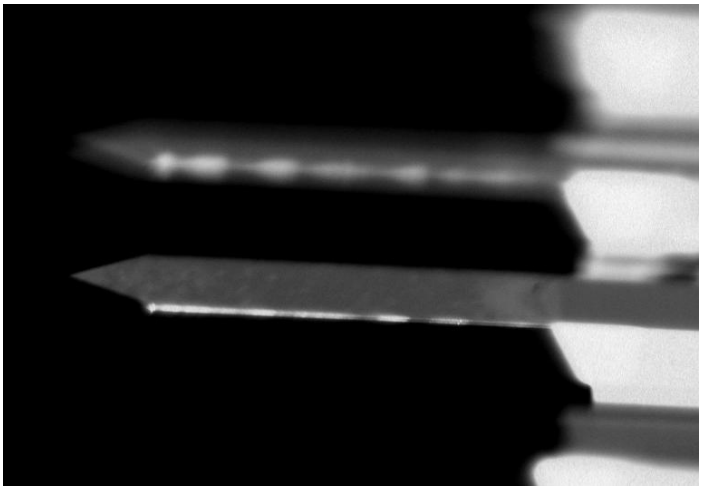

(b)

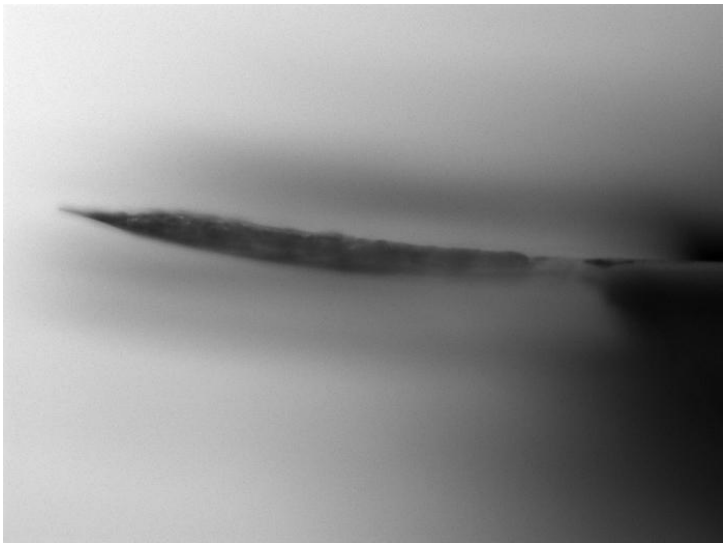

Figure 6.5: Side-view image of microcantilever array

Poly(methacrylic acid) crosslinked with 20 mol% polycaprolactone diacrylate photopolymerized atop 8 microcantilever array. Angled side-view images of (a) bare silicon array and (b) array with dry hydrogel atop beam.

(a)

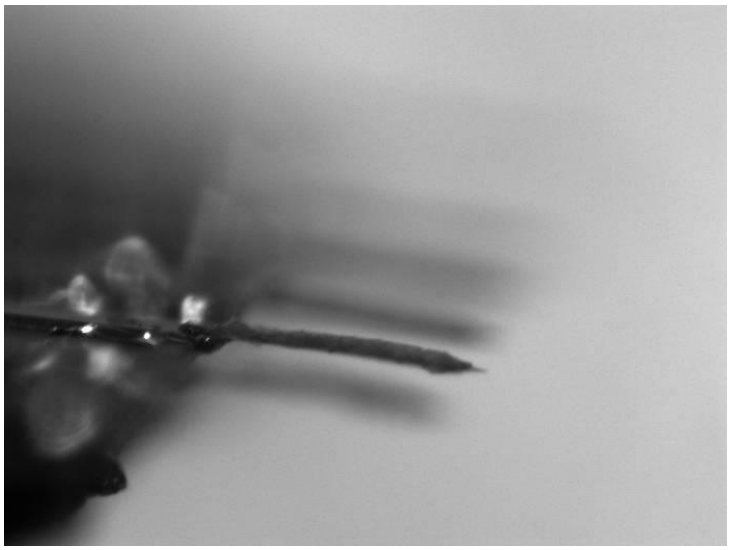

(b)

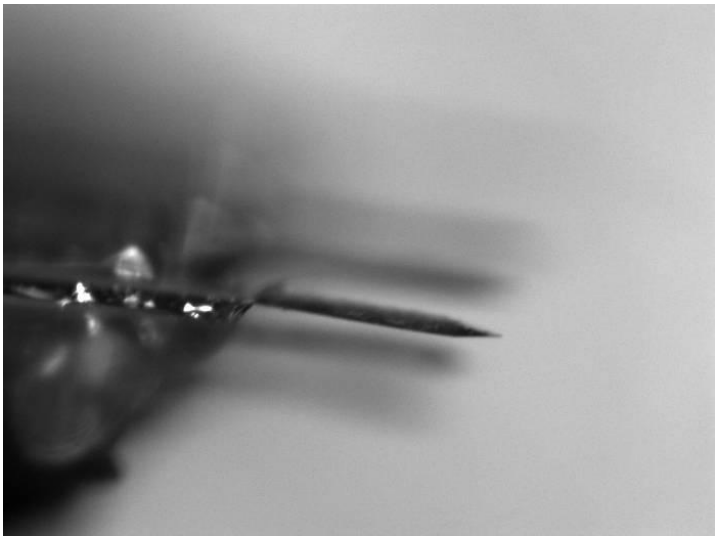

Figure 6.6: Microcantilever array with hydrogel atop beams

Poly(methacrylic acid) crosslinked with 20 mol% polycaprolactone diacrylate photopolymerized atop 8 microcantilever array. Images of (a) second cantilever and (b) third cantilever in the array with swollen hydrogel causing beam to deflect downward

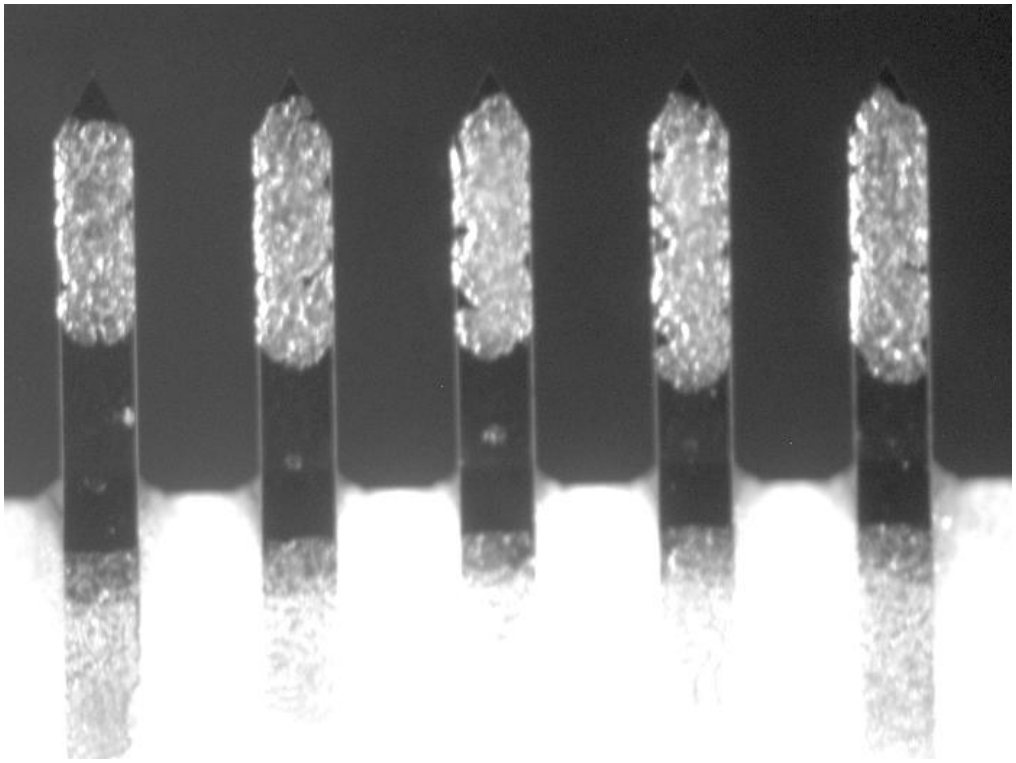

Figure 6.7: Microcantilever array with fluorescently-labeled hydrogel

Poly(methacrylic acid) crosslinked with 20 mol% polycaprolactone diacrylate and 1% fluorescent monomer was photopolymerized atop an 8 microcantilever array and imaged with a FITC filter.

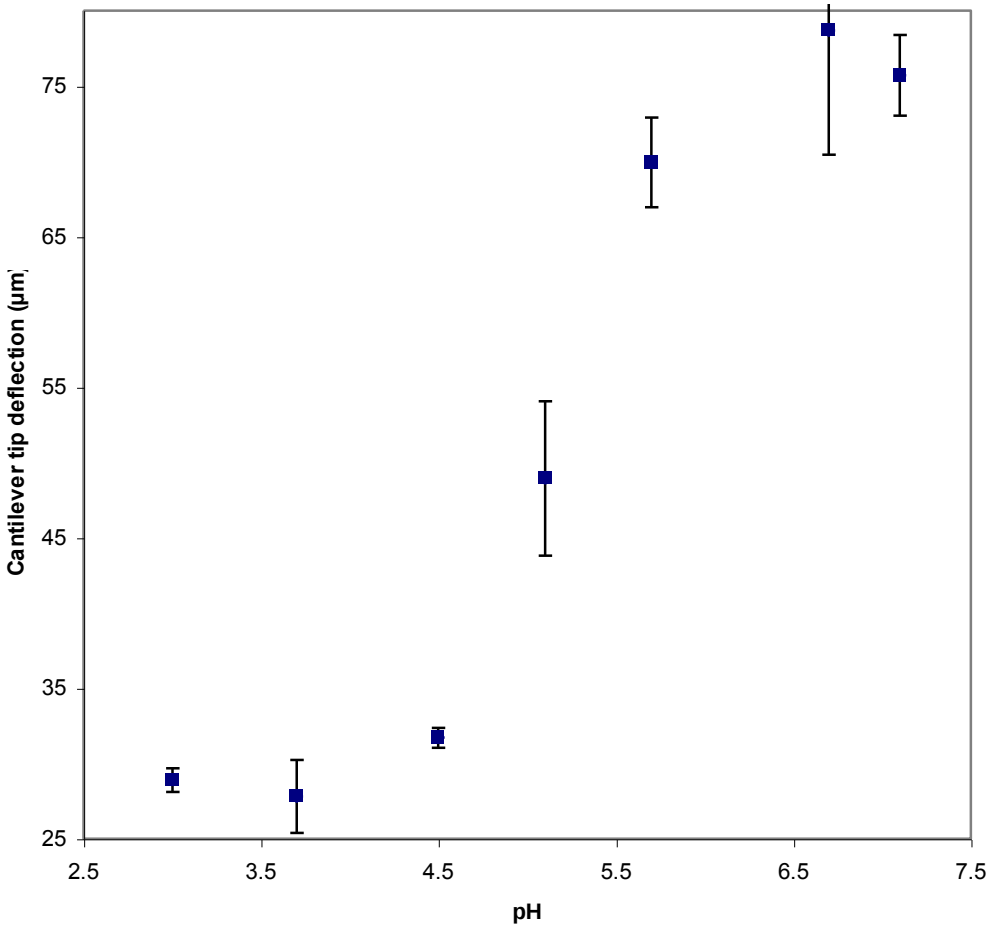

Figure 6.8: Microcantilever with pH-responsive hydrogel atop beam

Poly(methacrylic acid) crosslinked with 20 mol% polycaprolactone diacrylate was photopolymerized atop single microcantilevers and swollen in phosphate-citrate buffers of varying pH and constant ionic strength (0.5M).

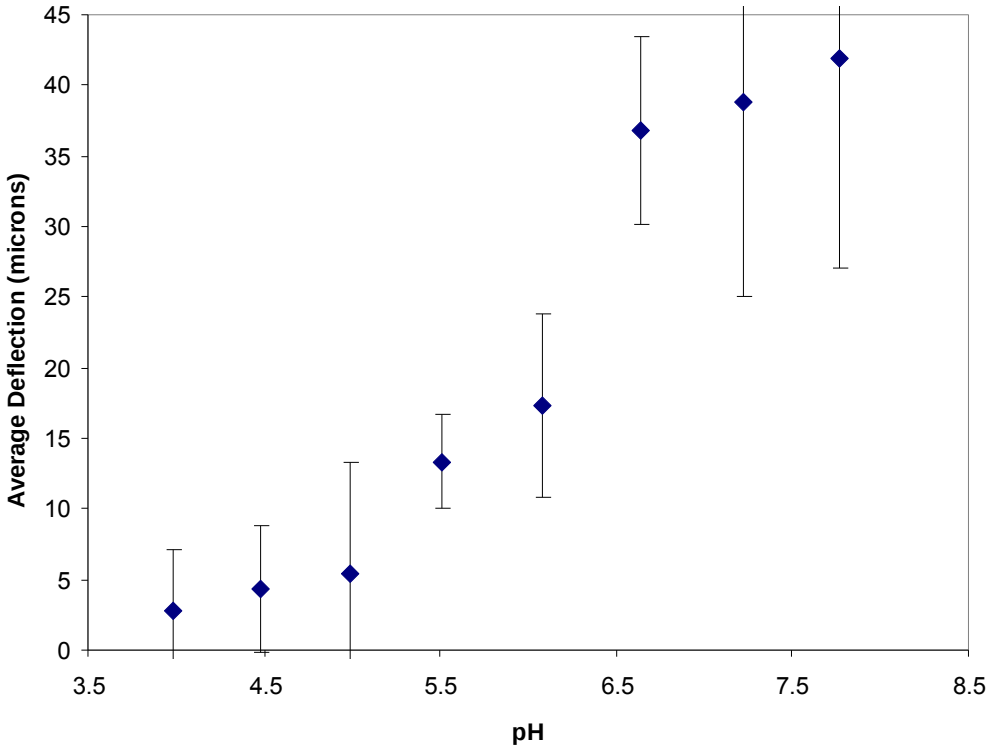

Figure 6.9: Average deflection versus pH from high pH to low pH

Poly(methacrylic acid) crosslinked with 20 mol% polycaprolactone diacrylate photopolymerized atop microcantilever array and swollen in phosphate-citrate buffers of varying pH and constant ionic strength (0.5M) from high pH to low pH

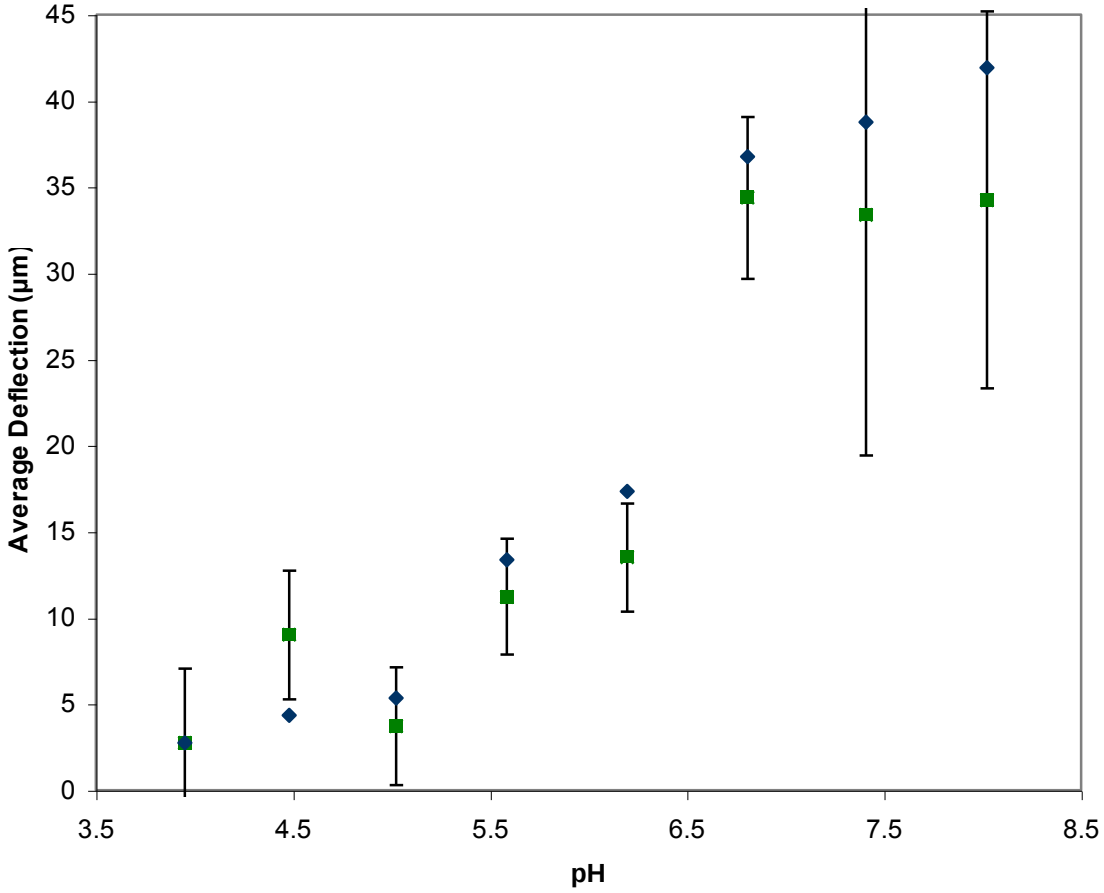

Figure 6.10: Average deflection versus pH from low pH to high pH

Poly(methacrylic acid) crosslinked with 20 mol% polycaprolactone diacrylate photopolymerized atop microcantilever array and swollen in phosphate-citrate buffers of varying pH and constant ionic strength (0.5M). Equilibrium deflection of microcantilevers in array when measured from low pH to high pH -■-, and high to low pH -♦-

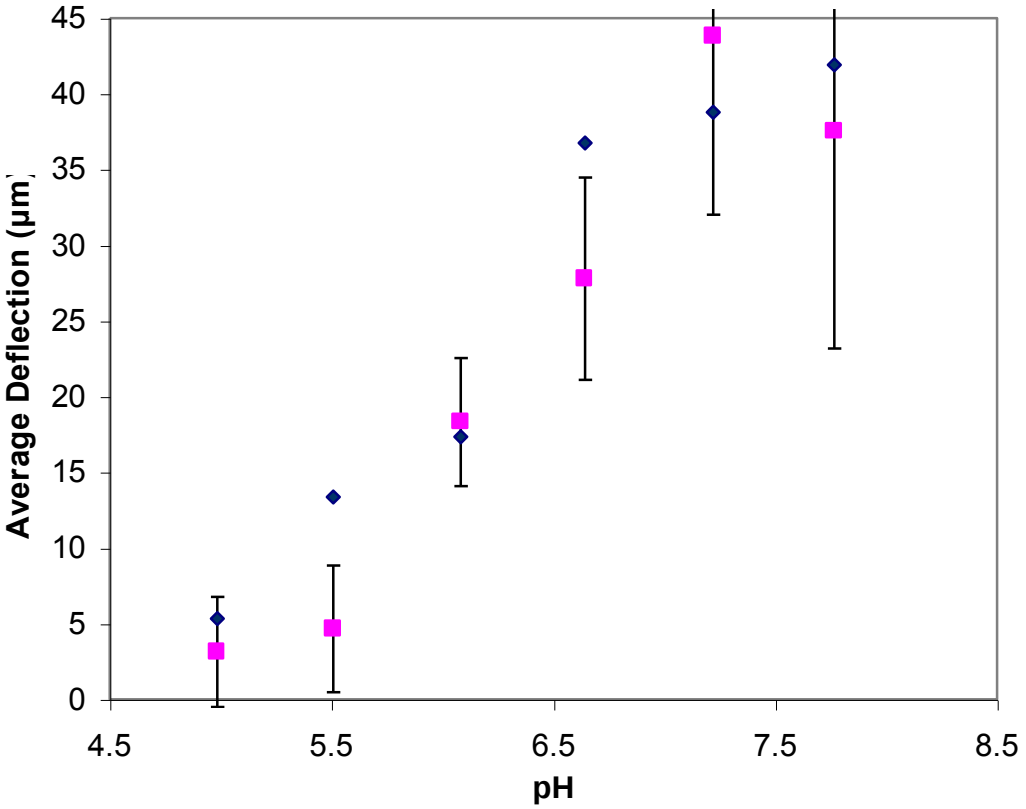

Figure 6.11: Average deflection versus pH with different equilibration times

Equilibration time of array with phosphate-citrate buffer was 5 minutes -■-, and 2 hours -♦-.

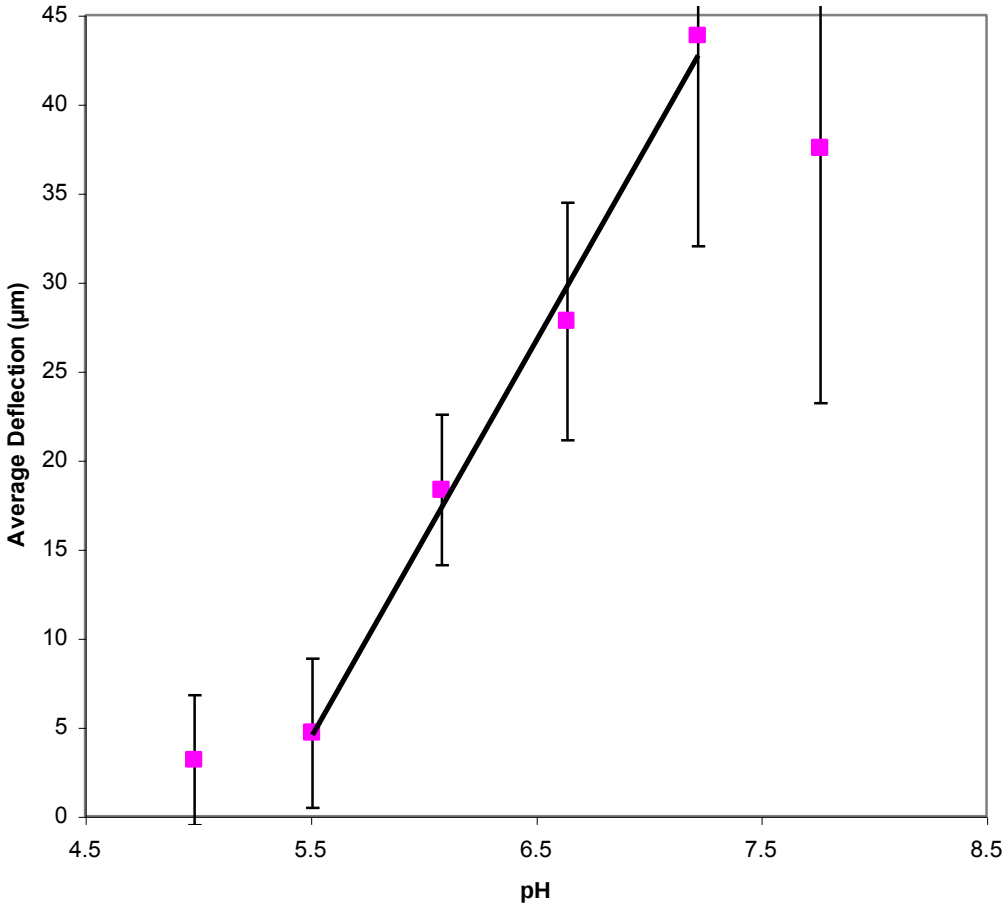

Figure 6.12: Ultrahigh sensitivity of microcantilever sensing array

Average deflection versus pH of poly(methacrylic acid) crosslinked with polycaprolactone diacrylate on 8 microcantilever array and equilibration time of 5 minutes. Linear fit of data in maximum sensitivity region yielded sensitivity of 1nm / 4.5e-5 ΔpH.

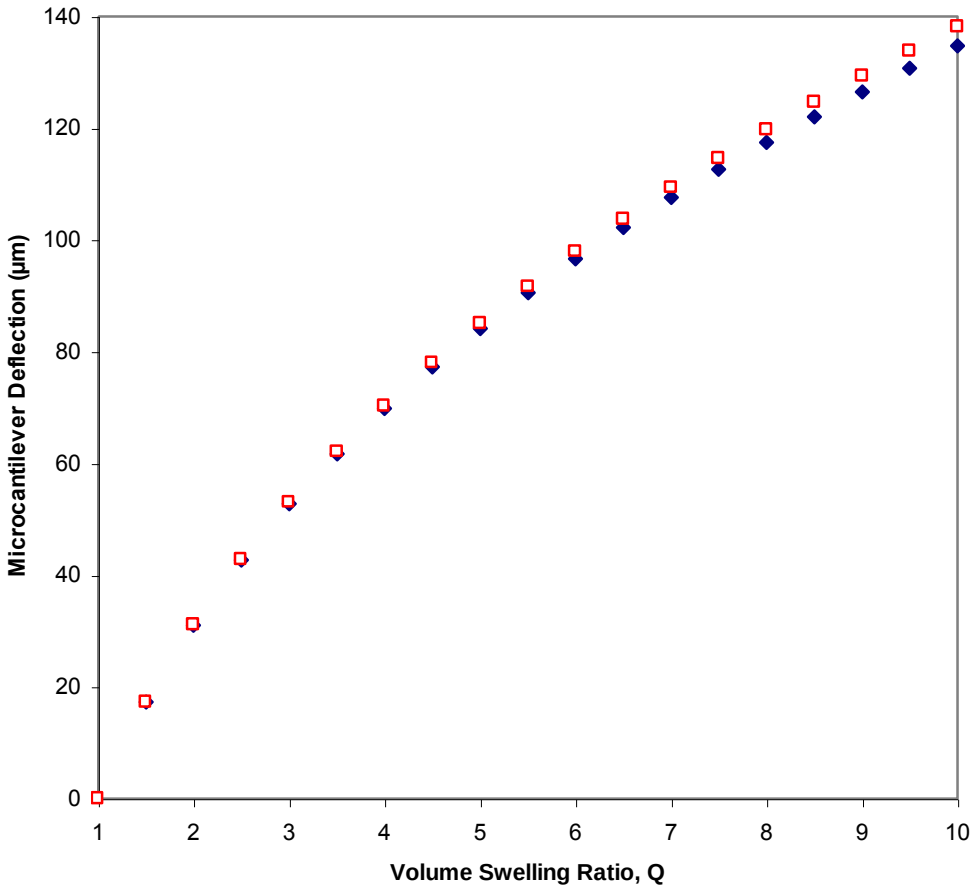

Figure 6.13: Test of small deflection assumption in composite beam with no slip at the boundary

Small deflection assumption in composite beam model showed less than 1% error up to 85 microns of deflection for the composite beams fabricated in this thesis. Without assumption -□- and with small deflection assumption -♦-

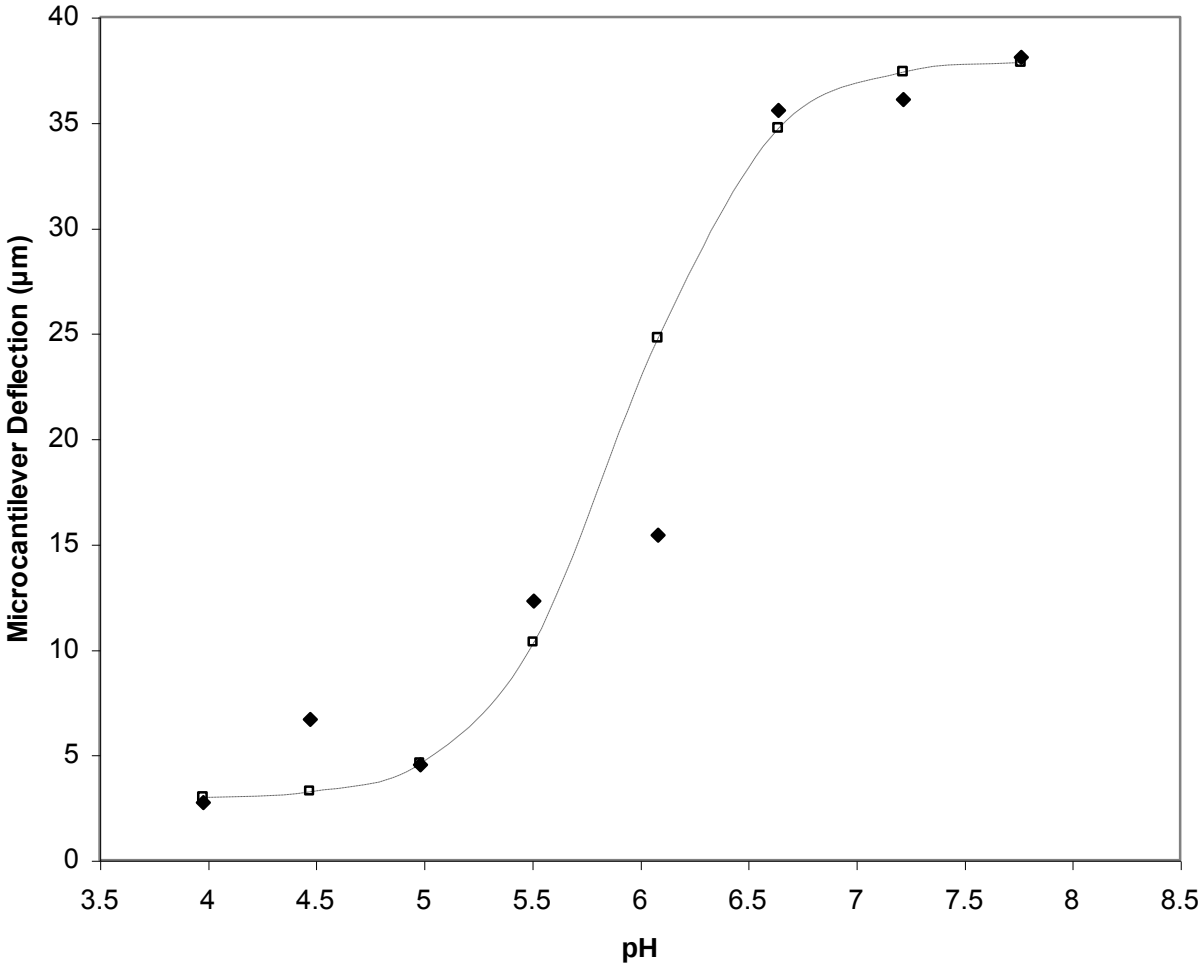

Figure 6.14: Composite cantilever model comparison to experimental deflection data

Composite Cantilever Model -□- and experimental deflection data -♦- averaged from high pH to low pH and low pH to high pH equilibrium deflection studies.

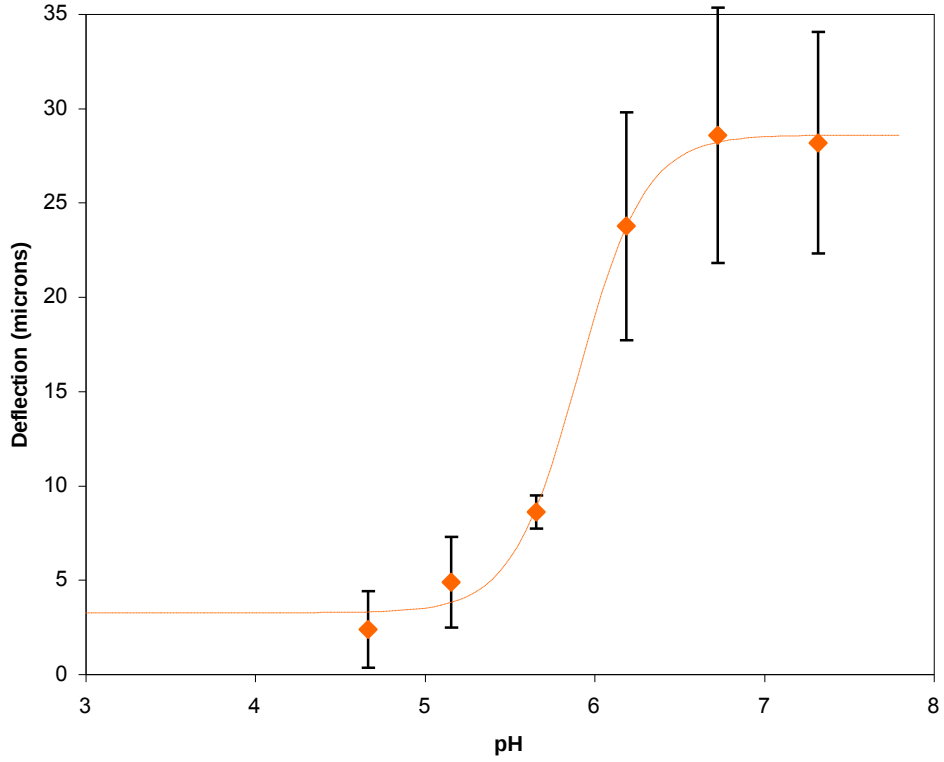

Figure 6.15: Microcantilever deflection versus pH in serum

Microcantilever array with poly(methacyrlic acid) crosslinked with 20% polycaprolactone diacrylate in pH buffers with 10% fetal bovine serum (FBS). Solid line is hyperbolic tangent fit of the data.

REFERENCES

1. Hansma, P.K., et al., *Scanning tunneling microscopy and atomic force microscopy: application to biology and technology.* Science, 1988. **242**: p. 209-216.
2. Boisen, A. and Thundat, T., *Design & fabrication of cantilever array biosensors.* Mater Today, 2009. **12**(9): p. 32-38.
3. Moulin, A.M., et al., *Microcantilever-based biosensors.* Ultramicroscopy, 2000. **82**(1-4): p. 23-31.
4. Chilkoti, A., et al., *The relationship between ligand-binding thermodynamics and protein-ligand interaction forces measured by atomic force microscopy*. Biophys J, 1995. **69**(5): p. 2125-30.
5. Boland, T., Ratner, B.D., *Direct measurement of hydrogen bonding in DNA nucleotide bases by atomic force microscopy.* Proc Natl Acad Sci USA, 1995. **12**: p. 5297-301.
6. Moulin, A.M., et al., *Microcantilever-based biosensors.* Ultramicroscopy, 2000. **82**(1-4): p. 23-31.
7. Timoshenko, S., *Analysis of bimetal thermostats*, J Opt Soc Am, 1925. **11**: p. 233.
8. Chu, W., et al., *Analysis of tip deflection and force bimetallic cantilever microactuator*, J Micromech Microeng, 1993. **3**: p. 4-7.

9. Lavrik, N.V., M.J. Sepaniak, and P.G. Datskos, *Cantilever transducers as a platform for chemical and biological sensors.* Rev Sci Instrum, 2004. **75**(7): p. 2229-2253.

10. Bergese, P., et al., *Investigation of a biofunctional polymeric coating deposited onto silicon microcantilevers.* Appl Surf Sci, 2007. **253**(9): p. 4226-4231.

11. Itoga, K., et al., *Cell micropatterning using photopolymerization with a liquid crystal device commercial projector.* Biomaterials, 2004. **25**(11): p. 2047-2053.

12. Itoga, K., et al., *Micropatterned surfaces prepared using a liquid crystal projector-modified photopolymerization device and microfluidics.* J Biomed Mater Res A, 2004. **69A**(3): p. 391-397.

13. Itoga, K., et al., *Maskless liquid-crystal-display projection photolithography for improved design flexibility of cellular micropatterns.* Biomaterials, 2006. **27**(15): p. 3005-3009.

14. Itoga, K., et al., *Second-generation maskless photolithography device for surface micropatterning and microfluidic channel fabrication.* Anal Chem, 2008. **80**: p. 1323-1327.

15. Giessibl, F. J., *Advances in atomic force microscopy*. Rev Mod Phys, 2003. **75**: p. 949.

16. Humphris, A.D., Miles, M.J. and Hobbs, J.K.*, A mechanical microscope: High-speed atomic force microscopy*, Appl Phys Lett, 2005. **86**.

17. Hilt, J.Z., *Novel micro- and nanoscale diagnostic and therapeutic devices based on intelligent polymer networks*, in *Chemical Engineering*. 2004, The University of Texas: Austin, TX.

18. Bashir, R., et al., *Micromechanical cantilever as an ultrasensitive pH microsensor.* Appl Phys Lett, 2002. **81**(16): p. 3091-3093.

19. Lei, M., et al., *Integration of hydrogels with hard and soft microstructures.* J Nanosci Nanotechno, 2007. **7**(3): p. 780-789.

20. Sorber, J., et al., *Hydrogel-based piezoresistive pH sensors: Investigations using FT-IR attenuated total reflection spectroscopic Imaging.* Anal Chem, 2008. **80**(8): p. 2957-2962.

21. Hilt, J.Z., et al., *Ultrasensitive biomems sensors based on microcantilevers patterned with environmentally responsive hydrogels*. Biomed Microdevices, 2003. **5**(3): p. 177-184.

CHAPTER 7: BIODEGRADABLE MICROSENSORS FROM POROUS SILICON RUGATE FILTERS AND PH-RESPONSIVE HYDROGELS

7.1 Introduction

The incorporation of environmentally responsive hydrogels and porous silicon rugate filters is an exciting prospect for *in vivo* biosensing. This is primarily because the resulting composite achieves both sensing and self-reporting without the need for an energy source within the body. The porous silicon rugate filter's characteristic wavelength of reflectance is dependent on the average refractive index of the composite (Figure 7.1). As the hydrogel responds to a change in its environment by swelling, the peak reflectance of the sensing device will shift. This shift could be observed wirelessly through several centimeters of biological tissue. The incorporation of stimuli responsive hydrogels with any transducer is promising since hydrogels can be made to respond to such a variety of biological stimuli. Previously, a thermoresponsive poly(N-isopropyl acrylamide) hydrogel has been polymerized within porous silicon to generate sensing nanoparticles. The volume phase transition correlated to a change in optical thickness in a reversible manner [1].

Porous silicon rugate filters and poly(methacrylic acid)-based hydrogels have both been separately synthesized to biodegrade *in vivo*. If combined, the resulting sensor would be a novel completely biodegradable biosensor. A

biodegradable, pH-responsive hydrogel network consisting of poly(methacrylic acid) crosslinked with polycaprolactone diacrylate is particularly appealing for biosensing applications because polycaprolactone undergoes slow degradation. Polycaprolactone is also desirable as a crosslinker since its degradation products are either metabolized or easily eliminated by renal secretion from the body[2]. Because the degradation of this hydrogel occurs exclusively at the crosslinks, the degradation rate of these networks can be tuned by the quantity of crosslinking.

Similarly, the degradation rate of the porous silicon transducer can be tuned. This is achieved either by varying the pore volume of the filter or by chemically altering the surface. In the following studies, all PSiRF were immediately chemically treated with 1,8-Nonadiyne, which reacts covalently with silicon. The π bonds present in this molecule interact strongly with each other to create a very chemically stable surface. An advantage of 1,8-Nonadiyne over standard self assembled monolayer treatments is that this chemistry will not create multilayers.

When designing a microsensor for *in vivo* use, a primary concern must be the biocompatibility of the device and the toxicity of its degradation products. Silicon is an essential trace element in the body. While some degradation products of porous silicon, particularly the silicic acid compounds, can be toxic at high doses, it is known how these are processed and efficiently eliminated from the body through the urine [3]. The primary biodegradation product of porous silicon, orthosilicic acid (Si(OH)4), is predominantly absorbed by humans and is

naturally found in numerous tissues. The biocompatibility of porous silicon appears to depend on its surface functionality and thus degradation rate. Previous work has established the relatively low toxicity of porous silicon both in cell and live animal studies[4].

Prof. John Justin Gooding and his Biosensors and Biodevices research group at the University of New South Wales in Sydney, Australia, have made significant progress towards *in vivo* sensing utilizing porous silicon rugate filters. These filters contain a sinusoidally varying refractive index created by electrochemical etching of a silicon substrate[4] (Figure 7.2). By varying the current density across a silicon wafer during the etching process, regions of high and low porosity are created. Constructive interference is generated when light is shined on a porous silicon rugate filter and this leads to a sharp reflectivity maximum (Figure 7.3).

Porous silicon rugate filters are inexpensive to produce and easy to make. Gooding *et al*. have produced these filters to reflect strongly and narrowly at a characteristic wavelength in the near infrared (IR) region[5]. The reflectivity peak is tuned by varying the substrate dopant type and level, the applied current density, and the electrolyte type and concentration [6]. This particular region of reflectance is desirable because near IR light is known to penetrate tissue to a depth of several centimeters[7]. This would enable the monitoring of an implanted sensor by simply irradiating the area with light and collecting the reflectance spectrum with specialized equipment.

The porosity of rugate filters can be varied to allow specific absorption of proteins from solution. Gooding *et al*. demonstrated the absorption of carbonic anhydrase and the exclusion of bovine serum albumin (BSA) due to size[8]. In these filters, protein absorption results in a density change within the pores and thus a shift in the reflective IR peak. Since the filter is naturally hydrophobic, the surface chemistry must be changed to allow biological fluids to penetrate the pores. The Gooding lab utilizes its expertise in self assembled monolayers (SAMs) to generate hydrophilic pores. Through further changes of the surface chemistry, that laboratory has shown the ability to resist biofouling and thus increase the lifetime of these sensing devices for *in vivo* applications[9].

Thus far, the absorption of proteins into porous silicon sensing devices has been dictated by the size of pores created in silicon. By polymerizing a hydrogel layer atop porous silicon, one could vary and control this size exclusion. Stimuli responsive hydrogels change their network mesh size in response to their environment. It is in this way that Peppas *et al*. have developed particles for oral protein delivery[10, 11]. In their collapsed state, the mesh size of certain hydrogels is too small to allow proteins to diffuse through the network. In the swollen state of the hydrogel, the mesh size is increased and allows protein to freely diffuse through.

The incorporation of stimuli responsive hydrogels and silicon rugate filters would also have interesting applications in drug delivery. If loaded with drug, the porous silicon filter could be utilized as an easily monitored drug reservoir *in vivo*.

As the drug is dispensed, the density of the rugate filter would change and a reflectivity shift would be experienced. The diffusion rate of the drug from the reservoir would vary depending on whether the hydrogel existed in its swollen or deswollen state. In this way, controlled drug delivery from a monitorable drug reservoir would be achieved.

In this chapter, p-type silicon wafers were electrochemically etched to produce porous silicon rugate filters (PSiRF) which reflect strongly and narrowly in the first optical window for biological tissue (Figure 7.4) [12]. PSiRFs were immediately stabilized with a dense alkyl monolayer of 1,8-Nonadiyne. A biodegradable, pH-responsive hydrogel composed of poly(methacrylic acid) crosslinked with polycaprolactone diacrylate was photopolymerized within the pores. This incorporation resulted in a red-shift of the reflectance peak. The reflectance spectra of the resulting composite was measured in phosphate-citrate buffer solutions of varying pH and constant ionic strength from 400-1200nm when exposed to white light. A linear shift in the reflectance peak was seen over the pH range 2.2 to 8.8. PSiRFs reflectance was also measured in solutions of varying salt concentration and without hydrogel.

The overall objective of these studies was to discover if a porous silicon rugate filter could serve as a transducer for a biodegradable, environmentally-responsive hydrogel. It was hypothesized that the pH-responsive hydrogel would experience a change in its swollen volume with pH change while contained within the pore. This volume difference would result in a change to the average

refractive index within the nanopore. Since the reflectivity peak of the PSiRF is dependent upon the average refractive index, a shift would be seen corresponding to the pH change (Figure 7.5). If successful, this would prove to be a particularly novel hydrogel-based microsensor because the reflectance peak of PSiRFs can exist in the optical tissue window enabling communication with these sensors *in vivo* through several centimeters of tissue. Additionally, this microdevice would demonstrate a completely biodegradable sensor where both the sensing component and the transducer are degraded by hydrolysis. Figure 7.6 shows the proposed lifecycle of this microsensor *in vivo*.

7.2 Materials and Methods

7.2.1 Preparation of Porous Silicon Rugate Filters

P-type silicon (100) wafers of thickness 350 nm (0.007 Ω cm, Institute of Electronics Materials Technology, Warsaw, Poland) were cut into 1 cm squares, and then sonicated in ethanol (Sigma-Aldrich, St. Louis, MO, distilled from sodium) and acetone each for 5 minutes. The wafers were placed in a 25% hydrofluoric acid (Sigma-Aldrich, St. Louis, MO) in ethanol solution that allowed them to be electrochemically etched to 55% porosity. A platinum electrode was placed in the hydrofluoric acid solution, and the silicon wafer was directly connected to the current source (Figure 7.7). Etching lasted approximately 15 minutes. After etching, the PSiRF was washed with ethanol to remove any residual hydrofluoric acid and dried with nitrogen. Immediately following etching,

the porous silicon was stabilized against further oxidation and corrosion by the creation of a dense alkyl monolayer of 1,8-Nonadiyne.

The 1,8-Nonadiyne (98%, Sigma-Aldrich, St. Louis, MO) was redistilled from sodium borohydride (Sigma-Aldrich, St. Louis, MO) under reduced pressure and collected over molecular sieves [6]. Immediately prior to reaction, 1,8-Nonadiyne was dried by a freeze-thaw method in an atmosphere alternated between argon and vacuum. The porous silicon was reacted with 1,8-Nonadiyne for 3 hours at 170°C under argon then rinsed with dichloromethane (distilled from calcium hydride) and ethanol. The PSiRF was stored in dichloromethane overnight to remove any unreacted 1,8-Nonadiyne. The remaining alkyne was bound covalently to the silicon to block access by water to the silicon surface and passivate the material (Figure 7.8).

7.2.2 Photopolymerization of hydrogel within PSiRF

A monomer solution containing methacrylic acid, polycaprolactone diacrylate, and the UV free-radical initiator, 2,2-dimethoxy-2-phenylacetophenone, was prepared as described in Section 4.2.3. Prior to use, it was purged with argon for 30 minutes to remove oxygen from the monomer solution. The stabilized porous silicon rugate filter was immersed in monomer solution for 20 minutes to allow for diffusion of the solution into the chemically-stabilized nanopores. After removal from the solution, a microscopic glass slide was placed atop the PSiRF and hydrogel polymerization was initiated under UV light in an argon atmosphere for 30 minutes. The PSiRF filled with hydrogel was

rinsed in deionized water to remove any residual photoinitiator or unreacted monomer not covalently bound to the hydrogel. Additionally, a non-degradable hydrogel was photopolymerized within the pores using tetraethylene glycol dimethacrylate as the crosslinker.

7.2.3 Measurement of Reflectance

Porous silicon rugate filters were irradiated with white light and the percent reflectance recorded in the range 400 - 1600 nm with a J/Y SPEK 1681 spectrometer. The spectra were obtained as the average of 100 scans with the reference being single crystal silicon. Spectra were obtained from samples both in air and submerged in phosphate-citrate buffers of varying pH and ionic strength. In some studies, the dynamic behavior of this pH sensor was obtained by acquiring spectra as rapidly as was possible with this method of data acquisition. In all studies not designated as dynamic, one hour was used as the equilibration time for the porous silicon rugate filter and the buffer solution.

7.2.4 Refractive Index Measurement of Bulk Hydrogel

Hydrogel films of 1mm thickness were polymerized by pipetting monomer solution between two glass microscopic slides separated by a Teflon spacer and initiating polymerization under UV light in an argon atmosphere for 20 minutes. The refractive index of the bulk hydrogel was measured by placing these films atop silicon wafers and obtaining the reflectance spectra when light was focused on the top of the film. Hydrogel films were swollen in phosphate-citrate buffers in

the pH range of 3.7 to 7.4 of constant ionic strength and allowed to equilibrate for 2 hours. Films were blotted with a KimWipe and spectra were acquired immediately to minimize data shift due to drying of the film in air.

7.3 Results and Discussion

7.3.1 Hydrogel Polymerization within PSiRF

The polymerization of poly(methacrylic acid) crosslinked with 1 mol percent tetraethylene glycol dimethacrylate within the porous silicon rugate filter resulted in a 20 nm red shift of the reflectance peak as seen in Figure 7.9. This red shift confirmed the incorporation of hydrogel within the nanopores. Immersing the filter in water and allowing the hydrogel to swell resulted in an additional red shift of 14 nm. This red shift confirms that the nanopores were not completely filled with hydrogel prior to swelling. The wavelength of maximum reflectance for the PSiRF with swollen hydrogel was 711 nm. This reflectance is desirable since it occurs within the first optical window for biological tissue that exists between 650 and 950 nm [12].

7.3.2 Relating hydrogel volume change in PSiRF to reflectance peak shift

For these composites to be useful as pH microsensors, it was important to understand the volume of hydrogel present in the pores at both the swollen (high pH) and unswollen (low pH) states. Equation 7.1 was used to calculate the porosity of the PSiRF immediately after its passivation with 1,8-Nonadiyne. In Equation 7.1, n_{psi} is the refractive index of the porous silicon rugate filter, n_{si} is

the refractive index of silicon, and here n_{pore} is the refractive index of air. Upon measurement of the refractive index of the porous silicon rugate filter, Equation 7.1 was used to solve for the silicon porosity, P.

$$n_{psi}^{1/3} = (1-P)*n_{Si}^{1/3} + P*n_{pore}^{1/3} \quad \textbf{Equation 7.1}$$

$$n_{psi}^{1/3} = (1-P)* n_{Si}^{1/3} + Q*n_{layer}^{1/3} + (P-Q)*n_{pore}^{1/3} \quad \textbf{Equation 7.2}$$

After hydrogel was polymerized within the pores, the refractive index was measured again. This time, Equation 7.2 was used to calculate Q, the volume of hydrogel within the pores. Here, n_{layer} is the average refractive index of the hydrogel. From this calculation it was estimated that the pores were 20% filled with hydrogel. It was expected that completely filling the pores with hydrogel would be undesirable as nanoconfinement would not allow the hydrogel to swell in response to changes in its environment. Based on bulk equilibrium swelling studies presented in Chapter 5, it was hypothesized that this amount of hydrogel in the pores would allow ample volume for swelling at both high and low pH.

7.3.4 Dynamic behavior of PSiRF with pH-responsive hydrogel

The following study was performed to determine the response time of microsensors composed of PSiRF and pH-responsive hydrogel. The PSiRF was submerged in a phosphate-citrate buffer of pH 7 for 2 hours. The reflectance spectrum was recorded. At time zero, the buffer solution was removed and

replaced with one of pH 3. The reflectance spectrum was measured at varying intervals thereafter (Figure 7.10). The reflectance peak blue shifted 8 nm with the drop in pH. The sensor reached equilibrium between 10 and 30 minutes after the pH change. As a result of this dynamic study, one hour was used hereafter as the equilibration time for the porous silicon rugate filters.

7.3.5 Equilibrium Effect of pH on reflectance peak

A PSiRF with poly(methacrylic acid) crosslinked was 5 mol percent polycaprolactone diacrylate was submerged in phosphate-citrate buffer solutions of consistent ionic strength ranging from pH 2.2 to 8.8. One hour was allotted for the hydrogel within the pores to reach its equilibrium-swollen volume. The reflectance peak experienced a red shift with increased pH. This behavior appeared linear over the pH range 2.2 to 8.8 with a maximum reflectivity peak shift of approximately 13nm. These data are shown in Figure 7.11 (n=3).

The red shift in the reflectance peak is a result of an increase in the average refractive index of the nanopore. An increase in the average refractive index within the nanopore could occur in two ways. First, since the refractive index of hydrogel is higher than either air or water, if the percentage by volume of hydrogel within the pore increases, the average refractive index of the pore would increase. Second, the refractive index of the hydrogel increases with pH without the swollen volume of the material increasing.

This second phenomena appears more likely since the reflectance peak red-shifts linear over a very large pH range. If this shift were a result of a volume

change of the hydrogel within the pore, one would expect a steep transition around the pKa of the material or about pH 5.8. It is hypothesized that issues of nanoconfinement resist the large volume change commonly experienced in the transition of environmentally responsive hydrogels. Confinement of the hydrogel within rigid silicon nanopores might severely limit the swelling capacity of these materials and thus the average refractive index change of the pores are dominated by a change in the refractive index of the hydrogel, not resulting from a change in the percentage composition of the pore. Further studies were conducted on unconfined hydrogel thin films to determine whether these materials experienced a similar shift in refractive index as the nanoconfined ones and are discussed in Section 7.3.5.

The reflectance spectrum of a PSiRF without pH-responsive hydrogel was measured to serve as a control. The PSiRF was placed in phosphate-citrate buffers of pH 2.2 and 8.8 respectively (Figure 7.12). The pH shift resulted in no significant reflectivity peak shift. It was concluded from this study that without the photopolymerization of hydrogel within the nanopores, the PSiRF alone could not respond to pH changes in solution.

7.3.6 Effect of salt concentration on reflectivity peak

The reflectance spectrum from 900 to 1200 nm was obtained for a PSiRF with poly(methacrylic acid) crosslinked with 5 mol percent polycaprolactone diacrylate in solutions of varying ionic strength and consistent pH (Figure 7.13). Phosphate-citrate buffers were prepared with either no potassium chloride or

potassium chloride added to concentrations 0.5M and 1.5M. A pH of 5.8 was chosen for testing since these pH-responsive hydrogels undergo a steep volume transition around this pH. An equilibration time of 1 hour was allotted for each sensor. Varying the ionic strength of the buffer by the addition of different quantities of potassium chloride did not significantly affect the reflectivity peak. This result suggests that a pH microsensor of this type would be relatively stable to changes in ionic strength.

7.3.7 Effect of pH on refractive index of hydrogel

The relative reflectance of hydrogel thin films was measured for the wavelength range of 900 and 1200nm. First, hydrogel thin films of approximately 1mm thickness were swollen to equilibrium in a range of pH buffers. Next, the hydrogel was removed from solution, blotted with a Kimwipe to remove surface water, and placed on a silicon wafer. The reflectance spectra were obtained immediately to minimize shifting of data due to hydrogel drying. The refractive index of the bulk hydrogel was measured by placing these films atop silicon wafers and obtaining the reflectance spectra when light was focused on the top of the film.

The refractive index of these hydrogels around 1050nm is of most interest here (Figure 7.14). This study was conducted for comparison to the behavior observed with nanoconfined materials which resulted in a shift in reflectivity peak of the PSiRF from 1043 to 1056 nm (Figure 7.11). The objective of this study was to determine if the unconfined hydrogels demonstrate a large refractive

index change around the pK_a of the pH-responsive hydrogel. Based on previous studies with nanoconfined hydrogels, it was hypothesized that they would not. Indeed, these materials underwent a gradual increase in reflectance with pH and no stepwise change around the pK_a. This rudimentary study supports the hypothesis presented in Section 7.3.3 that the broad shift in reflectivity peak with pH is due to a shift in refractive index of the hydrogel that exists outside of the pH-responsive volume transition of this material.

7. 4 Conclusions

A novel microsensor which consisted of a PSiRF with pH-responsive hydrogel photopolymerized within the pores was successfully fabricated. Two hydrogel formulation, one degradable and one nondegradable, were tested to determine the effect degradation had on the sensing element. The hydrogels tested were poly(methacrylic acid) crosslinked with tetraethylene glycol dimethacrylate and poly(methacrylic acid) crosslinked with polycaprolactone diacrylate. Silicon was electrochemically etched in hydrofluoric acid to generate the porous silicon rugate filter with its reflectivity peak in the near IR region. A pH-responsive hydrogel was photopolymerized within the pores using a UV free-radical polymerization. In one study, the silicon nanopores were calculated to consist of 20% dry hydrogel. The reflectivity peak of this sensor varied linearly with pH in the range 2.2 to 8.8 pH. The reflectivity peak did not change significantly when the ionic strength of the pH buffers was altered using potassium chloride.

This work shows promise towards utilizing porous silicon rugate filters as transducers for environmentally responsive hydrogels for biosensing applications. Porous silicon rugate filters are garnering increased attention as components for *in vivo* biosensors due to their ability for remote readout through tissue. Additionally, PSiRFs show promise as transducers since their hydrolytic degradation is tunable based on the surface stabilization chemistry employed. A biodegradable, pH-responsive hydrogel was polymerized within the pores of a porous silicon rugate filter to successfully generate a novel, completely degradable sensor.

FIGURES

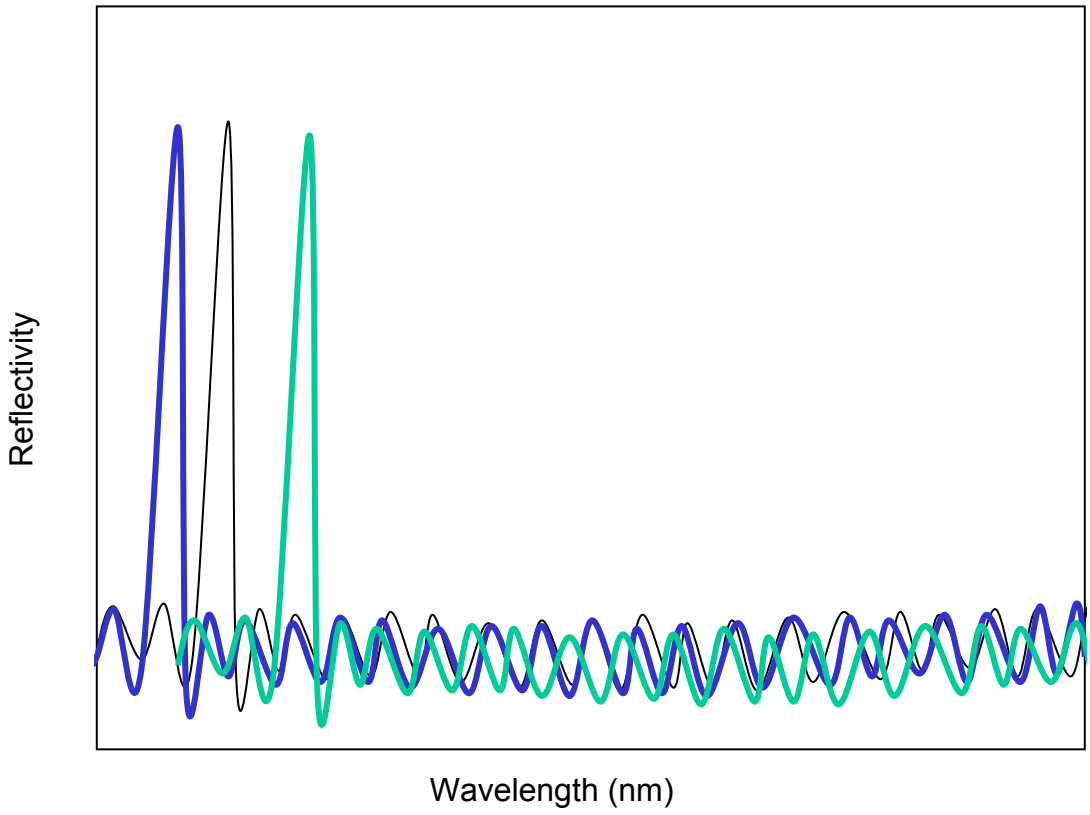

Figure 7.1: Porous Silicon Rugate Filter (PSiRF) reflectivity

PSiRF shows a high reflectivity "stop-band" around a characteristic wavelength and very low reflectivity elsewhere. A shift in the reflectivity peak to higher wavelength corresponds to an overall increase in the refractive index (green). A shift to lower wavelength corresponds to an overall decrease in refractive index (blue).

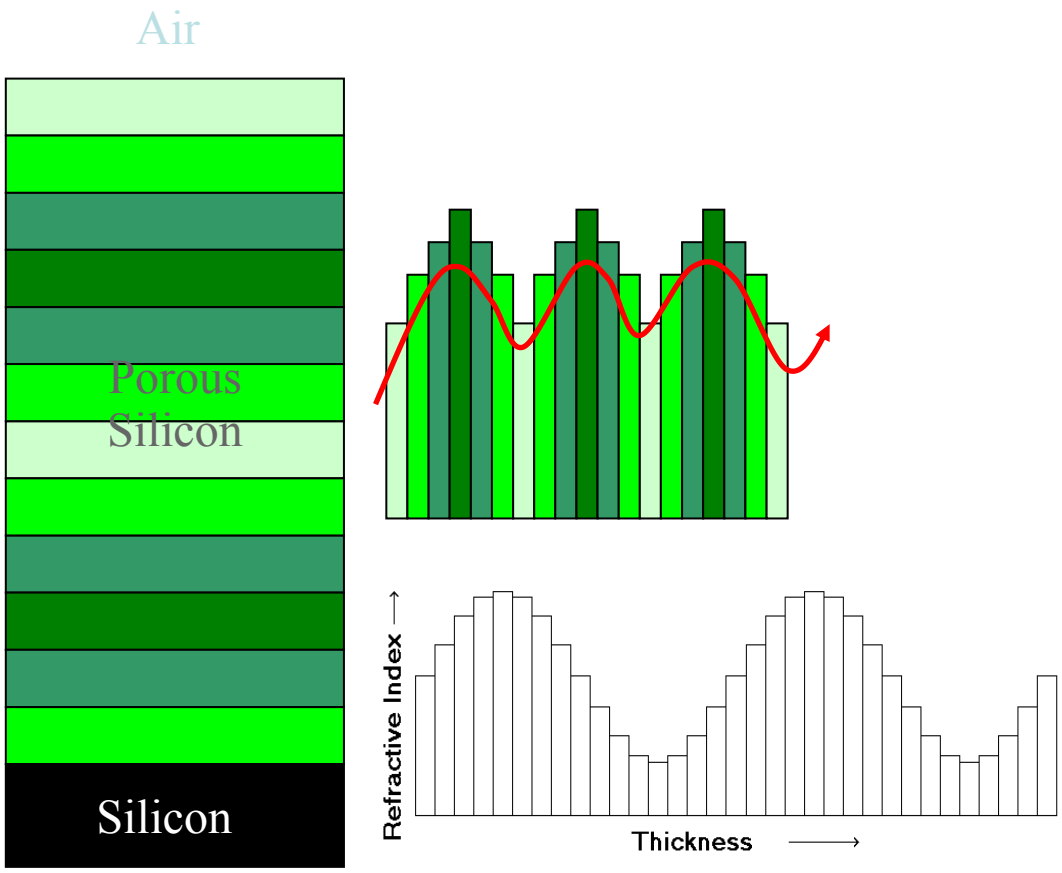

Figure 7.2: Varying refractive index across thickness of Porous Silicon Rugate Filter

PSiRFs incorporate a sinusoidally varying refractive index to generate sharp reflectivity peaks caused by constructive interference of light [13].

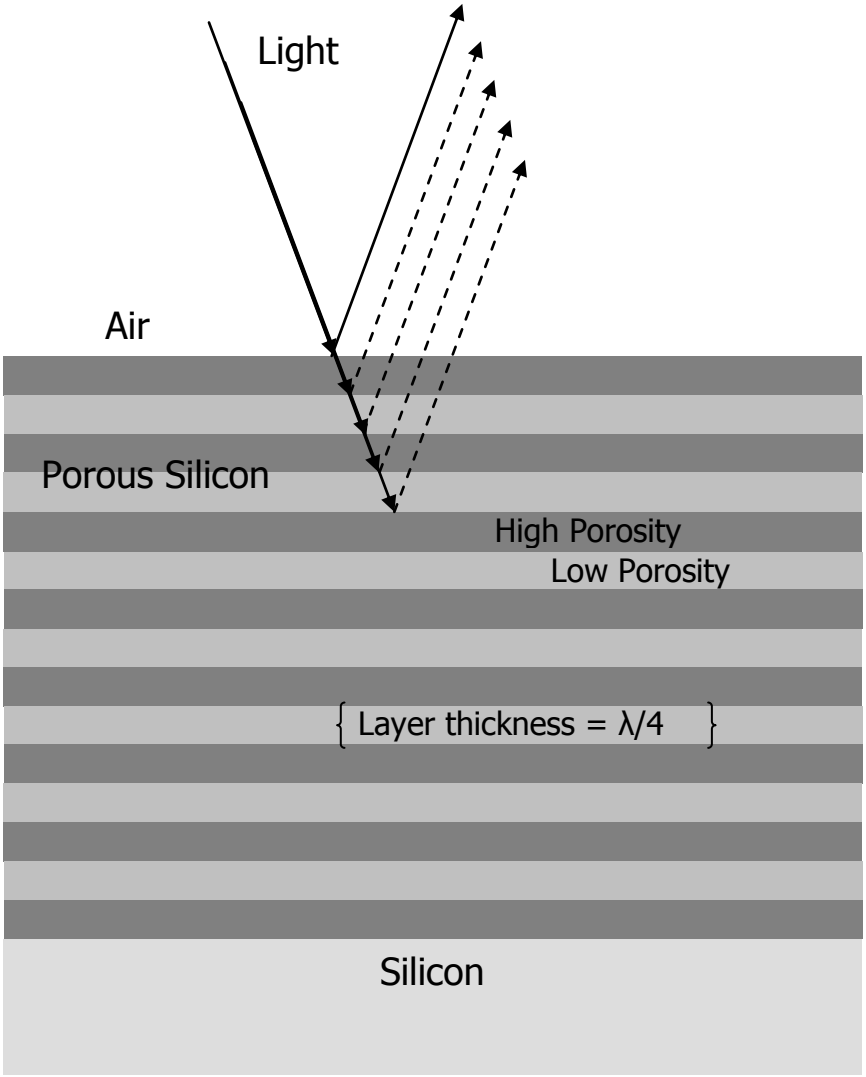

Figure 7.3: Constructive interferance of reflected light from Porous Silicon Rugate Filter

Regions of high and low density silicon create constructive interferance and a sharp reflectivity maximum.

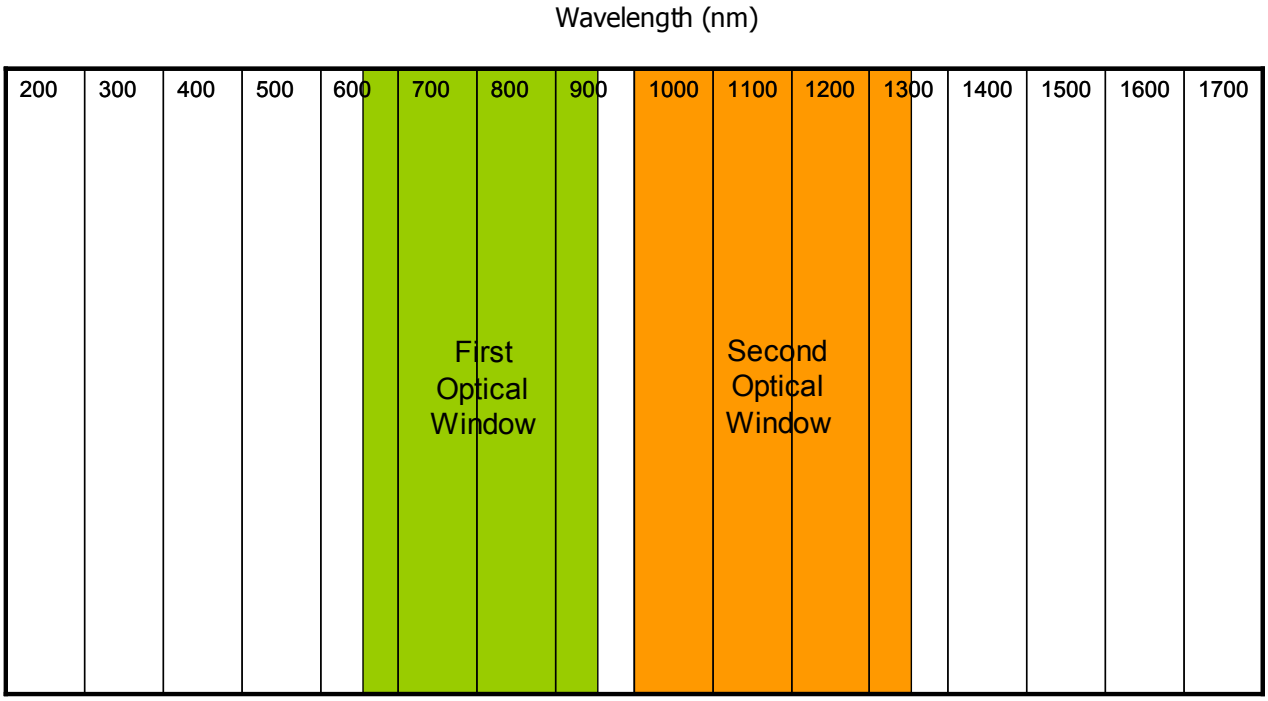

Figure 7.4: First and second optical windows

Regions of lowest absorption from biological tissue are called the optical windows. These are the best wavelengths for optical monitoring *in vivo*.

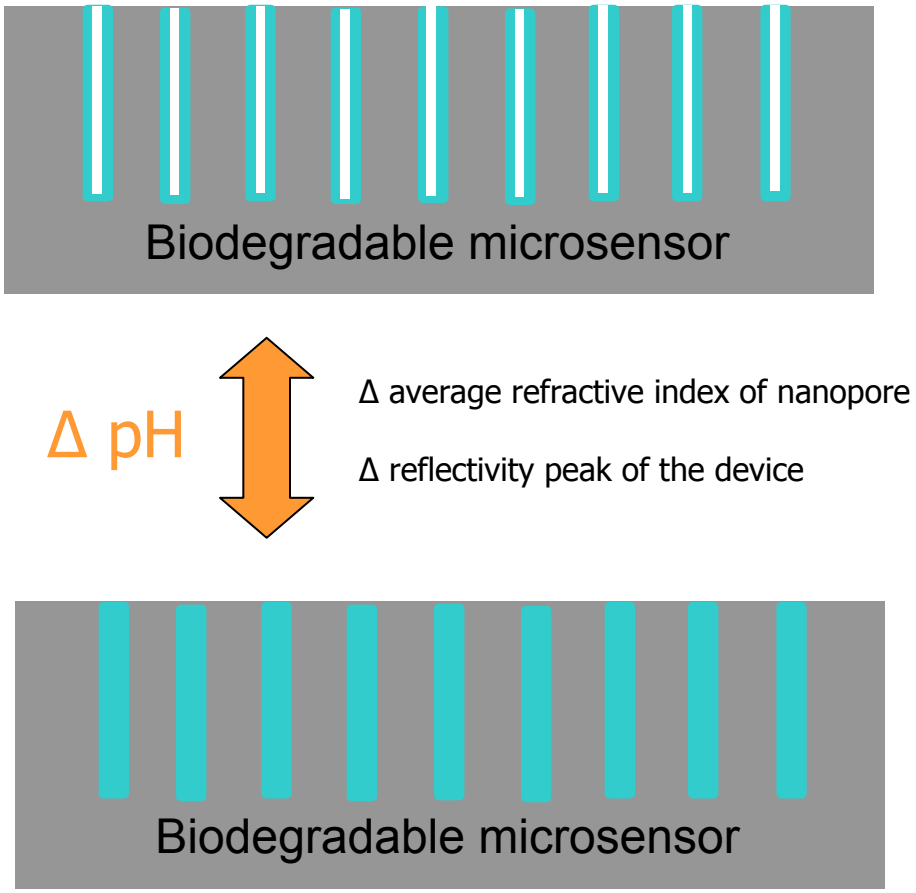

Figure 7.5: Diagram of hydrogel swelling within PSiRF

The volume change of the pH-responsive hydrogel within the pores (blue) results in a change in the reflectivity peak of the PSiRF.

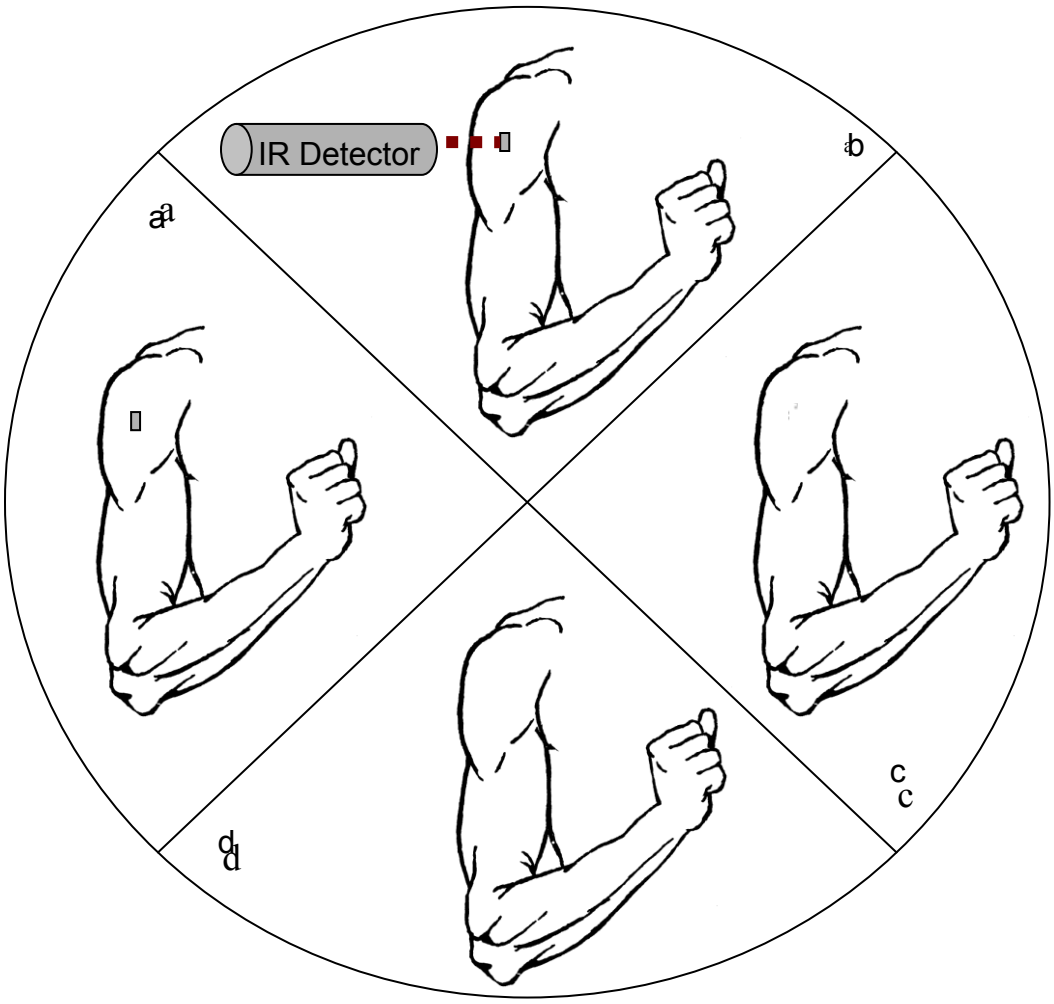

Figure 7.6: Lifecycle of Hydrogel-based PSiRF Microsensor

(a) Implant microsensor into tissue, (b) Sensing phase: Aim laser at microsensor and record reflected IR spectrum. Shift in reflectance peak corresponds with pH shift, (c) Degradation phase, (d) No surgery is required for removal of microsensor

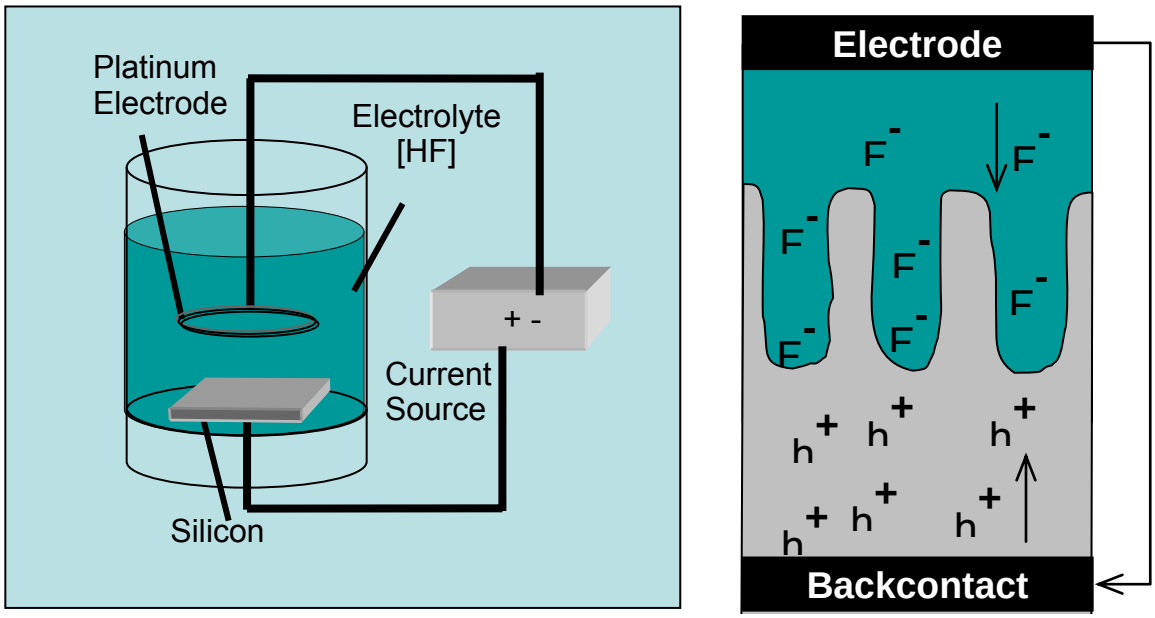

Figure 7.7: Schematic of silicon etching setup

Silicon is electrochemically etched by contacting it with a computer-controlled current source [13].

(a)

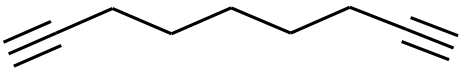

(b)

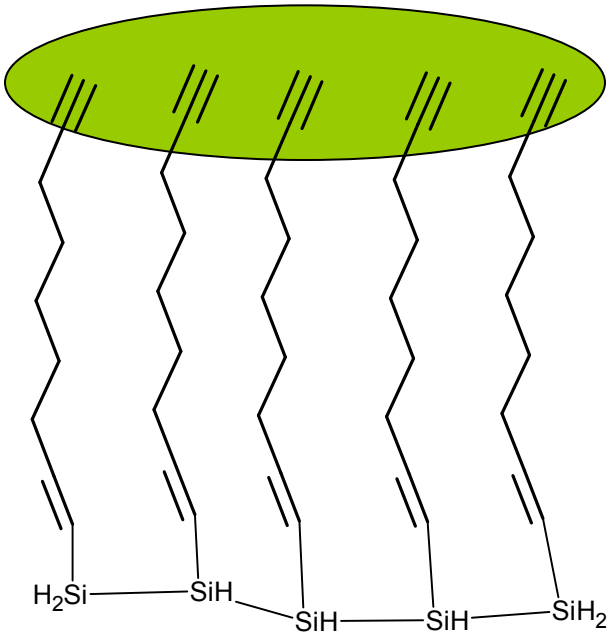

Figure 7.8: 1,8-Nonadiyne (a) chemical structure and (b) monolayer on silicon

1,8-Nonadiyne reacts with the freshly etched silicon to passivate the material

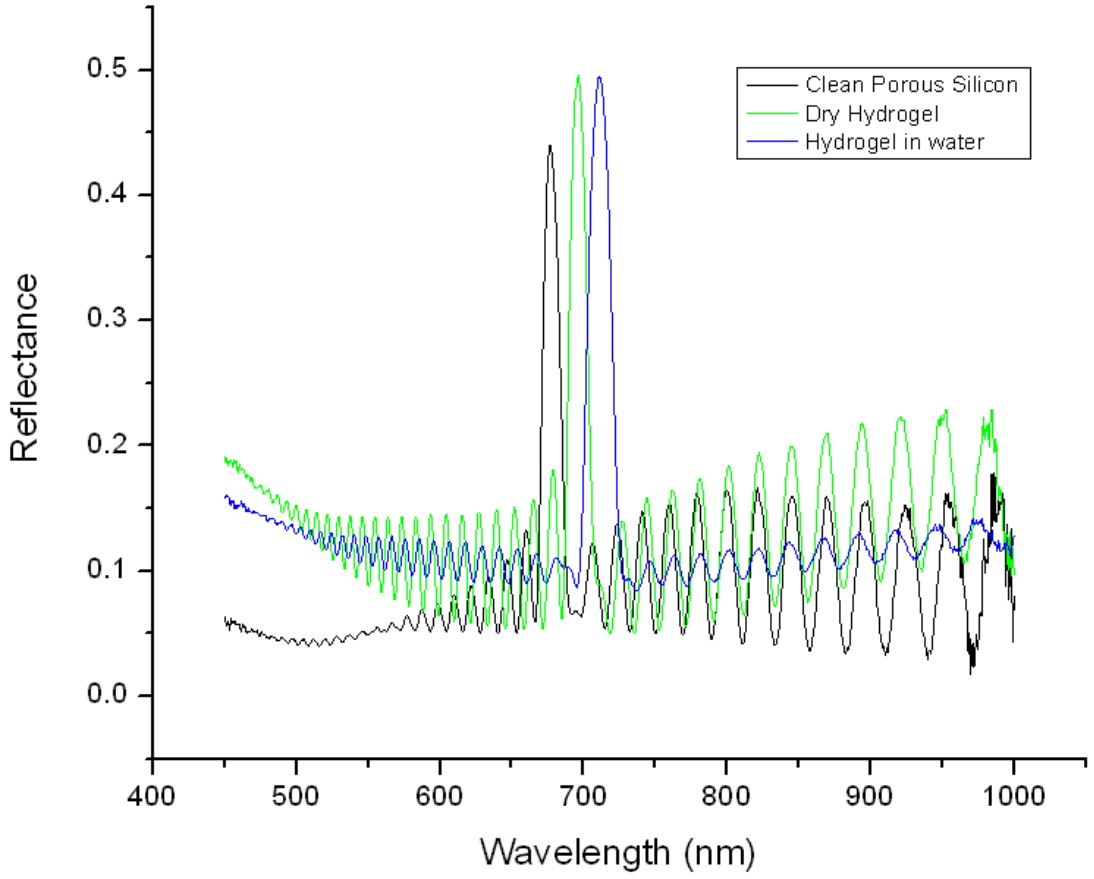

Figure 7.9: Reflectivity spectra of PSiRF with no hydrogel, with dry PMAA crosslinked with 1%TEGDMA, and with swollen PMAA crosslinked with 1%TEGDMA

The red-shift in the reflectivity peak indicates that hydrogel has been photopolymerized in the pores.

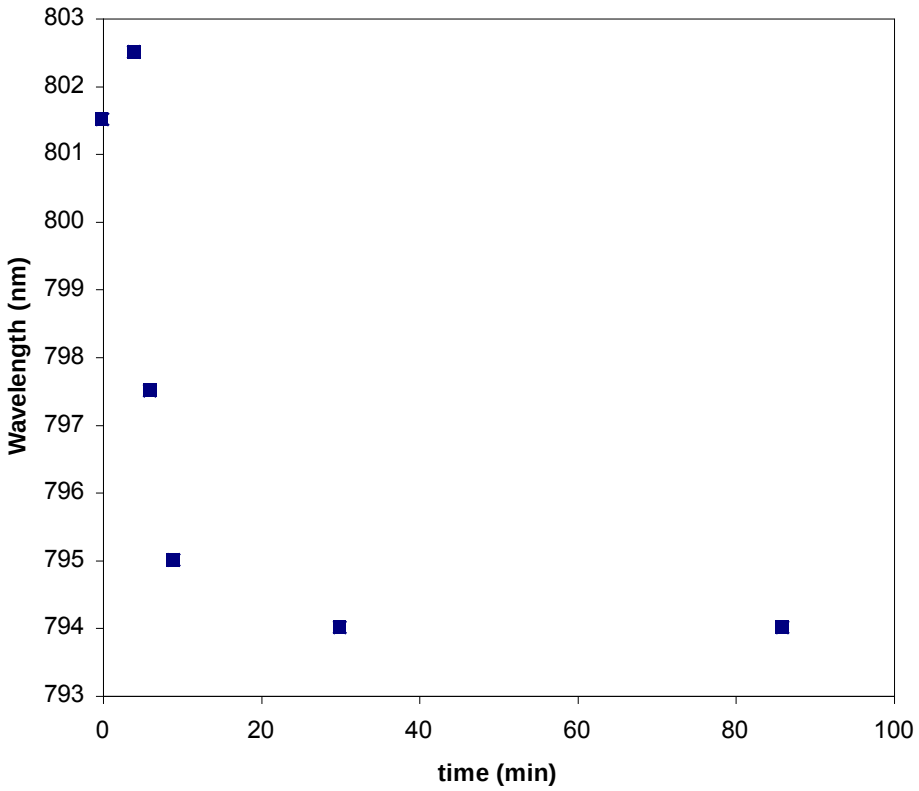

Figure 7.10: Reflectivity peaks of PSiRF with PMAA crosslinked with 1%TEGDMA following a change in phosphate-citrate buffer from pH 7 to pH 3 at time zero

This dynamic study suggests that these composite sensors will reach equilibrium between 10 and 30 minutes after a buffer solution is changed.

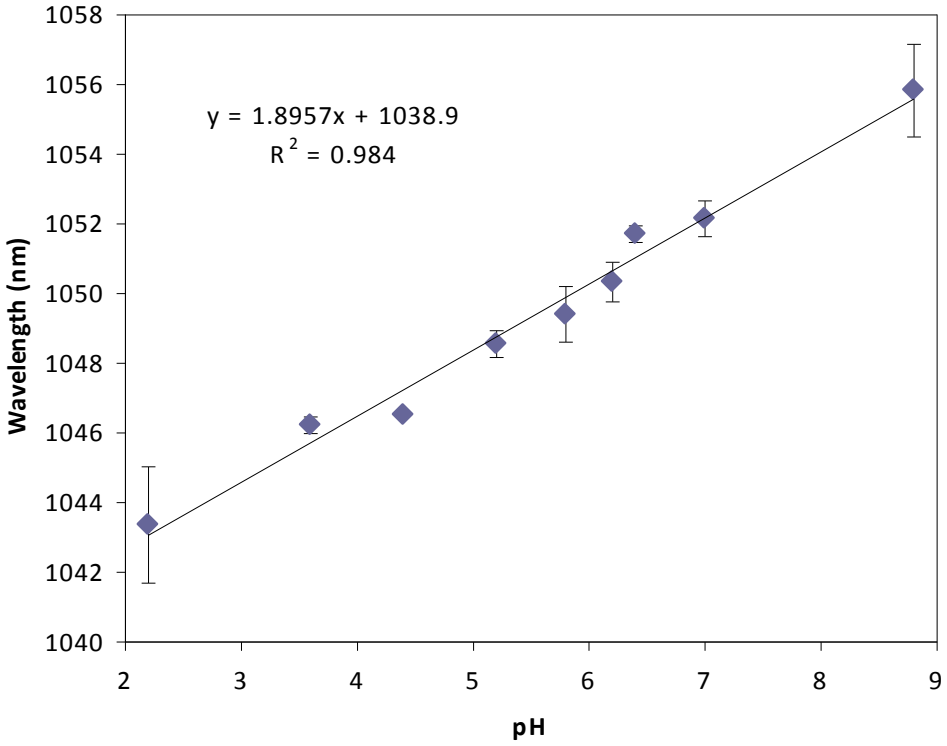

Figure 7.11: Reflectivity peaks of PSiRF with PMAA_5%PCLDA obtained in phosphate-citrate buffer solutions ranging from pH 2.2 to 8.8

Reflectivity peaks shows linear increase with pH in solutions of consistent ionic strength.

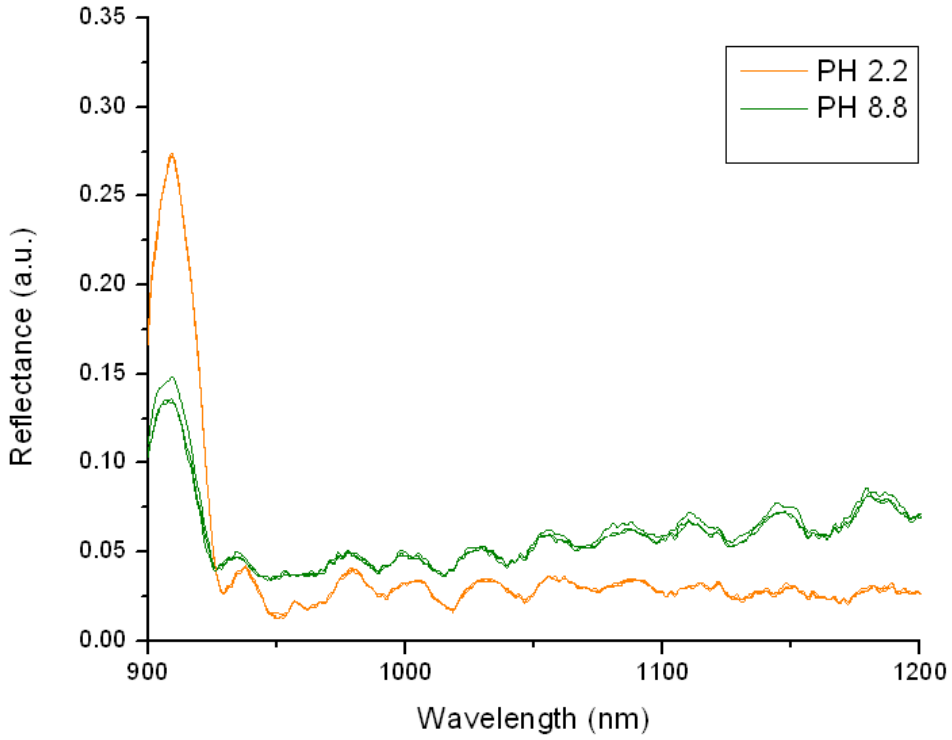

Figure 7.12: Reflectivity Spectra of PSiRF (no hydrogel) in phosphate-citrate buffer solutions of pH 2.2 and 8.8

Comparison of reflectivity spectra show no significant reflectivity peak shift without the incorporation of the pH-responsive hydrogel

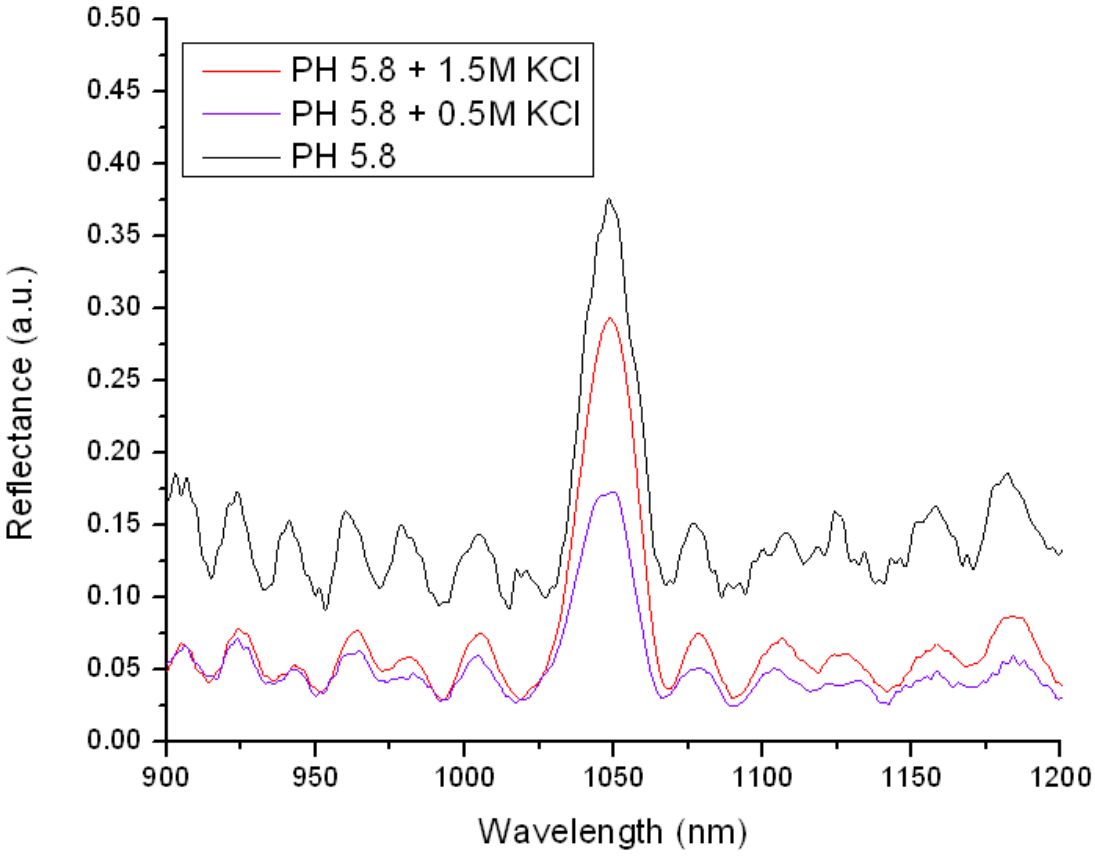

Figure 7.13: Reflectivity Spectra of PMAA crosslinked with 5%PCLDA in PSiRF in phosphate-citrate buffer solutions of pH 5.8 and varying salt concentrations

Comparison of reflectivity spectra show no significant reflectivity peak shift by varying salt concentration in phosphate-citrate buffers

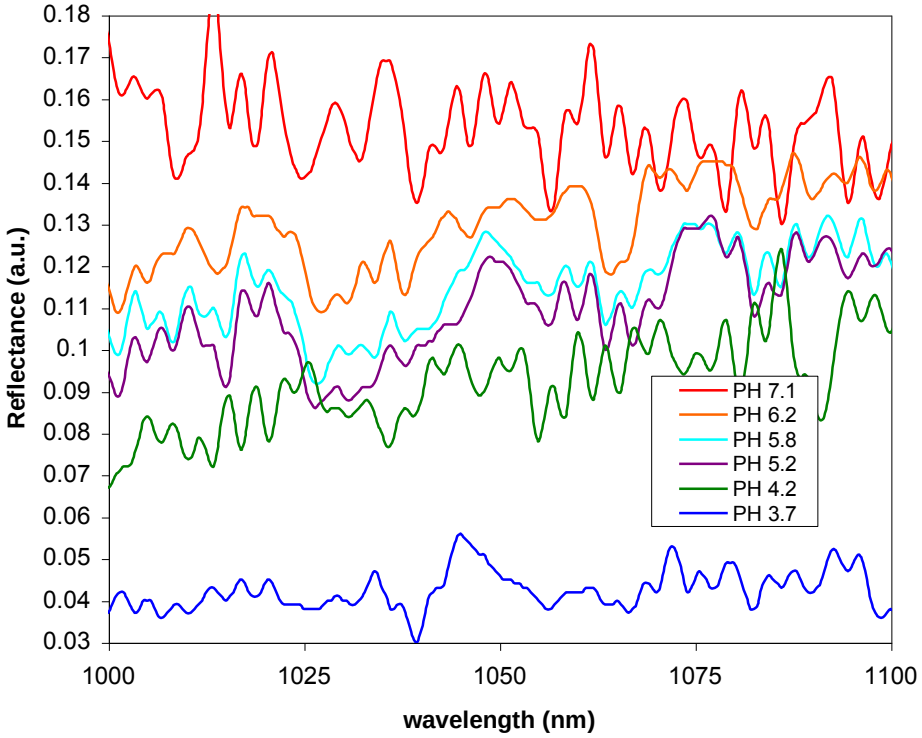

Figure 7.14: Reflectivity Spectra of PMAA_5%PCLDA in phosphate-citrate buffer solutions of ranging from pH 3.7 to 7.1

Comparison of reflectivity spectra shows general decrease in reflectance with pH.

REFERENCES

1. Segal, E., et al., *Confinement of thermoresponsive hydrogels in nanostructured porous silicon dioxide templates.* Adv Funct Mater, 2007. **17**(7): p. 1153-1162.
2. Kweon, H., et al., *A novel degradable polycaprolactone networks for tissue engineering.* Biomaterials, 2003. **24**(5): p. 801-808.
3. Park, J-H, Sailor, M.J., *Biodegradable luminescent porous silicon nanoparticles for in vivo applications* . Nat Mater, 2009.
4. Anglin, E.J., et al., *Porous silicon in drug delivery devices and materials.* Adv Drug Deliver Rev, 2008. **60**(11): p. 1266-1277.
5. Ilyas, S., et al., *Porous silicon based narrow line-width rugate filters.* Opt Mater, 2007. **29**(6): p. 619-622.
6. Ciampi S., et al., *Silicon (100) electrodes resistant to oxidation in aqueous solutions: An unexpected benefit of wurface acetylene moieties* Langmuir, 2009. **25**(4): p. 2530-2539.
7. Olive, D.M. *Near infrared technology and optical agents for molecular imaging*. Biomedicine, 2008.
8. Kilian, K.A., et al., *Forming antifouling organic multilayers on porous silicon rugate filters towards in vivo/ex vivo biophotonic devices.* Adv Funct Mater, 2007. **17**(15): p. 2884-2890.

9. Ciampi, S., et al., *Click chemistry in mesoporous materials: Functionalization of porous silicon rugate filters.* Langmuir, 2008. **24**(11): p. 5888-5892.

10. Fisher, O.Z. and N.A. Peppas, *Quantifying tight junction disruption caused by biomimetic pH-sensitive hydrogel drug carriers.* J Drug Deliv Sci Tec, 2008. **18**(1): p. 47-50.

11. Torres-Lugo, M. and N.A. Peppas, *Molecular design and in vitro studies of novel pH-sensitive hydrogels for the oral delivery of calcitonin.* Macromolecules, 1999. **32**(20): p. 6646-6651.

12. Smith, A.M., et al., *Bioimaging: Second window for* in vivo *imaging.* Nat Nanotechnol, 2009. **4**, p. 710-711.

13. Kilian, K. (2006, November 22) *Optical transducers of biomolecular interactions*. Powerpoint presented at Flinder's University, NSW, Australia.

CHAPTER 8: CONCLUSIONS

The goal of this thesis was to develop biodegradable microsensors that might someday contribute to improved *in vivo* sensing. Biodegradable, pH-responsive hydrogels were utilized as microsensing elements in two different types of silicon-based microsensors. First, novel hydrogels composed of pH-responsive, poly(methacrylic acid) crosslinked with varying amounts of biodegradable, polycaprolactone diacrylate were synthesized. The chemical composition of these materials was characterized using NMR, FTIR, and GPC.

The equilibrium and dynamic swelling behavior of these hydrogels was analyzed to better understand the sensitivity and range possible from a resulting microsensor. From these studies, it was concluded that the pH-responsive volume change experienced by the hydrogels would be sufficient to deflect a microcantilever transducer. The degradation rate of the hydrogels was studied to anticipate the sensing lifetime of the produced microsensor. Degradation products were analyzed to understand the biocompatibility of the novel hydrogel, and thus its potential for *in vivo* sensing.

Two types of transducers were utilized to fabricate novel sensors. The first produced a microcantilever-based sensing array. The advantages of this transducer include ultrasensitivity and the potential to produce a diverse biosensing array. The second was a porous silicon rugate filter-based microsensor. The advantages of this sensor are most appealing if the device's

ultimate use were *in vivo* biosensing. They include slow hydrolytic degradation and remote readout through several centimeters of tissue. This thesis successfully utilized biodegradable, environmentally-responsive hydrogels as sensing components in novel microscale devices.

Polycaprolactone-based crosslinkers were demonstrated to be ideal for synthesizing degradable, pH-responsive hydrogels for use in microsensing elements. This was due to their long degradation times, found to be approximately 1.5 years in biologically mimicking solutions studied in this thesis. A long degradation time is desirable for a hydrogel that will be utilized in a microsensor as the device must present a sensing lifetime useful for a patient. Since this thesis aimed to develop microsensors towards *in vivo* sensing, polycaprolactone was chosen as it has been previously FDA-approved for *in vivo* devices [1].

Hydrogels composed of poly(methacrylic acid) crosslinked with varying percentages of polycaprolactone diacrylate were synthesized by UV-free radical photopholymerization. These particular hydrogels were designed to undergo biodegradation by hydrolytic cleavage of their polycaprolactone crosslinks. Hydrogel are held together as insoluble networks because of their crosslinking, and once removed, the poly(methacrylic acid) chains would simply dissolve. Gel permeation chromatography of the poly(methacrylic acid) chains of the hydrogel was conducted to insure these polymers were of molecular weight that could be cleared from the body. The number average molecular weight of 48 kDa

obtained for poly(methacrylic acid) falls within the threshold for renal filtration of polymers [2].

The dynamic and equilibrium swelling behavior of these materials were studied. The change in swollen volume of pH-responsive hydrogels is critical for the material's use as a sensing element. It is this change in the hydrogel thin film that is transduced in this thesis to yield ultrasensitive microsensors. Thus, the swelling of these hydrogel was thoroughly studied. Additionally, the pK_a of the hydrogel, a property that affects the pH sensing range of the resulting sensor, was shifted by the quantity of crosslinking. Ultimately, pH-responsive volume changes in the hydrogel are correlated to response time of a resulting sensors. Theoretically, a larger change in volume from low to high pH results in a higher sensitivity sensors. It was shown that by varying the crosslinking density, factors relating to the sensitivity, range, and sensing lifetime of the resulting sensor could be varied.

By changing the crosslinking density from 20 to 2.5%, the weight swelling ratio,q, at high pH (above the pKa) was shown to increase 3-fold. The q at low pH varied little with crosslinking density. The dynamic swelling behavior was studied with varying crosslinking density. The highest crosslinked material reached equilibrium swelling most rapidly. As the intended application of these materials is in sensing, a shorter time to equilibrium is desirable. A slowly degrading hydrogel is needed if these materials are to be utilized as sensing elements for *in vivo* microsensors. Degradation studies conducted on

poly(methacrylic acid) crosslinked with 20 mol% polycaprolactone diacrylate in phosphate buffered saline solution at 37°C predict a complete degradation time of 1.5 years. Up to 3 months, the ratio of weight swelling ratio, q/q_0, increased linearly with time for this biodegradable hydrogel while a similar hydrogel with nondegradable crosslinks (polyethylene glycol-based) showed no change.

This knowledge makes it possible to approximate the performance of these hydrogels as sensing elements in certain types of microsensors. The microcantilever-based sensors reported in Chapter 6 rely on changes to the swollen volume of hydrogels with pH. It is known that very thin hydrogel films that are covalently adhered to a substrate, such as silicon or glass, will not swell in the same way as unconstrained materials that are free to swell in all three dimensions. However, it is still important to understand the swelling potential of these materials in the bulk to help predict their performance when utilized as thin films in sensing applications.

A primary goal of this dissertation was to integrate hydrogels as sensing elements that were also biodegradable. This goal might at first seem counterintuitive. Traditionally sensors are engineer to increase the sensing lifetime of the device. However, for certain *in vivo* applications, a longer lifetime of the sensor is not needed. One such example is diagnosing ischemia in transplanted tissue. The need to monitor sufficient blood supply to a newly transplanted tissue is short, on the order of days [3]. Thus a microsensor that would be implanted along with a tissue as it was transplanted would need only

sense the pH of its microenvironment reliably for a short time. Then it would be ideal if this microsensor simply biodegraded and was cleared from the body. This would eliminate the need for a second surgery for sensor removal. Ideally, a sensing element would be designed such that it exhibited a useable lifetime in the body, followed by a tunable degradation and clearance from the body.

Biodegradable, pH-responsive hydrogel networks composed of poly(methacrylic acid) crosslinked with polycaprolactone diacrylate were photopolymerized atop microcantilever arrays. Microcantilever beams of varying force constant were tested and the crosslinking ratio of the hydrogel was varied to generate the highest sensitivity sensor. In general, a lower force constant silicon microcantilever and a thicker hydrogel thin film resulted in a higher sensitivity sensors. It was determined that a microcantilever of force constant 0.03 N/m and a 20% crosslinked hydrogel allowed the fabrication of the highest sensitivity sensor, 1nm/4.5e-5ΔpH. These sensors were tested in a variety of biologically mimicking solutions of varying pH, including protein-rich solutions, which did not significantly interfere with the function of the sensor.

Imaging the hydrogel atop the cantilever was undertaken with an optical microscope and satisfactory images were obtained using a fluorescently labeled hydrogel. These images were used to evaluate the consistency of hydrogel deposition across an array. A composite cantilever deflection equation, based on the bimetallic cantilever deflection equation first presented by Timoshenko in 1925, was evaluated for the microcantilever sensors fabricated and tested in this

thesis. A “small deflection” assumption present in this composite cantilever deflection equation was tested for the sensors and tip deflections presented here. Given the parameters of these microcantilever pH sensors, the composite cantilever equation agrees with experimentally obtained deflection data within the error of those experiments. This theory appears sufficient to describe the microcantilever pH sensors fabricated and tested in this thesis.

A novel microsensor consisting of a porous silicon rugate filter with a pH-responsive hydrogel photopolymerized within the pores was successfully fabricated. Two hydrogel formulation were tested to determine the affect of a degradable sensing element: poly(methacrylic acid) crosslinked with tetraethylene glycol dimethacrylate and poly(methacrylic acid) crosslinked with polycaprolactone diacrylate. Silicon was electrochemically etched in hydrofluoric acid to generate the porous silicon rugate filter with its reflectivity peak in the near infrared region. pH-Responsive hydrogel was photopolymerized within the pores using a UV free-radical polymerization. In one study, the silicon nanopores were calculated to consist of 20% dry hydrogel. The reflectivity peak of this sensor varied linearly with pH in the range 2.2 to 8.8 pH. The reflectivity peak did not change significantly when the ionic strength of the pH buffers was altered using potassium chloride.

This work showed promise towards utilizing porous silicon rugate filters as transducers for a wider variety of hydrogels in biosensing applications. Porous silicon rugate filters are garnering increased attention as components for *in vivo*

biosensors due to their ability for remote readout through tissue. Additionally, PSiRFs show promise as transducers since their hydrolytic degradation is tunable based on the surface stabilization chemistry employed. A biodegradable, pH-responsive hydrogel was polymerized within the pores of a porous silicon rugate filter to successfully generate a novel, completely degradable sensor.

In conclusion, combining advanced microfabrication techniques for producing silicon-based transducers and environmentally-responsive hydrogels enables the production of novel microsensors. The development of a completely degradable microsensor in this thesis might offer new potential for short-term *in vivo* biosensing. While pH-responsive hydrogels have been utilized here, the methods of fabrication and associated theory developed and tested herein enable future work with a wide variety of environmentally-responsive hydrogels. Molecularly imprinted polymers might be used with these transducers to produce protein-specific sensing arrays. The microfabrication of responsive hydrogel thin films with silicon microdevices is an exciting and promising route in developing novel microsensors.

REFERENCES

1. Atzet, S., et al., *Degradable poly(2-hydroxyethyl methacrylate)-co-polycaprolactone hydrogels for tissue engineering scaffolds*. Biomacromolecules, 2008. **9**: p. 3370-33377.
2. Fox, M.E., et al., *Soluble polymer carriers for the treatment of cancer: the importance of molecular architecture*. Accounts Chem Res, 2009. **42**(8): p. 1141-1151.
3. Gumbrell, G.P., et al., *Evaluation of a minimally invasive pH based microvascular ischemial monitor*. J Clin Eng, 1998. **23**: p. 344-353.

BIBLIOGRAPHY

Anglin, E.J., et al., *Porous silicon in drug delivery devices and materials.* Adv Drug Deliver Rev, 2008. **60**(11): p. 1266-1277.

Anseth, K.S., et al., *Mechanical properties of hydrogels and their experimental determination*. Biomaterials, 1996. **17**: p.1647-1657.

Asher, S.A., et al., *Enabling thermoreversible physically cross-linked polymerized colloidal array photonic crystals*. Chem Mater, 2008. **20**(24): p. 7501-7509.

Atzet, S., et al., *Degradable poly(2-hydroxyethyl methacrylate)-co-polycaprolactone hydrogels for tissue engineering scaffolds*. Biomacromolecules, 2008. **9**: p. 3370-33377.

Bashir, R., et al., *Micromechanical cantilever as an ultrasensitive pH microsensor.* Appl Phys Lett, 2002. **81**(16): p. 3091-3093.

Baxamusa, S.H. et al., *Protection of sensors for biological applications by photoinitiated chemical vapor deposition of hydrogel thin films*. Biomacromolecules, 2008. **9**(10): p. 2857-2862.

Bayer, C.L. and N.A. Peppas, *Advances in recognitive, conductive and responsive delivery systems.* J Control Release, 2008.

Bergese, P., et al., *Investigation of a biofunctional polymeric coating deposited onto silicon microcantilevers.* Appl Surf Sci, 2007. **253**(9): p. 4226-4231.

Boland, T., Ratner, B.D., *Direct measurement of hydrogen bonding in DNA nucleotide bases by atomic force microscopy.* Proc Natl Acad Sci USA, 1995. **12**: p. 5297-301.

Boisen, A. and Thundat, T., *Design & fabrication of cantilever array biosensors.* Mater Today, 2009. **12**(9): p. 32-38.

Brahim, S., et al., *Chemical and biological sensors based on electrochemical detection using conducting electroactive polymers*. Microchim Acta, 2003. **143**(2): p. 123-137.

Bramfeldt, H., P. Sarazin, and P. Vermette, *Characterization, degradation, and mechanical strength of poly(D,L-lactide-co-epsilon-caprolactone)-poly(ethylene glycol)-poly(D,L-lactide-co-epsilon-caprolactone).* J Biomed Mater Res A, 2007. **83A**: p. 503-511.

Buerk, D.G., *Biosensors, Theory and Applications*. 1993, Lancaster, PA: Technomic Publishing Company, Inc.

Calvert, P., *Gel sensors and actuators.* Mrs Bull, 2008. **33**(3): p. 207-212.

Carr, D.A. and Peppas, N.A., *Assessment of poly(methacrylic acid-co-N-vinyl pyrrolidone) as a carrier for the oral delivery of therapeutic proteins using Caco-2 and HT29-MTX cell lines.* J Biomed Mater Res A, 2010. **92A**(2): p. 504-512.

Chao, G.T., et al., *Synthesis, characterization, and hydrolytic degradation behavior of a novel biodegradable pH-sensitive hydrogel based on polycaprolactone, methacrylic acid, and poly(ethylene glycol).* J Biomed Mater Res A, 2008. **85A**(1): p. 36-46.

Chilkoti, A., et al., *The relationship between ligand-binding thermodynamics and protein-ligand interaction forces measured by atomic force microscopy*. Biophys J, 1995. **69**(5): p. 2125-30.

Chu, W., et al., *Analysis of tip deflection and force bimetallic cantilever microactuator*, J Micromech Microeng, 1993. **3**: p. 4-7.

Ciampi, S., et al., *Click chemistry in mesoporous materials: Functionalization of porous silicon rugate filters.* Langmuir, 2008. **24**(11): p. 5888-5892.

Ciampi S., et al., *Silicon (100) electrodes resistant to oxidation in aqueous solutions: An unexpected benefit of wurface acetylene moieties* Langmuir, 2009. **25**(4): p. 2530-2539.

De, S.K., et al., *Equilibrium swelling and kinetics of pH-responsive hydrogels: Models, experiments, and simulations.* J Microelectromech S, 2002. **11**(5): p. 544-555.

Eichenbaum, G.M., et al., *Investigation of the swelling response and loading of ionic microgels with drugs and proteins: The dependence on cross-link density.* Macromolecules, 2001. **34**(18): p. 6526-6526.

Endo, T., et al., *Stimuli-responsive hydrogel–silver nanoparticles composite for development of localized surface plasmon resonance-based optical biosensor*. Anal Chim Acta, 2008. **611**(2): p. 205-211.

Fagerstam, L.G., et al., *Biospecific interaction analysis using surface-plasmon resonance detection applied to kinetic binding-site and concentration analysis.* J Chromatogr, 1992. **597**: p. 397-410.

Fisher, O.Z. and N.A. Peppas, *Quantifying tight junction disruption caused by biomimetic pH-sensitive hydrogel drug carriers.* J Drug Deliv Sci Tec, 2008. **18**(1): p. 47-50.

Fisher, O.Z., et al., *Enhanced core hydrophobicity, functionalization and cell penetration of polybasic nanomatrices*. Pharm Res, 2009. **26**(1): p. 51-60.

Flory, P.J. and J. Rehner, *Statistical mechanics of cross-linked polymer networks.* J Chem Phys, 1943. **11**(11): p. 521-526.

Fox, M.E., et al., *Soluble polymer carriers for the treatment of cancer: the importance of molecular architecture*. Accounts Chem Res, 2009. **42**(8): p. 1141-1151.

Giessibl, F. J., *Advances in atomic force microscopy*. Rev Mod Phys, 2003. **75**: p. 949.

Green Book, *IUPAC Quantities, Units and Symbols in Physical Chemistry*. Second Edition, 1993. Oxford: Blackwell Scientific Publications.

Guiseppi-Elie, A., et al., *Enzyme microgels in packed-bed bioreactors with downstream amperometric detection using microfabricated interdigitated microsensor electrode arrays*. Biotechno Bioeng, 2001. **75**(4): p. 475-484.

Gumbrell, G.P., et al., *Evaluation of a minimally invasive pH based microvascular ischemial monitor*. J Clin Eng, 1998. **23**: p. 344-353.

Guo, W., Hu, N., *Interaction of myoglobin with poly(methacrylic acid) at different pH in their layer-by-layer assembly films: an electrochemical study* Biophys Chem, 2007. **129**(2-3): p. 163-71.

Hansma, P.K., et al., *Scanning tunneling microscopy and atomic force microscopy: application to biology and technology.* Science, 1988. **242**: p. 209-216.

Hilt, J.Z., et al., *Ultrasensitive biomems sensors based on microcantilevers patterned with environmentally responsive hydrogels*. Biomed Microdevices, 2003. **5**(3): p. 177-184.

Hilt, J.Z., *Novel micro- and nanoscale diagnostic and therapeutic devices based on intelligent polymer networks*, in *Chemical Engineering*. 2004, The University of Texas: Austin, TX.

Hull, T.H., *The challenge of contraceptive implant removals in east Nusa Tenggara, Indonesia.* Int Fam Plan Perspec, 1998. **24**(4): p. 176.

Humphris, A.D., Miles, M.J. and Hobbs, J.K.*, A mechanical microscope: High-speed atomic force microscopy*, Appl Phys Lett, 2005. **86**.

Ilyas, S., et al., *Porous silicon based narrow line-width rugate filters.* Opt Mater, 2007. **29**(6): p. 619-622.

Instron Material Testing Solutions, Grip Solution for Testing Polymer Hydrogels, 12-14-2009. http://www.instron.us/wa/solutions/Polymer_Hydrogels_ Testing_ Grip_Solution.aspx

Itoga, K., et al., *Cell micropatterning using photopolymerization with a liquid crystal device commercial projector.* Biomaterials, 2004. **25**(11): p. 2047-2053.

Itoga, K., et al., *Micropatterned surfaces prepared using a liquid crystal projector-modified photopolymerization device and microfluidics.* J Biomed Mater Res A, 2004. **69A**(3): p. 391-397.

Itoga, K., et al., *Maskless liquid-crystal-display projection photolithography for improved design flexibility of cellular micropatterns.* Biomaterials, 2006. **27**(15): p. 3005-3009.

Itoga, K., et al., *Second-generation maskless photolithography device for surface micropatterning and microfluidic channel fabrication.* Anal Chem, 2008. **80**: p. 1323-1327.

Kanekiyo, Y., et al., *Novel nucleotide-responsive hydrogels designed from copolymers of boronic acid and cationic units and their applications as a QCM resonator system to nucleotide sensing*. J Polym Sci A1, 2000. **38**(8): p. 1302-1310.

Karlsson, S., Albertsson, A.-C., *Biodegradable polymers and environmental interaction.* Polym Eng Sci**, 38**(8): p. 1251-1253.

Kilian, K.A., et al., *Forming antifouling organic multilayers on porous silicon rugate filters towards in vivo/ex vivo biophotonic devices.* Adv Funct Mater, 2007. **17**(15): p. 2884-2890.

Kilian, K. (2006, November 22) *Optical transducers of biomolecular interactions*. Powerpoint presented at Flinder's University, NSW, Australia.

Kim, J.H., S.K. Park, and Y.H. Bae, *In situ accelerated degradation of polyoxyethylene/poly(epsilon-caprolactone) multiblock copolymer by moderate thermal treatment.* J Biomat Sci-Polym E, 2003. **14**(9): p. 903-916.

Knerr, P.J., et al., *Zinc-triggered hydrogelation of designed beta-hairpin peptides*. Biopolymers, 2007. **88**(4): p. 639.

Kocincova, A.S., et al., *Multiplex bacterial growth monitoring in 24-well microplates using a dual optical sensor for dissolved oxygen and pH*. Biotechnol Bioeng, 2008. **100**(3): p. 430-438.

Kweon, H., et al., *A novel degradable polycaprolactone networks for tissue engineering.* Biomaterials, 2003. **24**(5): p. 801-808.

Lavrik, N.V., M.J. Sepaniak, and P.G. Datskos, *Cantilever transducers as a platform for chemical and biological sensors.* Rev Sci Instrum, 2004. **75**(7): p. 2229-2253.

Lee, W.F. and T.S. Cheng, *Studies on preparation and properties of porous biodegradable poly(NIPAAm) hydrogels.* J Appl Polym Sci, 2008. **109**(3): p. 1982-1992.

Lei, M., et al., *Integration of hydrogels with hard and soft microstructures.* J Nanosci Nanotechno, 2007. **7**(3): p. 780-789.

Li, H. and Luo, R., *Modeling and characterization of glucose-sensitive hydrogel: Effect of Young's modulus.* Biosens Bioelectron, 2009. 24(12): p. 3630-3636.

Liu, Z., et al., *Structural and functional studies of aspergillus oryzae cutinase: enhanced thermostability and hydrolytic activity of synthetic ester and polyester degradation,* J Am Chem Soc, 2009. **131**(43): p. 15711–15716.

Lowman, A.M. and N.A. Peppas, *Solute transport analysis in pH-responsive, complexing hydrogels of poly(methacrylic acid-g-ethylene glycol).* J Biomat Sci-Polym E, 1999. **10**(9): p. 999-1009.

Maurer, M.K., et al., *Cholesterol oxidase functionalization of a polymerized crystalline colloidal array*. Sensor Actuat B-Chem, 2008. **134**(2): p. 736-742.

Meiring, J.E., et al., *Pattern recognition of shape-encoded hydrogel biosensor arrays*. Opt Eng, 2009. **48**(3).

Mikos, A.G. and N.A. Peppas, *Flory Interaction Parameter-Chi For Hydrophilic Copolymers With Water.* Biomaterials, 1988. **9**(5): p. 419-423.

Mohr, G.J., et al., *Design of acidochromic dyes for facile preparation of pH sensor layers*. Anal Bioanal Chem, 2008. **392**(7): p. 1411-1418.

Moulin, A.M., et al., *Microcantilever-based biosensors.* Ultramicroscopy, 2000. **82**(1-4): p. 23-31.

Oda, Y., et al., *Polycaprolactone depolymerase produced by the bacterium Alcaligenes faecalis,* FEMS Microbiol Lett, 1997. **152**: p. 339-343.

Olive, D.M. *Near infrared technology and optical agents for molecular imaging*. Biomedicine, 2008.

Owens, D.E., et al., *Temperature-responsive polymer-gold nanocomposites as intelligent therapeutic systems.* J Biomed Mater Res A, 2007. **83A**: p. 692-695.

Owens, D.E. and N.A. Peppas, *Opsonization, biodistribution, and pharmacokinetics of polymeric nanoparticles.* Int J Pharm, 2006. **307**(1): p. 93-102.

Park, J-H, Sailor, M.J., *Biodegradable luminescent porous silicon nanoparticles for in vivo applications* . Nat Mater, 2009.

Peppas, N.A., et al., *Hydrogels in pharmaceutical formulations.* Eur Journal Pharm Biopharm, 2000. **50**(1): p. 27-46.

Peppas, N.A., et al., *Hydrogels in biology and medicine: From molecular principles to bionanotechnology.* Adv Mater, 2006. **18**(11): p. 1345-1360.

Peppas, N.A., *Kinetics of Smart Hydrogels*, in *Reflexive Polymers and Hydrogels*, N. Yui, R.J. Mrsny, and K. Park, Editors. 2004, CRC Press LLC. p. 99-113.

Peppas, N.A., *Hydrogels*, in *Biomaterials Science*, A.S.H. Buddy D. Ratner, Frederick J. Shoen, Jack E. Lemons, Editor. 2004, Elsevier: San Diego, California.

Qin, D., Y.N. Xia, and G.M. Whitesides, *Rapid prototyping of complex structures with feature sizes larger than 20 mu m.* Adv Mater, 1996. **8**(11): p. 917.

Rice, M.A., J. Sanchez-Adams, and K.S. Anseth, *Exogenously triggered, enzymatic degradation of photopolymerized hydrogels with polycaprolactone subunits: Experimental observation and modeling of mass loss behavior.* Biomacromolecules, 2006. **7**(6): p. 1968-1975.

Richter, A., et al., *Review on hydrogel-based pH sensors and microsensors.* Sensors, 2008. **8**: p. 561-581.

Richter, A., et al., *Characterization of a microgravimetric sensor based on pH sensitive hydrogels*, Sensor Actuat B-Chem, 2004. **99**(2): p. 579-585.

Ruan, C.M., et al., *A mass-sensitive pH sensor based on a stimuli-responsive polymer*. Anal Chim Acta, 2003. **497**(1): p. 123-131.

Ruzin, *Plant Microtechnique and Microscopy.* 1999, Oxford University Press.

Salehi-Khojin A., et al., *Nanomechanical cantilever active probes for ultrasmall mass detection*. J Appl Phys, 2009. **105**(1).

Schrenkhammer, P., Wolfbeis, O.S., *Fully reversible optical biosensors for uric acid using oxygen transduction*. Biosens Bioelectron, 2008. **24**(4): p. 994-999.

Segal, E., et al., *Confinement of thermoresponsive hydrogels in nanostructured porous silicon dioxide templates.* Adv Funct Mater, 2007. **17**(7): p. 1153-1162.

Sheppard, N.F., et al., *Microfabricated conductimetric pH sensor*. Sensor Actuat B-Chem, 1995. **28**(2): p. 95-102.

Siepmann, J. and A. Gopferich, *Mathematical modeling of bioerodible, polymeric drug delivery systems.* Adv Drug Deliver Rev, 2001. **48**(2-3): p. 229-247.

Sikes, H.D., et al., *Antigen detection using polymerization-based amplification*. Lab Chip, 2009. **9**(5): p. 653-656.

Siparsky, G.L., K.J. Voorhees, and F.D. Miao, *Hydrolysis of polylactic acid (PLA) and polycaprolactone (PCL) in aqueous acetonitrile solutions: Autocatalysis.* J Environ Polym Degr, 1998. **6**(1): p. 31-41.

Smith, A.M., et al., *Bioimaging: Second window for* in vivo *imaging.* Nat Nanotechnol, 2009. **4**, p. 710-711.

Sorber, J., et al., *Hydrogel-based piezoresistive pH sensors: Investigations using FT-IR attenuated total reflection spectroscopic Imaging.* Anal Chem, 2008. **80**(8): p. 2957-2962.

Sperling, L.H., *Introduction to Physical Polymer Science*, 3rd Edition. p. 428.

Stair, J.L., et al., *Sensor materials for the detection of proteases*. Biosens Bioelectron, 2009. **24**(7): p. 2113-2118.

Tang, J., Xiao, P.F., *Polymerizing immobilization of acrylamide-modified nucleic acids and its applications.* Biosens Bioelectron, 2009. **24**(7): p. 1817-1824.

Thete, A.R. et al., *A hydrogel based fluorescent micro array used for the characterization of liquid analytes*. Anal Chim Acta, 2009. **633**(1): p. 81-89.

Tierney, S., et al., *Determination of swelling of responsive gels with nanometer resolution. Fiber-optic based platform for hydrogels as signal transducers*. Anal Chem, 2008. **80**(13): p. 5086-5093.

Timoshenko, S., *Analysis of bimetal thermostats*, J Opt Soc Am, 1925. **11**: p. 233.

Torres-Lugo, M. and N.A. Peppas, *Molecular design and in vitro studies of novel pH-sensitive hydrogels for the oral delivery of calcitonin.* Macromolecules, 1999. **32**(20): p. 6646-6651.

Webb, A.R., J. Yang, and G.A. Ameer, *Biodegradable polyester elastomers in tissue engineering.* Expert Opin On Biol Th, 2004. **4**(6): p. 801-812.

Wu, Z., *Direct and label-free detection of cholic acid based on molecularly imprinted photonic hydrogels*, J Mater Chem, 2008. **18**: p. 5452-5458.

Zhu, Y., et al., *Surface modification of polycaprolactone with poly(methacrylic acid) and gelatin covalent immobilization for promoting its cytocompatibility*. Biomaterials, 2002. **23**(24): p. 4889-4895.

Zourob, M., et al., *A wireless magnetoelastic biosensor for the direct detection of organophosphorus pesticides*. Analyst, 2007. **132**(4): p. 338-343.

VITA

Diana Kathryn Snelling was born in Kettering, Ohio, on January 7, 1983. She is the daughter of Larry and Kathy Snelling. She attended Middletown High School in Middletown, Ohio, and graduated first in her class in 2001. Diana immediately enrolled at The Ohio State University in Columbus, Ohio. While pursuing her undergraduate degree in Chemical Engineering, Diana participated in a cooperative education program. She worked for DuPont in Teflon® Technology at their plant in Parkersburg, West Virginia.

Upon receiving her Bachelor's degree in Chemical Engineering, Diana proceeded to the University of Texas at Austin to begin doctoral study in the Department of Chemical Engineering. She was awarded a National Science Foundation Graduate Research Fellowship while in attendance. Her project which focused on using biodegradable, stimuli-responsive hydrogels in microsensing devices was supervised by Professor Nicholas A. Peppas. Diana married Tom Van Blarcom on March 27, 2010, in Austin, Texas.

Permanent Address: 6516 Jennifer Lane, Franklin, OH 45005

This dissertation was typed by the author.